

**ULTRASOUND ASSISTED BIODIESEL SYNTHESIS
FROM JATROPHA OILSEEDS USING IN-SITU REACTIVE
EXTRACTION**

TAN SHIOU XUAN

**FACULTY OF ENGINEERING
UNIVERSITY OF MALAYA
KUALA LUMPUR**

2019

**ULTRASOUND ASSISTED BIODIESEL SYNTHESIS
FROM JATROPHA OILSEEDS USING IN-SITU
REACTIVE EXTRACTION**

TAN SHIOU XUAN

**DISSERTATION SUBMITTED IN FULFILMENT OF THE
REQUIREMENTS FOR THE DEGREE OF MASTER OF
ENGINEERING SCIENCE**

**FACULTY OF ENGINEERING
UNIVERSITY OF MALAYA
KUALA LUMPUR**

2019

UNIVERSITY OF MALAYA
ORIGINAL LITERARY WORK DECLARATION

Name of Candidate: Tan Shiou Xuan

Matric No: KGA160024

Name of Degree: Master of Engineering Science

Title of Project Paper/Research Report/Dissertation/Thesis ("this Work"):

ULTRASOUND ASSISTED BIODIESEL SYNTHESIS FROM JATROPHA
OILSEEDS USING IN-SITU REACTIVE EXTRACTION

Field of Study: Energy

I do solemnly and sincerely declare that:

- (1) I am the sole author/writer of this Work;
- (2) This Work is original;
- (3) Any use of any work in which copyright exists was done by way of fair dealing and for permitted purposes and any excerpt or extract from, or reference to or reproduction of any copyright work has been disclosed expressly and sufficiently and the title of the Work and its authorship have been acknowledged in this Work;
- (4) I do not have any actual knowledge nor do I ought reasonably to know that the making of this work constitutes an infringement of any copyright work;
- (5) I hereby assign all and every rights in the copyright to this Work to the University of Malaya ("UM"), who henceforth shall be owner of the copyright in this Work and that any reproduction or use in any form or by any means whatsoever is prohibited without the written consent of UM having been first had and obtained;
- (6) I am fully aware that if in the course of making this Work I have infringed any copyright whether intentionally or otherwise, I may be subject to legal action or any other action as may be determined by UM.

Candidate's Signature

Date:

Subscribed and solemnly declared before,

Witness's Signature

Date:

Name:

Designation:

ULTRASOUND ASSISTED BIODIESEL SYNTHESIS FROM JATROPHA OILSEEDS USING IN-SITU REACTIVE EXTRACTION

ABSTRACT

Utilisation of edible feedstock in biodiesel production had caused food versus fuel crisis. Mechanical stirring was found to be a cost-ineffective approach as excessive energy was needed with the requirement for external heating while consuming more catalyst. Furthermore, several intermediate steps between oilseeds harvesting and biodiesel synthesis could be integrated, thereby simplifying the process and reduced the production cost. The main aim of the present study was to produce biodiesel with satisfactory fatty acid methyl ester (FAME) purity ($\geq 96.5\%$) after two-step ultrasound assisted in-situ esterification and ultrasound assisted transesterification by directly utilising non-edible *Jatropha* oilseeds containing high acid value (AV) as feedstock. Ultrasound assisted in-situ esterification utilising sulphuric acid (H_2SO_4) as catalyst and the reaction parameters affecting the extraction, esterification efficiencies and FAME purity such as ultrasonic pulse mode, *Jatropha* oilseed particle size, n-hexane to methanol volume ratio, H_2SO_4 loading, reaction time and ultrasonic amplitude were investigated in detail. For ultrasound assisted transesterification, potassium hydroxide (KOH) was utilised as catalyst and the optimum reaction parameters of KOH loading, methanol to esterified oil molar ratio, reaction time and ultrasonic amplitude were investigated. *Jatropha* oilseeds before and after ultrasound assisted in-situ esterification were characterized and the fuel properties of the biodiesel produced were examined. The results showed that ultrasound assisted in-situ esterification obtained extraction efficiency of 83.96%, esterification efficiency of 71.10% and FAME purity of 38.58% at optimum reaction parameters of ultrasonic pulse mode 5s on/2s off, particle size of 1–2 mm, n-hexane to methanol volume ratio of 3:1, H_2SO_4 loading of 5 vol.%, reaction time of 150 min and ultrasonic amplitude of 60%. It was revealed from the results that ultrasonic pulse mode had significant effects on

esterification efficiency and FAME purity. On the other hand, *Jatropha* oilseed particle size and n-hexane to methanol volume ratio significantly affected extraction efficiency. Other reaction variables (H_2SO_4 loading, reaction time and ultrasonic amplitude) had considerable effects on extraction, esterification efficiencies and FAME purity. The esterified *Jatropha* oil produced from esterification was then subjected to transesterification in order to further improve the FAME purity and minimized the AV to acceptable limit according to American Standards for Testing Materials (ASTM D6751) and European Union Standards for Biodiesel (EN14214). In the subsequent ultrasound assisted transesterification, high FAME purity of 99.03% and biodiesel yield of 85.20% were attained at KOH loading of 1.5 wt.%, methanol to esterified oil molar ratio of 12:1, reaction time of 15 min and ultrasonic amplitude of 60%. It was revealed from ultrasound assisted transesterification that ultrasound could produce biodiesel within a short reaction time while producing high FAME purity at the same time. In conclusion, ultrasound assisted in-situ esterification and transesterification can be a feasible biodiesel production method using solid oil bearing seeds directly without pre-extraction in the future. Detailed and in-depth information of the influence of each reaction parameters in ultrasound assisted in-situ esterification of *Jatropha* oilseeds on extraction efficiency, esterification efficiency and FAME purity was contributed to current literatures, specific to *Jatropha* oilseeds. These information would be crucial for the commercialisation of the process in the future.

Keywords: *Jatropha* seeds, ultrasound, in-situ esterification, biodiesel

**PENGHASILAN BIODIESEL DARI BIJI BENIH JATROPHA
MENGUNAKAN *IN-SITU* EKSTRAKSI REAKTIF DENGAN BANTUAN
ULTRABUNYI**

ABSTRAK

Penggunaan bahan mentah yang boleh dimakan dalam penghasilan biodiesel telah menimbulkan kontroversi antara makanan dengan bahan api. Pengadukan mekanikal didapati tidak berkesan dari segi kos kerana tenaga berlebihan yang diperlukan untuk pemanasan luar dengan mengambil lebih banyak pemangkin. Tambahan pula, beberapa langkah perantaraan antara penuaian benih dan sintesis biodiesel dapat diintegrasikan untuk memudahkan proses dan mengurangkan kos pengeluaran. Matlamat kajian ini adalah untuk menghasilkan biodiesel dengan kemurnian FAME yang memuaskan ($\geq 96.5\%$) selepas *in-situ* esterifikasi dan transesterifikasi dengan bantuan ultrabunyi menggunakan biji benih *Jatropha* yang mengandungi nilai asid (AV) tinggi sebagai bahan mentah secara langsung. *In-situ* esterifikasi dibantu ultrabunyi dengan menggunakan asid sulfurik (H_2SO_4) sebagai pemangkin. Parameter tindak balas yang mempengaruhi kecekapan pengekstrakan dan eksterifikasi dengan kemurnian FAME seperti mod denyut ultrabunyi, saiz zarah biji benih minyak *Jatropha*, nisbah isipadu n-heksana kepada metanol, pemuatan H_2SO_4 , masa tindak balas dan amplitud ultrasonik telah diselidiki secara terperinci. Untuk transesterifikasi dengan bantuan ultrabunyi, kalium hidroksida (KOH) telah digunakan sebagai pemangkin dan parameter tindak balas optimum untuk pemuatan KOH, nisbah molar metanol kepada minyak esterified, masa tindak balas dan amplitud ultrasonik telah diselidiki. Biji benih minyak *Jatropha* sebelum dan selepas *in-situ* esterifikasi dengan bantuan ultrabunyi dan sifat bahan api biodiesel yang dihasilkan telah diperiksa. Keputusan menunjukkan bahawa *in-situ* esterifikasi dengan bantuan ultrabunyi memperoleh 83.96% kecekapan pengekstrakan, 71.10% kecekapan esterifikasi dan 38.58% kemurnian FAME pada parameter tindak balas

optimum 5s buka / 2s tutup mod denyut ultrasonik, 1-2 mm saiz zarah, 3: 1 nisbah isipadu n-heksana kepada metanol, 5 vol.% pemuatan H_2SO_4 , 150 minit masa tindak balas dan 60% amplitud ultrasonik. Keputusan yang diperolehi menunjukkan bahawa mod denyut ultrasonik mempunyai kesan ketara ke atas kecekapan esterifikasi dan kemurnian FAME. Sebaliknya, saiz zarah biji benih minyak *Jatropha* dan nisbah isipadu n-heksana kepada metanol mempunyai kesan kecekapan pengekstrakan yang ketara. Pemboleh ubah reaksi lain (pemuatan H_2SO_4 , masa tindak balas dan amplitud ultrasonik) mempunyai kesan yang besar ke atas kecekapan pengekstrakan dan esterifikasi dan kemurnian FAME. Minyak *Jatropha* yang dihasilkan daripada esterifikasi diteruskan dengan transesterifikasi untuk meningkatkan kemurnian FAME dan mengurangkan AV ke had yang boleh diterima mengikut *Standard American for Materials Testing* (ASTM D6751) dan *European Union Standards for Biodiesel* (EN14214). Dalam transesterifikasi dengan bantuan ultrasound, kemurnian FAME yang tinggi sebanyak 99.03% dan hasil biodiesel sebanyak 85.20% telah diperolehi pada 1.5 wt% pemuatan KOH, 12: 1 nisbah molar metanol kepada minyak esterified, 15 minit masa tindak balas dan 60% amplitud ultrasonik. Keputusan yang diperolehi menunjukkan bahawa transesterifikasi dengan bantuan ultrasound boleh menghasilkan biodiesel dalam masa tindak balas yang pendek dan menghasilkan kemurnian FAME yang tinggi. Kesimpulannya, *in-situ* esterifikasi dan transesterification dengan bantuan ultrabunyi boleh menjadi kaedah penghasilan biodiesel untuk biji benih minyak tanpa pre-ekstraksi dalam masa akan datang. Maklumat terperinci dan mendalam tentang kesan setiap parameter tindak balas dalam *in-situ* esterifikasi dengan menggunakan biji benih *Jatropha* pada kecekapan pengekstrakan, kecekapan esterifikasi dan kemurnian FAME disumbangkan kepada literatur semasa, khusus untuk biji benih minyak *Jatropha*. Maklumat ini penting untuk proses pengkomersialan pada masa akan datang.

Kata kunci: biji benih *Jatropha*, ultrabunyi, *in-situ* esterifikasi, biodiesel

ACKNOWLEDGEMENTS

I would like to express my special thanks of gratitude to my supervisors, Dr. Ong Hwai Chyuan and Dr. Steven Lim for their kind support and guidance throughout my master degree.

I would also like to thank the laboratory technicians and staffs at Department of Mechanical Engineering and Chemistry for their helpful assistance.

Finally, I would like to thank all my friends and family for their kind help and support, and for always being there for me throughout my study.

University of Malaya

TABLE OF CONTENTS

Abstract	iii
Abstrak	v
Acknowledgements	vii
Table of Contents	viii
List of Figures	xii
List of Tables.....	xv
List of Symbols and Abbreviations.....	xvi
List of Appendices	xviii
 CHAPTER 1: INTRODUCTION.....	1
1.1 Background.....	1
1.2 Problem statement	4
1.3 Significance of the study	5
1.4 Aim and research objectives.....	5
1.5 Outline of research work	6
1.6 Thesis outline.....	8
 CHAPTER 2: LITERATURE REVIEW.....	9
2.1 Biodiesel synthesis.....	9
2.2 Ultrasound assisted biodiesel production	14
2.2.1 Ultrasound assisted homogeneous alkaline-catalysed transesterification	16
2.2.2 Ultrasound assisted homogeneous acid-catalysed transesterification	18
2.2.3 Two-step homogeneous ultrasound assisted transesterification.....	20
2.2.4 Ultrasound assisted interesterification.....	22
2.3 Primary factors for ultrasound assisted transesterification.....	25

2.3.1	Alcohol to oil molar ratio	25
2.3.2	Catalyst loading	29
2.3.3	Reaction time	32
2.3.4	Reaction temperature	35
2.3.5	Energy consumption	37
2.3.6	Phase separation time	38
2.3.7	Ultrasonic pulse mode	39
2.3.8	Biodiesel conversion and yield	41
2.4	Ultrasonic reactive extraction for biodiesel production	43
2.4.1	Mechanism of ultrasonic reactive extraction on oilseed for biodiesel production	45
2.5	Research gaps	48
CHAPTER 3: MATERIALS AND METHODS		49
3.1	Introduction	49
3.2	Materials	49
3.3	Equipment	51
3.4	Measurement of moisture and oil content of <i>Jatropha</i> seeds	51
3.5	Ultrasound assisted in-situ esterification	51
3.6	Ultrasound assisted transesterification	53
3.7	Seed characterization	55
3.7.1	FESEM	55
3.7.2	TGA	55
3.7.3	FTIR	55
3.7.4	Elemental analysis	56
3.8	Fuel properties	56
3.8.1	Acid value (AV)	57

3.8.2	FAME purity	58
3.8.3	Density at 15°C	58
3.8.4	Calorific value	59
3.8.5	Flash point	59
3.8.6	Kinematic viscosity at 40°C	59
3.8.7	Oxidation stability	61
3.8.8	Copper strip corrosion	62
3.8.9	Group I and II metals	63
CHAPTER 4: RESULTS AND DISCUSSION		64
4.1	Moisture and oil contents of <i>Jatropha</i> seeds	64
4.2	Parameters screening for ultrasound assisted in-situ esterification	65
4.2.1	Effect of ultrasonic pulse mode	65
4.2.2	Effect of ultrasonic amplitude	66
4.2.3	Effect of H ₂ SO ₄ loading	68
4.3	Parameters study of ultrasound assisted in-situ esterification	70
4.3.1	Effect of particle size	71
4.3.2	Effect of n-hexane to methanol volume ratio	72
4.3.3	Effect of H ₂ SO ₄ loading	74
4.3.4	Reaction time and ultrasonic amplitude	76
4.4	Seed characterization	79
4.4.1	FESEM	79
4.4.2	FTIR	81
4.4.3	TGA	84
4.4.4	Elemental analysis	85
4.5	Parameter study of ultrasound assisted transesterification	86
4.5.1	Effect of KOH loading	86

4.5.2	Effect of methanol to esterified oil molar ratio	87
4.5.3	Effect of reaction time and ultrasonic amplitude	88
4.5.4	Physicochemical properties of biodiesel	90
4.6	Comparison of ultrasound technique with conventional stirring approach	94
4.7	Brief summary	95

CHAPTER 5: CONCLUSIONS AND RECOMMENDATIONS.....98

5.1	Recommendations for future work	99
	References	101
	List of Publications and Papers Presented	118
	Appendix	120

LIST OF FIGURES

Figure 1.1: Estimated global gross domestic product (GDP), population, TPEC, and carbon dioxide (CO ₂) emissions trends from 2010 to 2030 (Hajjari <i>et al.</i> , 2017).....	1
Figure 1.2: Molecular structure of biodiesel.	2
Figure 2.1: Energy forms and their corresponding effects in ultrasonic application.	14
Figure 2.2: Interesterification reaction (Initial 3 equations show the initial steps whereas final equation gives the overall reaction) (Maddikeri <i>et al.</i> , 2013).....	22
Figure 2.3: Wave profiles for (a) continuous sonication (b) pulse sonication (Martinez-Guerra & Gude, 2015).....	40
Figure 2.4: Ultrasonic extraction mechanism (Jadhav <i>et al.</i> , 2016).	45
Figure 2.5: FESEM images of raw date seed at (a) 2000 × and (c) 10000 × and ultrasonicated date seed at (b) 2000× and (d) 10000× (Jadhav <i>et al.</i> , 2016).....	47
Figure 2.6: Particle size distribution of fresh date seed powder and ultrasonicated date seed powder (Jadhav <i>et al.</i> , 2016).....	47
Figure 3.1: Overview of research methodology.....	50
Figure 3.2: Overall flowchart of ultrasound assisted in-situ esterification process.	53
Figure 3.3: Overall flowchart of ultrasound assisted transesterification process.....	54
Figure 3.4: Measuring cell of viscometer.	60
Figure 3.5: Corrosion standards according to ASTM D130 (Hafez <i>et al.</i> , 2017).....	62
Figure 4.1: Effects of ultrasonic pulse mode on extraction efficiency, esterification efficiency and FAME purity at n-hexane to methanol volume ratio of 3:1, 5 vol.% H ₂ SO ₄ , 50% ultrasonic amplitude and 150 min reaction time.....	66
Figure 4.2: Effects of ultrasonic amplitude on extraction efficiency, esterification efficiency and FAME purity at n-hexane to methanol volume ratio of 3:1, 5 vol.% H ₂ SO ₄ , pulse mode of 5 s on/2 s off and 150 min reaction time.	67
Figure 4.3: Effects of H ₂ SO ₄ loading on extraction efficiency, esterification efficiency and FAME purity at n-hexane to methanol volume ratio of 3:1, 60% ultrasonic amplitude, pulse mode of 5 s on/2 s off and 150 min reaction time.	70

Figure 4.4: Effect of particle size on extraction efficiency, esterification efficiency and FAME purity at n-hexane to methanol volume ratio of 1.5:1, 5 vol.% H ₂ SO ₄ , 60% ultrasonic amplitude and reaction time of 60 min.....	72
Figure 4.5: Effect of n-hexane to methanol volume ratio on extraction efficiency, esterification efficiency and FAME purity at particle size of 1–2 mm, 5 vol.% H ₂ SO ₄ , 60% ultrasonic amplitude and reaction time of 60 min.	74
Figure 4.6: Effect of H ₂ SO ₄ loading on extraction efficiency, esterification efficiency and FAME purity at particle size of 1–2 mm, n-hexane to methanol volume ratio of 3:1, 60% ultrasonic amplitude and reaction time of 60 min.....	75
Figure 4.7: Effect of various reaction times and ultrasonic amplitudes on extraction efficiency at particle size of 1–2 mm, n-hexane to methanol volume ratio of 3:1, 5 vol.% H ₂ SO ₄	77
Figure 4.8: Effect of various reaction times and ultrasonic amplitudes on esterification efficiency at particle size of 1–2 mm, n-hexane to methanol volume ratio of 3:1, 5 vol.% H ₂ SO ₄	78
Figure 4.9: Effect of various reaction times and ultrasonic amplitudes on FAME purity at particle size of 1–2 mm, n-hexane to methanol volume ratio of 3:1, 5 vol.% H ₂ SO ₄	78
Figure 4.10: FESEM images of raw de-oiled <i>Jatropha</i> seeds at magnification of (a) 500× (b) 1000× and ultrasonic esterified <i>Jatropha</i> seeds at magnification of (c) 500× (d) 1000×.	81
Figure 4.11: FTIR spectra of <i>Jatropha</i> seeds (a) before and (b) after ultrasound assisted in-situ esterification.....	83
Figure 4.12: TGA curves of raw <i>Jatropha</i> seeds and ultrasonic esterified <i>Jatropha</i> seeds.	84
Figure 4.13: Elemental analyses of raw <i>Jatropha</i> seeds and ultrasonic esterified <i>Jatropha</i> seeds.	85
Figure 4.14: Effect on KOH loading on FAME purity and biodiesel yield at methanol to esterified oil molar ratio of 12:1, amplitude of 60% and reaction time of 15 min.....	86
Figure 4.15: Effect of methanol to esterified oil molar ratio on FAME purity and biodiesel yield at KOH loading of 1.5 wt.%, ultrasonic amplitude of 60% and reaction time of 15 min.	87
Figure 4.16: Effect of various reaction times and ultrasonic amplitudes on FAME purity at methanol to esterified oil molar ratio of 12:1 and KOH loading of 1.5 wt.%.....	89

Figure 4.17: Effect of various reaction times and ultrasonic amplitudes on biodiesel yield at methanol to esterified oil molar ratio of 12:1 and KOH loading of 1.5 wt.%..... 90

University of Malaya

LIST OF TABLES

Table 2.1: Comparison between different biodiesel production approaches.	11
Table 2.2: Biodiesel conversion or yields at optimum conditions by employing two-step homogeneous ultrasound assisted transesterification.	21
Table 2.3: Optimum reaction conditions for ultrasound assisted interesterification of non-edible oil.....	24
Table 2.4: Effect of methanol to oil molar ratio on ultrasound assisted homogeneous and heterogeneous base-catalysed transesterification.....	28
Table 2.5: Effect of catalyst loading on ultrasound assisted homogeneous and heterogeneous base-catalysed transesterification.....	31
Table 2.6: Reaction time needed by employing ultrasonic cavitation and conventional stirring.	33
Table 2.7: Comparison of biodiesel yield or conversion of different feedstocks using ultrasound and conventional stirring approaches.	42
Table 3.1: List of equipment for fuel properties tests.	56
Table 4.1: Properties of <i>Jatropha</i> biodiesel in comparison to standards	90
Table 4.2: Comparison of <i>Jatropha</i> biodiesel properties with existing literatures using ultrasonication technique.	94
Table 4.3: Comparison between ultrasound technique and conventional magnetic stirring approach.	95
Table 5.1: Volume of H ₂ SO ₄ required at various H ₂ SO ₄ loadings.....	120
Table 5.2: Mass of KOH required at various KOH loadings.....	121
Table 5.3: Volume of methanol required to prepare different molar ratios of methanol to esterified <i>Jatropha</i> oil	122

LIST OF SYMBOLS AND ABBREVIATIONS

ASTM	: American Society for Testing and Materials
AV	: Acid value
C	: Carbon
Ca	: Calcium
CaDG	: Calcium diglyceroxide
CaO	: Calcium oxide
CO	: Carbon monoxide
CO ₂	: Carbon dioxide
DTA-TG	: Differential thermal analysis-thermogravimetry
E_a	: Activation energy
FAME	: Fatty acid methyl ester
FESEM	: Field emission scanning electron microscopy
FFA	: Free fatty acid
FID	: Flame ionization detector
FTIR	: Fourier-transform infrared spectroscopy
GC	: Gas chromatography
GDP	: Gross domestic product
GHG	: Greenhouse gas
H	: Hydrogen
H ₂ SO ₄	: Sulphuric acid
HCl	: Hydrochloric acid
HC	: Hydrocarbon
HNO ₃	: Nitric acid
ICP-MS	: Inductively coupled plasma mass spectrometry

IS	: Internal standard
K	: Potassium
KBr	: Potassium bromide
KOH	: Potassium hydroxide
K ₃ PO ₄	: Tripotassium phosphate
KH ₂ PO ₄	: Monopotassium phosphate
K ₂ HPO ₄	: Dipotassium phosphate
Mg	: Magnesium
Mg/Al	: Magnesia-alumina
MOF	: Metal organic framework
N	: Nitrogen
Na	: Sodium
NaOH	: Sodium hydroxide
O	: Oxygen
P	: Potassium
PTA	: Phosphotungstic acid
SO ₂ Cl ₂	: Sulfuryl chloride
SO _x	: Sulphur oxides
THF	: Tetrahydrofuran
TGA	: Thermal gravimetric analysis
TPA/AC	: Tungstophosphoric acid/activated carbon
TPA/Al	: Tungstophosphoric acid/gamma alumina
TPA/Cs	: Tungstophosphoric acid/cesium
TPEC	: Total primary energy consumption
WCO	: Waste cooking oil
XRD	: X-ray powder diffraction

LIST OF APPENDICES

Appendix A: Calculations for H_2SO_4	120
Appendix B: Calculations for KOH	121
Appendix C: Calculations for methanol.....	122

University of Malaya

CHAPTER 1: INTRODUCTION

1.1 Background

The increasing population and modernization has led to increment in the world's daily total primary energy consumption (TPEC). In 2015 itself, the world's TPEC stood at 150 million GWh with an expected increment of 57% by the year 2050 (Figure 1.1). Currently, fossil fuels contribute over 80% of the world's total energy utilisation (Hajjari *et al.*, 2017). The dramatic growth of energy consumption will eventually result in higher greenhouse gas (GHG) emissions from the combustion of fossil fuel, leading to global warming and climate change as well as air pollution problems all over the world (Asif *et al.*, 2017a; Mohod *et al.*, 2017). Escalating environmental problems and health concerns pinned with extensive utilisation of fossil fuel have spurred the quest for renewable and environmentally benign biofuels. Meanwhile, biodiesel is a potential renewable energy to curb the global warming arising from the over-dependence on fossil fuel. In addition, energy crisis due to the over-exploitation of fossil fuels can be avoided with the utilisation of biodiesel.

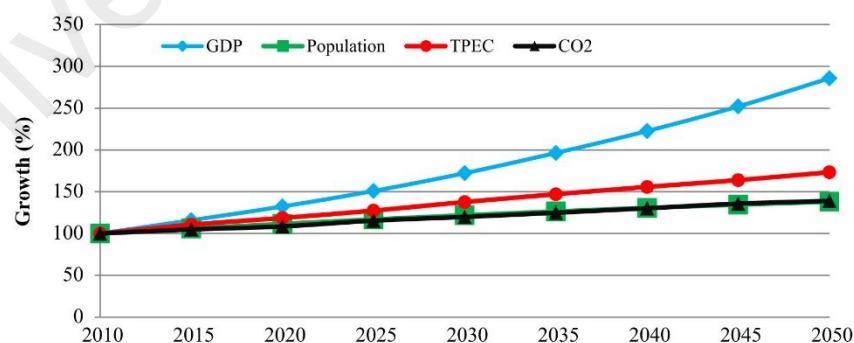


Figure 1.1: Estimated global gross domestic product (GDP), population, TPEC, and carbon dioxide (CO₂) emissions trends from 2010 to 2050 (Hajjari *et al.*, 2017).

Biodiesel can be defined as a liquid fuel comprising of mono alkyl ester of long-chain fatty acid (Figure 1.2). Theoretically, it is a sustainable source of liquid transportation fuel as it can be produced from a variety of feedstocks such as virgin vegetable oils, non-edible vegetable oils, waste vegetable oils and animal fats. Biodiesel is a promising substitute for diesel because it has various environmental benefits. Biodiesel has negligible sulphur and aromatics content and has about 11% built-in oxygen content, which helps it to undergo complete combustion (Parida *et al.*, 2016). Therefore, it tends to produce less smoke and particles during combustion, resulting in lower emissions of harmful pollutants such as particulates, carbon monoxide (CO), unburned hydrocarbons (HCs) and sulphur oxides (SO_x) (Lee *et al.*, 2014; Thanh *et al.*, 2010). By utilising biodiesel compared to diesel, the emission of particulates, CO, unburned HCs and SO_x would be lowered by 40, 44, 68 and 100%, respectively (Talebian-Kiakalaieh *et al.*, 2013). In contrast, diesel fuel does not contain any oxygen (Manickam *et al.*, 2014). The sulphur content in the diesel fuel contributes to the formation of SO_x and H₂SO₄, which lead to acid rain. The aromatic compounds in the diesel fuel contribute to particulate emissions and are considered toxic and carcinogenic. Benzene, toluene, ethylbenzene, and o-, m-, p-xylene, popularly known as BTEX compounds, are well documented carcinogenic compounds emitted from the exhaust of a diesel-powered compression ignition engine (Singh *et al.*, 2011). Furthermore, biodiesel can be directly used in a commercial diesel engine without any modifications due to its diesel-like properties (Chuah *et al.*, 2016b).

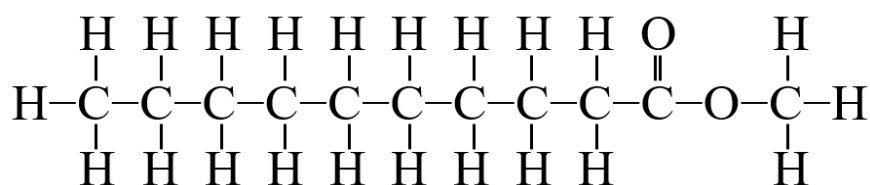


Figure 1.2: Molecular structure of biodiesel.

Common biodiesel feedstocks include edible oils (e.g. canola, soybean, sunflower and palm oils), non-edible oils (e.g. *Jatropha curcas*, *Calophyllum inophyllum*, and *Hevea brasiliensis* oils), waste oils as well as animal fats (e.g. chicken fat, beef tallow and poultry fat) (Dharma *et al.*, 2016b). 95% of the current world biodiesel production is derived from edible vegetable oils. Consumption of expensive edible oil for biodiesel production has led to the price of biodiesel to increase to 1.5 to 2-fold higher than diesel fuel. Moreover, non-edible oil plants can be grown all around the world regardless of weather and land conditions with relatively lower cost and high product yield (Asif *et al.*, 2017b; Chuah *et al.*, 2016b). Therefore, cheaper non-edible feedstocks such as *Jatropha curcas* are preferable in biodiesel production in order to alleviate the food crisis arising from the utilisation of edible feedstocks (Chuah *et al.*, 2016b; Koh & Ghazi, 2011; Su, 2013).

Transesterification is the most common process to produce biodiesel in the presence of alkali, acid or enzyme as catalyst. Mixing is a very crucial step in transesterification reaction as alcohol and oil are immiscible, resulting in limited mass transfer between the two phases (Ji *et al.*, 2006). Mechanical stirring is often used during transesterification process to improve the contact between the two phases with the assistance of external heating but it is costly since excessive energy is needed while consuming longer reaction time (Chuah *et al.*, 2016b). Higher molar ratio of alcohol to oil is also required since transesterification process is a reversible reaction. Ultrasonication appears to be a promising approach as it can be applied to improve the mixing, mass and heat transfer between different phases in transesterification reaction without heating requirement (Maddikeri *et al.*, 2012). Several researchers had also reported that ultrasonic irradiation could help to speed up transesterification reaction, increase reaction efficiency, shorten the phase separation time of glycerol and reduce the amount of alcohol, catalyst, cost and

energy required to produce biodiesel (Chuah *et al.*, 2016b; Gole & Gogate, 2012; Kumar *et al.*, 2012; Tan *et al.*, 2019; Thanh *et al.*, 2010).

The conventional production of biodiesel from oilseeds includes various steps such as oil extraction, purification (degumming, deacidification, dewaxing, dephosphorization, dehydration, etc.) followed by the esterification/transesterification process. These oil refining processing stages constitutes to over 70% of the total production costs of biodiesel (Haas *et al.*, 2006). Therefore, the combination of these processes into a single step reactive extraction is able to significantly reduce the production cost. Reactive extraction can also be known as in-situ transesterification in which the oil bearing material is in direct contact with an alcohol solution in the presence of a catalyst at ambient temperature and pressure conditions. Alcohol will have two functions in this process, acting as an extracting solvent and esterification reagent, thus combining both the oil extraction and transesterification processes into one single step (Veljković *et al.*, 2012). In other words, the oil extracted out from the seeds will be converted to esters instantaneously (Banković-Ilić *et al.*, 2012). This technique disregards the need for isolation and further refining of seed oils. Consequently, the biodiesel production process could reduce the expensive costs employed for the oil extraction and degumming while at the same maximizing the biodiesel yield up to 98% (Baskar & Aiswarya, 2016; Veljković *et al.*, 2012).

1.2 Problem statement

Although it had been proven that reactive extraction or in-situ transesterification could conduct oil extraction and transesterification of oil into biodiesel in a single step, in-situ esterification should be performed first in the case of utilising *Jatropha* oilseeds containing high AV in order to avoid saponification side reaction. By incorporating ultrasound in the reaction, it is also necessary to understand the fundamental process of

ultrasound assisted in-situ esterification on *Jatropha* seeds. However, there were only few studies (Chadha *et al.* (2012), Zahari *et al.* (2014b), Koutsouki *et al.* (2015) and Kumar (2017)) which had conducted on ultrasound assisted in-situ transesterification directly from non-edible oilseeds and there is no publication reporting on ultrasound assisted in-situ esterification of non-edible oilseeds to date. Therefore, considerable effort is required to understand the effect of reaction parameters on in-situ esterification coupled with ultrasound. Furthermore, it is also important to bear in mind that reaction parameters are raw material dependent which implies that optimal process conditions must be established independently for new types of raw material.

1.3 Significance of the study

This study provided findings on improvements achieved by ultrasound technology and revealed it as a viable alternative in biodiesel production. Detailed information of the influence of each reaction parameters on ultrasound assisted in-situ esterification and ultrasound assisted transesterification were successfully investigated specifically to *Jatropha* oilseeds. The findings obtained would be useful for other types of non-edible oilseeds in the similar processes. Furthermore, utilisation of non-edible *Jatropha* oilseeds directly as feedstock in conjunction with ultrasound could avoid the dependency on edible feedstock and eliminated several energy intensive stages such as oil extraction and solvent recovery steps as well as due to the absence of external heating and agitation.

1.4 Aim and research objectives

The present study aims to produce biodiesel with satisfactory FAME purity ($\geq 96.5\%$) via two-step ultrasound assisted in-situ esterification and ultrasound assisted transesterification by directly utilising non-edible *Jatropha* oilseeds containing high AV as feedstock. In order to achieve this aim, the following objectives must be achieved:

- i. To investigate the feasibility of ultrasound assisted in-situ esterification in extracting oil from non-edible *Jatropha* oilseeds while reducing the AV of the extracted *Jatropha* oil to acceptable limit (>3 wt.% FFA) for subsequent ultrasound assisted transesterification.
- ii. To investigate the effect of parameters for ultrasound assisted in-situ esterification (ultrasonic pulse mode, particle size, n-hexane to methanol volume ratio, H_2SO_4 loading, reaction time and ultrasonic amplitude).
- iii. To identify the parameters relationships for ultrasound assisted transesterification (KOH loading, methanol to esterified oil molar ratio, reaction time and ultrasonic amplitude) towards biodiesel yield and FAME purity.
- iv. To characterize *Jatropha* oilseeds before and after ultrasound assisted in-situ esterification and the fuel properties of the biodiesel produced.

1.5 Outline of research work

There were three main sections in this research study which included the production of esterified oil from *Jatropha* seeds via ultrasound assisted in-situ esterification, subsequent transesterification of the esterified oil with ultrasound assistance and analysis on the fuel characteristics of the biodiesel produced.

In the ultrasound assisted in-situ esterification, the oil bearing materials (*Jatropha* seeds) contacted directly with solution containing methanol, n-hexane and H_2SO_4 at ambient temperature and pressure before undergo sonication. Methanol acts as an extractant and an esterification reagent, producing biodiesel from oilseeds in a single step. N-hexane was used as a co-solvent to increase oil solubility in the reaction mixture (Shuit *et al.*, 2010a) and concentrated H_2SO_4 was utilised as catalyst as crude *Jatropha* oil usually contains more than 2% FFA. During sonication, bubble formation and collapse

of the cavities at elevated temperature and pressure occurs in a very short time. The asymmetric collapse of these cavities resulted in violent shock waves and high-speed jets being generated. These shock waves impacted the seed surface, which created surface damage such as cracks, crevices, and microfractures. At the same time, surface peeling, erosion and particle breakdown also occur due to impingement by high-speed jets. Due to these, the solvent could easily penetrate the plant's cell wall into cell tissues, accelerated the extraction of oil bodies and permitted the release of oil bodies into the external environment (solvent phase) (Jadhav *et al.*, 2016; Shirsath *et al.*, 2012). Once the oil bodies were being extracted, they would be converted to biodiesel simultaneously (Shuit *et al.*, 2010a). The parameters which would be investigated in the ultrasound assisted in-situ esterification are ultrasonic pulse mode, particle size, n-hexane to methanol volume ratio, H₂SO₄ loading, reaction time and ultrasonic amplitude. The esterified oil with the optimum esterification and extraction efficiencies and FAME purity was then subjected to transesterification in order to increase the FAME purity further.

In the ultrasound assisted transesterification, the esterified *Jatropha* oil would be loaded into solution containing methanol and KOH. In the presence of two immiscible liquids (oil and methanol), ultrasound formed fine emulsions, thereby increasing the reaction surface area between the two phases. The cavitation might also lead to a localized increment of temperature at the phase boundary. As a consequence, both mass transfer rates and overall reaction rate were expected to increase (Boffito *et al.*, 2014). The parameters examined would be KOH loading, methanol to esterified oil molar ratio, reaction time and ultrasonic amplitude. Lastly, fuel characteristics such as AV, FAME purity, density, calorific value, flash point, kinematic viscosity, oxidation stability, copper strip corrosion, group I metals: sodium (Na) + potassium (K) and group II metals: calcium (Ca) + magnesium (Mg)) of the biodiesel produced would be assayed.

1.6 Thesis outline

This thesis is structured into five chapters accordingly. Chapter 1 presents a brief introduction of the research background, problem statements, significance of the study, aim and research objectives, research framework and lastly an overview of the thesis. Chapter 2 presents a review of different approaches in biodiesel production. Moreover, this chapter also explains the effects of various parameters in the esterification and transesterification processes assisted by ultrasound. Chapter 3 describes the research methodology of ultrasound assisted in-situ esterification and ultrasound assisted transesterification in details. Chapter 4 presents the experimental results and the discussion of the effects of various parameters on the esterified oil and biodiesel produced, respectively. Brief summary of the results is provided at the end of Chapter 4. Chapter 5 concludes this research with the presentation of key findings and recommendations for future work.

CHAPTER 2: LITERATURE REVIEW

2.1 Biodiesel synthesis

There are several other transesterification techniques to produce biodiesel such as non-catalytic supercritical method, biox process, microwave, membrane technology, reactive distillation and ultrasonication. Non-catalytic supercritical method does not require catalyst, thus it does not face the disadvantages encountered in the catalysed route such as the necessity of treating the free fatty acids (FFAs) and triglycerides in different reaction stages, the inhibitory effects of water molecules present in the mixture, catalyst consumption, separation of the catalyst from the product mixture, low glycerol purity, and generation of waste water. However, it is an energy intensive and economic infeasible process because it requires high operating temperature (553–673 K) and pressure (10–30 MPa) as well as high methanol-to-triglycerides molar ratio up to 42:1 (Aransiola *et al.*, 2014). For biox process, it employs co-solvents such as tetrahydrofuran (THF) to solubilize methanol for faster reaction. THF is commonly used due to its boiling point (66°C) is similar to methanol (64.7°C) which allows the removal of excess solvents in a single step once the reaction is completed (Meira *et al.*, 2014; Monisha *et al.*, 2013). This process is capable to convert oil containing high FFA content (more than 10%) into biodiesel and can be conducted under ambient temperature and pressure. However, economical barrier arises due to their close proximity of boiling point between methanol and co-solvent which makes the product separation to be very challenging (Badday *et al.*, 2012). In addition, complete removal of co-solvent from both the glycerol and biodiesel is compulsory due to its hazardous and toxicity natures (Abbasi & Diwekar, 2014; Singh, 2014). Comparing to conventional transesterification, microwave method requires about 23 times lower energy consumption. This is because microwave energy is transmitted directly to the reactant, thus eliminating the preheating step. Furthermore, microwave

process has more effective heat transfer system than conventional method. Conventional method transfers heat to the reaction via thermal heat reflux whereas microwave transfers energy in the form of electromagnetic wave (Talebian-Kiakalaieh *et al.*, 2013). Nonetheless, low penetration depth of microwave radiation into the absorbing materials limits the scaled-up to industrial scale (Vyas *et al.*, 2010). On the other hand, membrane technology integrates reaction and separation into one step, thus minimizing separation costs and recycling requirements. However, membrane technology still requires further downstream purification since the FAME-rich phase will still contain methanol, glycerol and water (Aransiola *et al.*, 2014; Saleh *et al.*, 2010). For reactive distillation, it is advantageous for esterification process especially when dealing with high FFA feedstocks. Compared to the conventional method, it does not require excess alcohol due to the continuous removal of by-product (water) and is able to reduce the alcohol usage by 66% (Aransiola *et al.*, 2014; Oh *et al.*, 2012). Even though reactive distillation process has less number of connections between instruments (due to smaller amount of equipment) which reduces the safety issues (Mohapatra *et al.*, 2016), the requirement for reboiler and condenser will increase the capital investment and operating costs tremendously (Kiss, 2009). Among the emerging transesterification techniques, ultrasonication appears to be a promising approach as it can enhance mixing, heat and mass transfer between different phases in alcoholysis process (Maddikeri *et al.*, 2012). Consequently, it can reduce the operating cost and energy consumption as it has lower requirement on alcohol to oil molar ratio, catalyst amount and reaction time as well as no external heating requirement. In addition, phase separation of biodiesel from glycerol is simpler with shorter separation time. An overview of the advantages, disadvantages and recommendations of various emerging biodiesel production approaches is tabulated in Table 2.1.

Table 2.1: Comparison between different biodiesel production approaches.

Methods	Description	Advantages	Disadvantages	Recommendations	References
Non-catalytic supercritical method	Biodiesel production in which transesterification occurs by an alcohol at supercritical conditions (high temperature and pressure) without catalyst.	<ul style="list-style-type: none"> • Requires no catalyst. • Achieves near complete conversion in a relatively short time (2–4 min). 	<ul style="list-style-type: none"> • Requires high operating temperature (553–673 K) and pressure (10–30 MPa) resulting in much higher heating and cooling costs. • Requires high methanol-to-triglycerides molar ratio up to 42:1. 	<p>Addition of co-solvents such as carbon dioxide (CO₂), hexane, propane, calcium oxide (CaO) and subcritical alcohol to reduce the reaction temperature, pressure and the amount of alcohol.</p> <p>*The supercritical condition of CO₂ is 304 K and 7.38 MPa which it is lower than the supercritical methanol conditions (512 K and 8.09 MPa).</p>	Helwani <i>et al.</i> , 2009; Koh & Ghazi, 2011; Maddikeri <i>et al.</i> , 2013; Mohapatra <i>et al.</i> , 2016
Biox process	Non-catalytic biodiesel production with the use of co-solvent (usually tetrahydrofuran, THF) that generates one phase oil-rich system.	<ul style="list-style-type: none"> • Short reaction time. • Able to handle feeds with high FFA. • Recovery of both the excess alcohol and the THF co-solvent in a single step. • Absence of catalyst residues in either the biodiesel phase or the glycerol phase. 	<ul style="list-style-type: none"> • Completely removal of co-solvent is compulsory due to its hazardous and toxicity natures. • Residual solvent in the biofuel product can affect the compliance with the international standards. 	–	Badday <i>et al.</i> , 2012

Table 2.1, continued

Methods	Description	Advantages	Disadvantages	Recommendations	References
Microwave	Continuous oscillation of polar ends of molecules or ions by microwave irradiation causes the collision and friction between the moving molecules and generates localized superheating.	<ul style="list-style-type: none"> • Short reaction time (10 times shorter than conventional methods). • Low oil to methanol ratio. • Ease of operation. • Higher quality and yield product. • Drastic reduction in quantity of by-products. 	<ul style="list-style-type: none"> • Not suitable to be used in industrial scale as high microwave output (power) may cause damage to organic molecules (triglycerides) and due to safety aspects. 	Combination effect of microwave (removal of heat transfer barrier and ultrasound (removal of mass transfer barrier) can lead to synergistic effects significantly which overcomes the limitation of low penetration depth. However, this technique leads to high energy consumption for maintaining higher temperature condition which is not applicable for industrial scale.	Islam <i>et al.</i> , 2014; Talebian-Kiakalaieh <i>et al.</i> , 2013; Vyas <i>et al.</i> , 2010)
Reactive distillation	Simultaneous chemical reaction and distillation separation in a single unit.	<ul style="list-style-type: none"> • Simultaneous separation of reactants and products boosts the conversion and improves the selectivity by breaking the reaction equilibrium restrictions. • Eliminates the need for reheating because the heat of vaporization provides the heat of reaction in exothermic reactions. 	<ul style="list-style-type: none"> • Thermal degradation of the products occurs due to a higher temperature profile in the column. 	Reactive absorption could replace reactive distillation as it reduces capital investment and operating costs due to the absence of the reboiler and condenser, higher conversion and selectivity as no products are recycled in the form of reflux or boil-up vapours, as well as no occurrence of thermal degradation of the products due to a lower temperature profile in the column.	Baskar & Aiswarya, 2016; Kiss, 2009; Oh <i>et al.</i> , 2012

Table 2.1, continued

Methods	Description	Advantages	Disadvantages	Recommendations	References
Membrane technology	Combination of reaction and membrane-based separation by taking advantage of the immiscibility of methanol and oil to create a better purification process.	<ul style="list-style-type: none"> Controlled contact of incompatible reactants. Produces FAME-rich products. Eliminates undesired side reactions. 	<ul style="list-style-type: none"> High fabrication cost. Fouling can occur which reduces the effectiveness over time. 	–	Aransiola <i>et al.</i> , 2014; Kiss & Bildea, 2012; Lee <i>et al.</i> , 2014; Oh <i>et al.</i> , 2012; Talebian-Kiakalaieh <i>et al.</i> , 2013
Ultrasonication	Cavitation bubbles are produced by sound waves in a liquid due to pressure variations.	<ul style="list-style-type: none"> Simple reaction setup. Shorter reaction time. Approximately one-third of the energy consumed by mechanical agitation Enhanced conversion. Higher oil extraction yield (30–40% more when compared to the conventional stirring reactor system). Higher quality of glycerol production. 	<ul style="list-style-type: none"> Necessity of downstream processing which increases the purification cost. Reaction temperature is slightly higher for long reactions. Ultrasonic power must be under control due to the soap formation in fast reaction. FAME purity can be reduced by higher frequencies (40 kHz). 	–	Islam <i>et al.</i> , 2014; Maddikeri <i>et al.</i> , 2012; Talebian-Kiakalaieh <i>et al.</i> , 2013; Vyas <i>et al.</i> , 2010

2.2 Ultrasound assisted biodiesel production

Ultrasonic irradiation devices can produce a variety of energy forms, which are shown in Figure 2.1. An ultrasonic probe transforms electrical energy input into heat energy and vibrational energy. The vibrational energy is then transformed into cavitation energy and some of them is lost through sound reflection. Based on the reaction environment and targeted application, the cavitation energy can then be further utilised for its physical, chemical and biological effects (Martinez-Guerra & Gude, 2015). Generally, the beneficial effects of ultrasound on chemical reactions come from the energy produced from the ultrasonic cavitation. Ultrasonic cavitation includes the formation, growth and implosive collapse of bubbles. Expansion and compression waves present during the introduction of ultrasound result in negative and positive pressure points. These fluctuations generate bubbles which are then filled with solvent, solute vapour and dissolved gases. These bubbles will then undergo growth and recompression (Veljković *et al.*, 2012). The cavitation bubbles often break down after approximately 400 μ s (Badday *et al.*, 2012). During the cavitation bubble collapse, extremely high local heating and pressure points enhance the mass and heat transfer within the reaction medium (Veljković *et al.*, 2012).

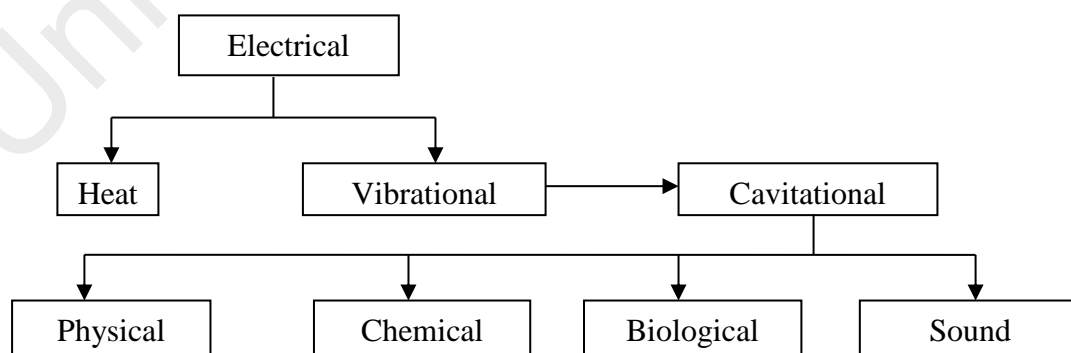


Figure 2.1: Energy forms and their corresponding effects in ultrasonic application.

In heterogeneous liquid reaction systems, ultrasound can render physical and chemical effects simultaneously through cavitation bubbles. The former emulsifies immiscible reactants by micro-turbulence produced by the cavitation bubbles' radial motion, subsequently increasing the interfacial area and reaction rate. The latter enhances the chemical reaction due to free radicals produced with the sudden collapse of cavitation bubbles.

The physical effect of ultrasound on transesterification reaction had been discussed by quite a number of researchers. In transesterification reaction, ultrasonic irradiation causes bubble cavitations near the alcohol-oil phase boundary, thus producing large amount of micro bubbles. Some bubbles are stable for the next cycle while the rest will be subjected to violent collapse upon expanding to certain critical size. The asymmetric collapse of the cavitation bubbles generates micro-turbulence and cause disruption at the phase boundary. Micro jets generated from the liquid impingement can reach to a speed up to 200 m/s, creating intimate mixing of the immiscible reactants near the phase boundary and thus induce emulsification. With the formation of such emulsion, the interfacial region and mass transfer between the alcohol and oil phases increases, thus the reaction kinetics will become faster (Badday *et al.*, 2012; Choudhury *et al.*, 2014; El-Ibiari *et al.*, 2014; Gogate *et al.*, 2006; Veljković *et al.*, 2012). According to He and Van Gerpen (2012), the formation and bursting of micro bubbles caused by ultrasonic cavitations intensified the local energy transfer and energized the reactant molecules, thus enhanced the overall reaction rate. The ultrasound is able to provide the mechanical energy for mixing and the activation energy (E_a) required for the transesterification process (Hajinezhad *et al.*, 2015). High local temperatures (≥ 5000 K) and pressures (≥ 1000 atm) (Mahamuni & Adewuyi, 2009) would be generated from the continuous compressions and rarefactions which then provided intense mixing for the immiscible reactants. This phenomenon automatically increased the reaction temperature with disruption of the

microbubbles which thus increased the heat and mass transfer in the medium and promoted the desired chemical reactions (Gude & Grant, 2013; Hong *et al.*, 2014; Kumar *et al.*, 2010b). Therefore, employment of ultrasound in the production of biodiesel eliminates the requirement of external agitation and heating because of the formation of micro jets and increment of localized temperature. For the chemical effect of ultrasound, highly reactive species such as $\text{OH}\cdot$, $\text{HO}_2\cdot$ and $\text{H}\cdot$ radicals are produced from the dissociation of solvent vapour trapped in the bubble during a transient implosive collapse of bubbles, which can help to accelerate the chemical reaction (Choudhury *et al.*, 2014; Mahamuni & Adewuyi, 2009).

2.2.1 Ultrasound assisted homogeneous alkaline-catalysed transesterification

Alkaline-catalysed transesterification is commonly applied in the production of biodiesel since alkaline catalysts can catalyse transesterification process faster than acid catalysts (Ho *et al.*, 2016). Alkaline metal alkoxides and hydroxides are most frequently used alkaline catalysts for ultrasound assisted transesterification. At low catalyst concentration (0.5 mol%), the former was capable of achieving significantly high yields (>98%) in short reaction times (30 min). Therefore, alkaline metal alkoxides were appraised as the most active catalysts (Ejikeme *et al.*, 2010). KOH and sodium hydroxide (NaOH) are the most commonly used alkaline metal hydroxides. They are normally inexpensive and able to catalyse at low reaction temperatures (from room temperature to around 333 K) as well as complete reaction in short reaction time (30 min) (Encinar *et al.*, 2002; Hara, 2009). On top of that, high conversion rate is achieved without intermediate steps (Leung *et al.*, 2010).

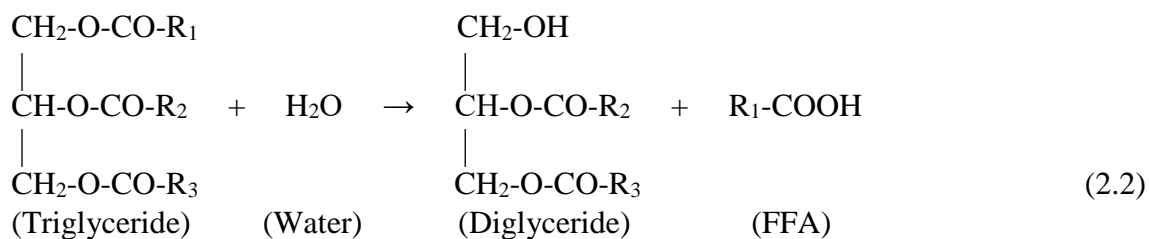
By employing ultrasound in alkaline-catalysed transesterification, cavitation events help to eliminate mass transfer resistance between immiscible reactants which then accelerate the chemical reaction. The E_a is also reduced which enables the reaction to be

conducted at room temperature (Yang *et al.*, 2011). In addition, homogeneous alkaline-catalysed transesterification assisted by ultrasound requires lower alcohol to oil molar ratio, catalyst amount, reaction temperature and energy consumption as well as shorter reaction time and phase separation time while attaining higher biodiesel yield as compared to those without ultrasound. The detailed beneficial effects of ultrasound could be found in Section 2.3.

Nonetheless, alkaline-catalysed transesterification only can be employed if the feedstock has FFA level less than 2 wt.%, which corresponds to AV of 4 mg KOH/g (Kumar *et al.*, 2010a). Oil containing high FFA cannot be transesterified directly using alkaline catalyst as the FFA reacts quickly with the alkaline catalyst through saponification side reaction which is presented in Equation 2.1 to produce soap and water. Excessive soap formation tends to gel-up the reaction mixture as solidification of soap tends to occur at ambient temperature (Lam *et al.*, 2010). The soap formed binds with the catalyst and partially consumes it and hence a higher cost will be incurred (Leung *et al.*, 2010). Consequently, viscosity of the reaction mixture increases which then interferes with the separation of ester from glycerol. This will reduce the biodiesel conversion and yield as well as increases the product separation cost (Chuah *et al.*, 2016b; Ramadhas *et al.*, 2005).

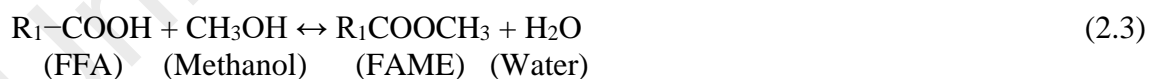


Furthermore, high percentage of water content in feedstock oil is also undesirable. The alkaline homogeneous catalysts must be handled properly as they are highly hygroscopic and tend to absorb water from air during storage. They can also form water when dissolved in the alcohol reactant (Leung *et al.*, 2010). Water can hydrolyse triglycerides to diglycerides and forms more FFA, with subsequent soap formation which is detrimental to the biodiesel yield. The hydrolysis reaction is presented in Equation 2.2 (Leung *et al.*, 2010).



2.2.2 Ultrasound assisted homogeneous acid-catalysed transesterification

For oil or fat containing high FFA content (>2 wt.%), it was reported that acid-catalysed transesterification performed better than base-catalysed transesterification as acid catalysts could catalyse both esterification and transesterification concurrently. This was because acid could act as esterification reagent and solvent at the same time. Unlike base-catalysed transesterification, there is no soap formation in the presence of acid catalyst (Talebian-Kiakalaieh *et al.*, 2013; Veljković *et al.*, 2012). Acid-catalysed transesterification has higher tolerance towards moisture content of feedstock, which could otherwise trigger the hydrolysis of esters resulting in regeneration of fatty acids (Leung *et al.*, 2010). For oil or fat with FFA less than 2 wt.%, the kinetic rate of homogeneous acid-catalysed transesterification was about 4000 times lower than homogeneous base-catalysed reaction which rendered it unfavourable in commercial applications (Yin *et al.*, 2012). Production of FAME through the reaction between FFA and methanol is presented in Equation 2.3.



H₂SO₄ is generally used as a catalyst in the homogeneous acid-catalysed transesterification because of its acid strength which is responsible for releasing more H⁺ species to protonate the carboxylic moiety of the fatty acid (Santos *et al.*, 2010). It was found out that mechanical stirring is not a feasible approach for homogeneous acid-catalysed transesterification as it requires high reaction temperature (343–473 K), high pressure (6–10 bar) and long reaction time (> 48 h). Biphasic nature of the reaction system

is the main cause for slow kinetics of homogeneous acid-catalysed transesterification which affects the catalyst accessibility to the triglyceride molecules. Although reaction kinetics could be improved by increasing alcohol to oil molar ratio (20:1 to 45:1) and acid concentration (≈ 5 wt.%), it is not practical for large scale process as higher operating cost incurred from the highly usage of alcohol amount and reactor corrosion from the higher acid concentration (Parker *et al.*, 2012). Therefore, ultrasound is a practical approach to increase the miscibility of the biphasic nature of the reaction system through the cavitation events.

Currently, researches on the homogeneous acid-catalysed transesterification of non-edible oil under ultrasonic irradiation condition were still limited. So far, only Choudhury *et al.* had conducted transesterification of *Jatropha* oil using H_2SO_4 (Choudhury *et al.*, 2013) and chlorosulfonic acid (Choudhury *et al.*, 2014) with the aid of ultrasonication. In their study, biodiesel yield of 80.12% was successfully obtained at optimum conditions of methanol to oil molar ratio of 7, catalyst concentration of 6 wt.%, temperature of 343 K and reaction time of 2 h. Simultaneous esterification/transesterification with sonication did not succeed due to formation of water in the esterification step, and sonication alone could not overcome this obstacle (Choudhury *et al.*, 2013). In order to overcome the inability of H_2SO_4 to carry out esterification/transesterification simultaneously, Choudhury *et al.* (2014) had utilised chlorosulfonic acid as catalyst instead. Chlorosulfonic acid possessed superior ability as it was capable to catalyse both esterification and transesterification reactions. Furthermore, chlorosulfonic acid also counteracted inhibition caused by water formed during esterification, which was the cause for very slow kinetics of acid catalysed transesterification. With the usage of chlorosulfonic acid, 93% of *Jatropha* biodiesel yield was achieved at optimum conditions of 8.5 wt.% catalyst, 20:1 methanol to oil molar ratio, temperature of 331 K and reaction

time of 4 h. The activation energy, E_a for the process (57 kJ/mol) was at least 3 times lower than H_2SO_4 catalysed transesterification.

Apart from chlorosulfonic acid, suluryl chloride (SO_2Cl_2) is also able to catalyse both esterification and transesterification reactions concurrently. It had been employed in the preparation of biodiesel from *Daturametel Linn* oilseeds containing high FFA content using ultrasonic cleaning bath (40 kHz, 130 W) (Mathiarasi & Partha, 2016). Strong acids such as hydrochloric acid (HCl) and H_2SO_4 were formed through the vigorous reaction between water molecules in *Daturametel Linn* oil and SO_2Cl_2 under intense mixing. The maximum biodiesel yield of 95.5% was attained at 8.0 wt % SO_2Cl_2 , 7:1 methanol to oil molar ratio and temperature of 318 K with reaction time of 2 h.

2.2.3 Two-step homogeneous ultrasound assisted transesterification

High initial acid content in non-edible oil will hamper transesterification approach using alkaline catalysts due to the soap formation. On the other hand, acid catalyst can catalyse non-edible feedstock containing high AV but with lower reaction rate. Therefore, a two-step esterification and transesterification process is an efficient approach to address the undesirable saponification side reaction and slow reaction rate while improving the biodiesel conversion or yield. The feedstock was usually first treated with acid catalysts to reduce FFA content to below 2 wt.%, followed by transesterification with alkaline catalysts. With the assistance of ultrasound in biodiesel production, the processing cost can be greatly reduced due to lower amount of methanol and operating temperature needed, compared to the conventional two-stage approach (Bahadur *et al.*, 2015b; Gole & Gogate, 2012; Worapun *et al.*, 2012). Biodiesel conversion or yield from different feedstocks at optimum conditions by employing two-step homogeneous ultrasound assisted transesterification is summarized in Table 2.2. High biodiesel conversion or yield (92.72–98.01%) can be achieved as observed from Table 2.2.

Table 2.2: Biodiesel conversion or yields at optimum conditions by employing two-step homogeneous ultrasound assisted transesterification.

Year	Ultrasonic reactor type	Frequency (kHz); Power (W)	Feedstock	Reaction conditions	Biodiesel conversion (%)	Yield (%)	References
2015	Direct sonication (horn)	20; 200	Neem oil	1 st step: methanol to oil (0.45 vol%), 0.75 vol% H ₂ SO ₄ , 333 K, 10 min 2 nd step: methanol to oil (0.2 vol%), 1.2% KOH, 333 K, 10 min	–	98.01	Bahadur <i>et al.</i> , 2015a
2015	Direct sonication (horn)	20; 400	Neem oil	1 st step: methanol to oil (6:1), 3 wt.% H ₂ SO ₄ , 303 K, 30 min 2 nd step: methanol to oil (7:1), 1.2% KOH, 323 K, 30 min	92.72	–	Prakash Maran & Priya, 2015
2015	Direct sonication (horn)	20–30; 1000	Mahua oil	1 st step: methanol to oil (0.35 mol%), 1 vol% H ₂ SO ₄ , 323 K, 5 min 2 nd step: methanol to oil (1.5 mol%), 0.75% KOH, 323 K, 5 min	–	97.4	Bahadur <i>et al.</i> , 2015b
2016	Direct sonication (horn)	28; 50	<i>Nerium oleander</i> oil	1 st step: methanol to oil (0.4 vol%), 1 vol% H ₂ SO ₄ , 328 K, 10–15 min 2 nd step: methanol to oil (0.2 vol%), 1 v/w% KOH, 328 K, 10–15 min	–	97	Yadav <i>et al.</i> , 2016a

2.2.4 Ultrasound assisted interesterification

Interesterification is different from transesterification in term of acryl acceptor used and the by-product produced. In biodiesel synthesis via interesterification process catalysed by base catalyst, alkyl acetate will replace alcohol as acryl acceptor which then produces a short chain triglyceride instead of glycerol. For instance, triacetin is yielded as by-product instead of glycerol when methyl acetate is used during interesterification (Tian *et al.*, 2018). The interesterification reaction is shown in Figure 2.2 (Maddikeri *et al.*, 2013). In interesterification reaction catalysed by acid catalyst, FFA in vegetable oil reacts with methyl acetate to form biodiesel and acetic acid (dos Santos Ribeiro *et al.*, 2017).

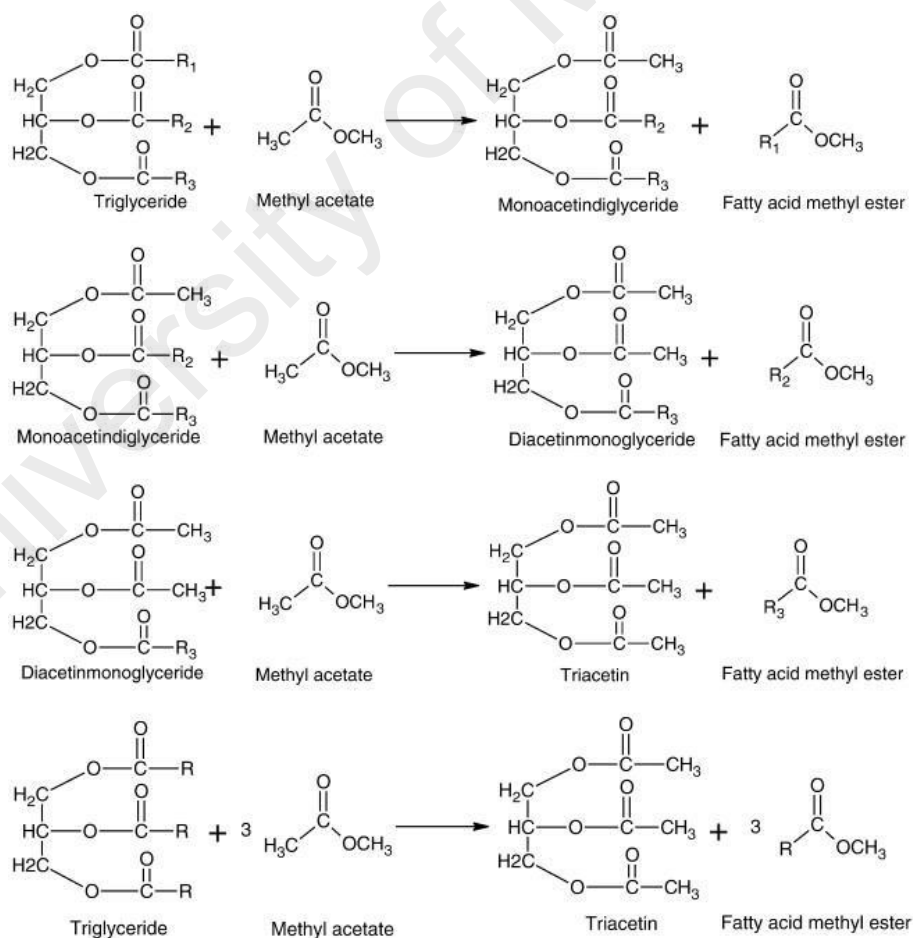


Figure 2.2: Interesterification reaction (Initial 3 equations show the initial steps whereas final equation gives the overall reaction) (Maddikeri *et al.*, 2013).

Generally, there are several drawbacks associated with the transesterification process. For enzyme catalyst, excess utilisation of methanol will lead to deactivation of enzyme and the by-product (glycerol) will have inhibitory effects on the enzymatic activity. These unfavourable issues will restrict the application of enzymatic route at industrial scale (Subhedar & Gogate, 2016). With the co-production of glycerol, neutralization is required to prevent biodiesel contamination. Separation and purification steps are needed for recovery of glycerol. All these steps are energy and resource intensive, decreasing the production efficiency and increasing the production costs. In addition, excessive supply of glycerol has caused it undervalued in the world market (dos Santos Ribeiro *et al.*, 2017; Tian *et al.*, 2018). With the employment of interesterification instead of transesterification, enzyme deactivation could be avoided as triacetin has no adverse effect on the activity of lipase enzyme (Subhedar & Gogate, 2016). Furthermore, production of triacetin is more preferable as it has higher commercial value than glycerol. Triacetin could be used as plasticizer or gelatinizing agent in polymers and explosives and as an additive in tobacco, pharmaceutical industries, and cosmetics. In addition, triacetin is soluble in biodiesel and could be added into biodiesel (up to 10 wt.%) as an additive which could help to improve oxidative stability and cold flow properties of biodiesel (Maddikeri *et al.*, 2013; Tian *et al.*, 2018).

By focusing on the non-edible feedstock, there are only several studies conducted on the ultrasound assisted interesterification. The biodiesel yield obtained at optimum reaction conditions using different catalysts is shown in Table 2.3. The superiority of ultrasound as compared to conventional approach in interesterification had been proven by researchers. For example, Maddikeri *et al.* (2013) observed that higher biodiesel yield was achieved by ultrasound (90%) than conventional stirring (70%) under the same optimum reaction conditions. In the study conducted by Subhedar and Gogate (2016), they discovered that ultrasound assisted interesterification required lower methyl acetate

Table 2.3: Optimum reaction conditions for ultrasound assisted interesterification of non-edible oil.

Feedstock	Catalyst	Temperature (K)	Methyl acetate to oil molar ratio	Catalyst concentration (wt.%)	Ultrasonic power (W)	Reaction time (h)	Biodiesel yield (%)	References
WCO	Potassium methoxide	313	12:1	1	450	0.5	90.0	Maddikeri <i>et al.</i> , 2013
WCO	<i>Thermomyces lanuginosus</i> (Lipozyme TLIM)	323	9:1	3% (w/v)	80	3	96.1	Subhedar & Gogate, 2016
Crambe oil	Novozym [®] 435	333	12:1	20	—	6	98.25	Tavares <i>et al.</i> , 2017a

to oil ratio (9:1 versus 12:1), lower enzyme loading (3% versus 6%), shorter reaction time (3 h versus 24 h) and achieved higher biodiesel yield (96.1% versus 90.1%) as compared to conventional stirring. Based on the several existing literatures, it is suggested that more studies should be conducted on the ultrasound assisted interesterification with the utilisation of different catalyst types to produce the optimum biodiesel yield (chemical and enzyme catalysts).

2.3 Primary factors for ultrasound assisted transesterification

There are several factors that will affect the biodiesel conversion or yield in the ultrasound assisted transesterification such as alcohol to oil molar ratio, catalyst loading, reaction time, reaction temperature, energy consumption and ultrasonic pulse mode. Although mechanical or magnetic stirring are commonly employed in the production of biodiesel, ultrasonic cavitation appears to be more resource-effective than conventional stirring approach in terms of alcohol to oil ratio, catalyst loading, reaction time, reaction temperature, energy consumption, phase separation time and biodiesel conversion or yield.

2.3.1 Alcohol to oil molar ratio

A lower alcohol to oil molar ratio will definitely minimize the energy consumption because alcohol separation using distillation is an energy-intensive operation, which controls the overall economics of biodiesel synthesis process (Gole & Gogate, 2012). By incorporating ultrasound in the biodiesel synthesis, lower molar ratio will be required as compared to conventional stirring. This is due to the intense micro-turbulence and microstreaming generated during the cavitation which contributes to the intensification of the transesterification or esterification processes (Mohan *et al.*, 2017). This claim had

been verified by several researchers through their studies such as Kumar *et al.* (2010a), Yin *et al.* (2012), Mohod *et al.* (2017) and Mohan *et al.* (2017).

Methanol is the most preferable alcohol in transesterification due to its lower cost, industrial availability and superior reactivity as compared to other alcohols. Its short molecular chain and polar properties serve as its physical and chemical advantages. It can also react with triglycerides efficiently and dissolve with the basic catalyst easily (Koh & Ghazi, 2011). Molar ratio of methanol to oil is one of the essential factors affecting the rate of formation and yield of FAME. Theoretically, methanol to oil molar ratio for the transesterification is 3:1. However, huge excessive methanol amount is required to drive the reversible transesterification reaction towards FAME (Thanh *et al.*, 2010). Excess alcohol in transesterification can enhance alcoholysis and ensure complete conversion of oils or fats into esters. Furthermore, better ester conversion can be achieved in a shorter time with a higher alcohol to triglyceride ratio (Leung *et al.*, 2010). For heterogeneous catalyst, excess alcohol can promote transesterification rate in addition to remove product molecules from the catalyst surface and regenerate the active sites (Kumar & Ali, 2013). The effects of molar ratio of methanol to oil on ultrasound assisted alkaline transesterification using homogeneous and heterogeneous catalysts are tabulated in Table 2.4. It is noticed from Table 2.4 that a molar ratio of more than 6:1 was mostly required to achieve optimum biodiesel yield.

Further increasing the molar ratio beyond the optimum will decrease the yield which might be caused by over dilution of biodiesel and glycerol (Gude & Grant, 2013; Jogi *et al.*, 2016; Samani *et al.*, 2016). This is because higher dissolution of glycerol and alcohol in biodiesel will affect the purity of biodiesel if the amount of methanol increases in the mixture (Samani *et al.*, 2016). Moreover, the equilibrium reaction might shift towards the reactant side, which reduces the effective yield (Pukale *et al.*, 2015). In addition, formation of undesirable suspension resulting from the unreacted methanol and oil

mixture has increased the difficulty of separation and longer duration is required as compared to lower methanol ratio (Gude & Grant, 2013).

The optimum methanol to oil molar ratio is also affected by the phase of catalyst. Generally, heterogeneous catalysts require slightly higher molar ratio than homogeneous catalysts due to slower rate which stemmed from mass transfer limitation (Mootabadi *et al.*, 2010). By comparing the optimum molar ratio required by both homogeneous and heterogeneous catalysts in Table 2.4, 16:1 is the highest molar ratio required by heterogeneous catalysts whereas 12:1 is the highest molar ratio required by homogeneous catalysts. This observation tallied with the statement that heterogeneous catalysts required slightly higher molar ratio than homogeneous catalysts. From Table 2.4, it is also observed that transesterification of WCO had been conducted by several groups of researchers by employing homogeneous (KOH and NaOH) and heterogeneous (K_3PO_4 and CaDG) catalysts. The general optimum molar ratios required by each type of catalyst were as followed: KOH and K_3PO_4 (6:1); NaOH and CaDG (9:1). Similar optimum molar ratio was reported using KOH and K_3PO_4 to achieve maximum biodiesel yield or conversion. This could be attributed to similar catalytic activity of K_3PO_4 and KOH (Jogi *et al.*, 2016).

Table 2.4: Effect of methanol to oil molar ratio on ultrasound assisted homogeneous and heterogeneous base-catalysed transesterification.

Year	Various molar ratio	Ultrasonic reactor type	Frequency (kHz)	Power (W)	Feedstock	Catalyst type; loading (wt.%)	Temperature (K)	Optimum molar ratio	Time (min)	Biodiesel conversion (%)	Yield (%)	References
2014*	4:1 to 7:1	Direct sonication (horn)	20	240	WCO	KOH; 1	–	6:1	8	~80	–	Fayyazi <i>et al.</i> , 2014
2014	8:1 to 18:1	Indirect sonication (bath)	40	250	<i>Silybum marianum</i> oil	KHC ₄ H ₄ O ₆ /Ti O ₂ ; 5.0	333	16:1	25	–	88.4	Takase <i>et al.</i> , 2014a
2015	4:1, 6:1, 8:1	Direct sonication (horn)	22	375	WCO	K ₃ PO ₄ ; 3.0	323	6:1	90	–	92.0	Pukale <i>et al.</i> , 2015
2015	6:1, 9:1, 12:1, 14:1	Direct sonication (horn)	22	120	WCO	CaDG; 1.0	333	9:1	30	–	93.5	Gupta <i>et al.</i> , 2015
2015*	4.5:1, 6:1, 9:1, 13.5:1	Direct sonication (horn) (Pulse mode)	20	150	WCO	NaOH; 1.25	–	9:1	2	–	96.8	Martinez-Guerra & Gude, 2015
2015*	4.5:1, 6:1, 9:1, 13.5:1	Direct sonication (horn) (Continuous mode)	20	150	WCO	NaOH; 1.25	–	9:1	2	–	81	Martinez-Guerra & Gude, 2015
2016*	6:1, 9:1, 12:1	Direct sonication (horn)	20	500	Karanj and soybean oil (40: 60) (w/w)	NaOH; 1.0	318	12:1	45	–	98	Parida <i>et al.</i> , 2016
2016*	4:1 to 7:1	Direct sonication (horn)	20	500	WCO	NaOH; 1.0	323	5:1	1	99	–	Khosravi <i>et al.</i> , 2016
2016*	4:1 to 7:1	Direct sonication (horn)	20	500	WCO	KOH; 1.0	323	7:1	1	99	–	Khosravi <i>et al.</i> , 2016
2016	3:1, 6:1, 9:1, 12:1	Direct sonication (probe)	20	250	<i>Schleichera triguga</i> oil	Ba(OH) ₂ ; 3.0	323	9:1	80	96.8	–	Sarve <i>et al.</i> , 2016
2016	9:1 to 17:1	Indirect sonication (bath)	20	600	<i>Jatropha</i> oil	K ₃ PO ₄ ; 1.0	323	12:1	60	–	98	Jogi <i>et al.</i> , 2016

Note: * denotes for ultrasound assisted homogeneous alkaline-catalysed transesterification

2.3.2 Catalyst loading

The reaction of oils and alcohols is a slow process due to the immiscibility between oils and alcohols (Talebian-Kiakalaieh *et al.*, 2013). Hence, catalyst is required for transesterification to accelerate the reaction and gives a better conversion efficiency of oil to biodiesel (Wang *et al.*, 2012). Ultrasonication had been proven by several researchers (Chen *et al.*, 2014; Kumar *et al.*, 2010a; Zhang *et al.*, 2015) that it could help in decreasing the catalyst loading required in either ultrasound assisted homogeneous or heterogeneous transesterification as compared to conventional stirring. In homogeneous transesterification, the beneficial effect was due to increased chemical activity in the presence of ultrasound cavitation (Kumar *et al.*, 2010a). In heterogeneous transesterification, the grinding effect of ultrasound on the catalyst could help to expose new catalytic active sites and increase the interfacial area between catalyst and reactant (Kumar *et al.*, 2010b; Sarve *et al.*, 2016). Therefore, emulsion droplets of alcohol and oil produced could contact with the catalyst particles easily, thus achieving effective mixing between liquid reactants and solid catalyst (Zhang *et al.*, 2015). In addition, microstreaming effect of ultrasound could also help to maintain the catalytic activity by dislodging the inactive surface formed and attached on the catalyst, thus providing more active sites for the catalytic reaction (Gaikwad & Gogate, 2015).

Inadequate catalyst loading can lead to incomplete conversion of triglyceride into FAME. As the catalyst loading increases, the conversion of triglyceride and the yield of biodiesel will also increase until an optimum catalyst loading is attained. Further increment in the catalyst loading will cause a decrement in the yield and increase the production cost. With excessive addition of alkaline catalyst beyond the optimum loading, alkaline catalyst can cause more triglycerides to react with the catalyst through saponification. The soap molecules inside FAME and water molecules will form emulsion, thus hindering the purification of FAME (Encinar *et al.*, 2012a). In addition,

large amount of catalyst increases the solubility of FAME in the glycerol, causing entrainment of FAME in the glycerol phase after phase separation (Noureddini *et al.*, 1998). Decrement in the FAME purity with excessive catalyst loading was encountered by Hingu *et al.* (2010) and Kesgin *et al.* (2014) in their studies.

In heterogeneous transesterification, the number of catalyst particles and active sites increase with the catalyst loading and thus increasing the accessibility of triglyceride and alcohol to the catalyst surface. Further increment of catalyst loading beyond the optimum value will cause either a decrement or negligible effect on the biodiesel conversion or yield due to the reduction of interspatial space between triglyceride and alcohol molecules (Sarve *et al.*, 2016). Moreover, increasing catalyst beyond the optimum loading will cause formation of emulsion layer which makes the biodiesel separation to be difficult (Jogi *et al.*, 2016). In *Jatropha* biodiesel synthesis assisted by ultrasonic irradiation, excessive magnesia-alumina (Mg/Al) (> 1.0 wt.%) as catalyst was found to cause a decrease in biodiesel yield in addition to the formation of emulsion layer (Deng *et al.*, 2011). It should be noted that inadequate catalyst loadings will give rise to unsatisfactory biodiesel yield and incur higher production costs. Therefore, optimum amount of catalyst is required to effectively convert the triglyceride into FAME. It is noticed from Table 2.5 that the range of catalyst loading to achieve maximum yield or conversion was between 0.5 and 1.5 wt.% for ultrasound assisted homogeneous alkaline-catalysed transesterification while higher range of catalyst loading (1.0 to 5.0 wt.%) was generally required for ultrasound assisted heterogeneous base-catalysed transesterification.

Table 2.5: Effect of catalyst loading on ultrasound assisted homogeneous and heterogeneous base-catalysed transesterification.

Year	Various catalyst loading (wt.%)	Ultrasonic reactor type	Frequency (kHz)	Power (W)	Feedstock	Catalyst type; optimum loading (wt.%)	Temperature (K)	Alcohol type; alcohol to oil molar ratio	Time (min)	Biodiesel conversion (%)	Yield (%)	References
2014*	0.5, 0.75, 1, 1.25	Direct sonication (horn)	20	240	WCO	KOH; 1.0	-	Methanol; 6:1	8	~85	-	Fayyazi <i>et al.</i> , 2014
2014	1.0 to 9.0	Indirect sonication (bath)	40	250	<i>Silybum marianum</i> oil	KHC ₄ H ₄ O ₆ /TiO ₂ ; 5.0	333	Methanol; 16:1	25	—	88.4	Takase <i>et al.</i> , 2014a
2015*	0.5, 1.25, 2	Direct sonication (horn) (Pulse mode)	20	150	WCO	NaOH; 1.25	-	Methanol; 9:1	2	-	96.8	Martinez-Guerra & Gude, 2015
2015*	0.5, 1.25, 2	Direct sonication (horn) (Continuous mode)	20	150	WCO	NaOH; 0.5	-	Methanol; 9:1	2	-	81	Martinez-Guerra & Gude, 2015
2015	1.0 to 4.0	Direct sonication (horn)	22	375	WCO	K ₃ PO ₄ ; 3.0	333	Methanol; 6:1	120	—	92.0	Pukale <i>et al.</i> , 2015
2015	0.5 to 1.25	Direct sonication (horn)	22	120	WCO	CaDG; 1.0	333	Methanol; 9:1	40	—	93.5	Gupta <i>et al.</i> , 2015
2016*	0.5, 1, 1.5	Direct sonication (horn)	20	500	Karanj and soybean oil (40: 60) (w/w)	NaOH; 1.5	318	Methanol; 6:1	45	-	98	Parida <i>et al.</i> , 2016
2016*	0.5, 0.75, 1, 1.25	Direct sonication (horn)	20	500	WCO	KOH; 1.25	323	Methanol; 6:1	1	99	-	Khosravi <i>et al.</i> , 2016
2016	1.0 to 4.0	Direct sonication (probe)	20	250	<i>Schleichera triguga</i> oil	Ba(OH) ₂ ; 3.0	323	Methanol; 9:1	100	96.8	—	Sarve <i>et al.</i> , 2016
2016	3.0 to 5.0	Direct sonication (horn)	20–30	50	Karabi oil	CaO; 5.0	333	Methanol; 12:1	120	—	94.1	Yadav <i>et al.</i> , 2016b

Note: * denotes for ultrasound assisted homogeneous alkaline-catalysed transesterification

2.3.3 Reaction time

It had been documented that shorter reaction time was required by ultrasonication compared to the conventional stirring. Many researchers had compared the reaction time needed by both approaches in their studies which are shown in Table 2.6. Ultrasonication can reduce the reaction time by at least 25% and as high as 95.8% compared to the conventional stirring. The reactions under ultrasonication are more reactive compared to mechanical stirring process. This could be attributed to the larger interfacial area of reactant droplets due to the physical effects of cavitation phenomena in terms of intense turbulence and mixing generated in the reactor which then led to the enhancement in the biodiesel yield or conversion (Guldhe *et al.*, 2014; Manickam *et al.*, 2014; Sebayang *et al.*, 2010). The average interfacial area generated by ultrasonication was found to be 67 times higher than that generated by mechanical agitation. The droplet sizes for ultrasonic emulsification were in the narrow range of 0.82–44.6 μm while wider range of 8.1–610 μm for emulsification by mechanical agitation (Ramachandran *et al.*, 2006).

Theoretically, the conversion of fatty acid esters will increase with reaction time (Freedman *et al.*, 1984). The reaction is slow initially due to the mixing and dispersion of alcohol into the oil. After some time, the reaction will proceed rapidly. However, prolonged reaction time will cause a decrement in the product yield due to the backward reaction of transesterification, causing more FFA to form soaps (Eevera *et al.*, 2009; Leung *et al.*, 2010). The transesterification reaction was found to be dependent on the reaction time in the ultrasonic transesterification of *Silybum marianum* oil catalysed by $\text{KHC}_4\text{H}_4\text{O}_6/\text{TiO}_2$ (Takase *et al.*, 2014a). Low reaction rate in the first 10 min could be due to inadequate agitation to enhance proper mixing and dispersion of methanol and catalyst onto the oil. The maximum biodiesel yield (90.1%) was attained in 30 min. However, excess reaction time (after 30 min) resulted in slight reduction in biodiesel yield due to reversible reaction.

Table 2.6: Reaction time needed by employing ultrasonic cavitation and conventional stirring.

Year	Feedstock	Reaction conditions	Ultrasonic cavitation			Conventional stirring			Reduction percentage (%)	References
			Reaction time (min)	Yield (%)	Conversion (%)	Reaction time (min)	Yield (%)	Conversion (%)		
2010	WCO	<ul style="list-style-type: none"> • Methanol to oil (9:1) • 1 wt.% NaOH • Temperature: 343 K^a 	5	–	94.6	120		89.3 (mechanical)	95.8	Sebayang <i>et al.</i> , 2010
2014	Palm oil	<ul style="list-style-type: none"> • Methanol to oil (9:1) • 1 wt.% KOH • Temperature: 333 K 	15	98.5	–	120	89.5 (mechanical)		87.5	Manickam <i>et al.</i> , 2014
	Palm oil	<ul style="list-style-type: none"> • Methanol to oil (3:1) • 1 wt.% KOH • Temperature: 333 K 	15	93	–	150	75 (mechanical)		90	
2014	Palm oil	<ul style="list-style-type: none"> • Methanol to oil ratio (9:1) • 8 wt.% CaO • Temperature: 333 K 	40	70	–	100	70 (magnetic)	–	60	Chen <i>et al.</i> , 2014
2014	<i>Silybum marianum</i> oil	<ul style="list-style-type: none"> • Methanol to oil (8:1) • 1 wt.% KOH • Temperature: 333 K 	15	82.46	–	50	82.35 (mechanical)	–	70	Takase <i>et al.</i> , 2014b
2015	Waste fish oil	<ul style="list-style-type: none"> • Methanol to oil (6:1) • 1 wt.% KOH • Temperature: 328 K 	30	79.6	–	60	78 (mechanical)	–	50	Maghami <i>et al.</i> , 2015
2015	<i>Cynara cardunculus</i> L. seed oil	<ul style="list-style-type: none"> • Methanol to oil (7:1) • 1 wt.% NaOH • Temperature: 333 K 	20	97	–	60	95.8 (mechanical)	–	40	Koutsouki <i>et al.</i> , 2015
2016	<i>Jatropha</i> oil	<ul style="list-style-type: none"> • Methanol to oil (12:1) • 1 wt.% K₃PO₄ • Temperature: 323 K^b 	45	98	–	60	92*	–	25	Jogi <i>et al.</i> , 2016

Table 2.6, continued

Year	Feedstock	Reaction conditions	Ultrasonic cavitation			Conventional stirring			Reduction percentage (%)	References
			Reaction time (min)	Yield (%)	Conversion (%)	Reaction time (min)	Yield (%)	Conversion (%)		
2016	<i>Citrullus vulgaris</i> seed oil	<ul style="list-style-type: none"> Ethanol to oil ratio (6:1) 1.5 wt.% crystalline manganese carbonate 	120	87	–	480	78*	–	75	Krishnaiah <i>et al.</i> , 2016
	<i>Citrullus vulgaris</i> seed oil	<ul style="list-style-type: none"> Isopropanol to oil ratio (6:1) 1.5 wt.% crystalline manganese carbonate 	180	86	–	720	74*	–	75	
2016	<i>Nerium oleander</i>	<ul style="list-style-type: none"> 1st step: Methanol to oil molar ratio (0.4 vol%), 1 vol% H₂SO₄, 328 K 2nd step: Methanol to oil molar ratio (0.2 vol%), 1 v/w% KOH, 328 K 	1 st step: 10–15 2 nd step: 10–15	97	–	1 st step: 60 2 nd step: 60	92 (magnetic)	–	75–83	Yadav <i>et al.</i> , 2016a
2017	<i>Jatropha</i> oil	<ul style="list-style-type: none"> Methanol to oil (10:1) 6 wt.% SrO-CaO Temperature: 338 K 	30	95.4	–	180	89.3 (magnetic)		≈ 83	Ali <i>et al.</i> , 2017

Note: * denotes for stirring type is not mentioned in the study; *a* denotes for temperature used in conventional stirring only; *b* denotes for temperature used in ultrasonication only

The influence of reaction time (from 0.5 to 2.5 min) on the transesterification of WCO was investigated by Martinez-Guerra and Gude (2015) for both pulse and continuous sonication conditions. The highest yield of 98% was achieved by pulse sonication at 2.5 min and 91% followed by continuous sonication at 1 min. During pulse sonication, the biodiesel yield increased with reaction time. On the other hand, the biodiesel yield began to drop upon reaching 1.5 min reaction time for continuous sonication. The drop in the biodiesel yield with increasing reaction time by the usage of continuous sonication had validated the recommendation given by Chand *et al.* (2008). Continuous sonication was not recommended for long reaction time due to local temperature increase (hot spots) which could degrade the oil and cause undesired reactions, leading to a decrement in the biodiesel yield (Salamatinia *et al.*, 2013).

2.3.4 Reaction temperature

For reactions with conventional stirring methods, external heating is paramount and reaction rate will heavily depend on the reaction temperature with vigorous mechanical mixing (Gude & Grant, 2013). On the other hand, ultrasonic mixing eliminates the need of external heating. The capability of ultrasound to increase the temperature inherently can be proven through the experiments performed by Boffito *et al.* (2014). In the ultrasound experiments at 336 K, the thermostat was set at 313 K and the ultrasound provided the heat to achieve the desired bath temperature. In fact, the bath temperature reached 336 K within seconds of initiating sonication which was a lot faster compared to conventional heating. The efficiency of sonication over magnetic stirring at room temperature had been studied by Ragavan and Roy (2011). Transesterification of rubber seed oil was completed at 305 K with an optimum yield of 80.7% which could not be achieved by magnetic stirring method. No visible separation of methyl esters was observed after 15 min of magnetic stirring with methanol/oil/KOH molar ratio 6:1:0.13

at room temperature. Higher temperature was required by magnetic stirring method to initiate the transesterification process. Since ultrasound assisted transesterification can take place at room temperature (303 K), which is much lower than the boiling point of alcohol obviously, it could reduce external heat energy effectively (Zou & Lei, 2012).

The reaction rate and yield of the biodiesel product are clearly influenced by reaction temperature (Koh & Ghazi, 2011). At lower reaction temperature, the oil has higher viscosity and impedes the bubble formation, resulting in poor mixing between the oil and alcohol-catalyst phases (Gude & Grant, 2013; Takase *et al.*, 2014b). As reaction temperature rises, the viscosity of oil will decrease and it becomes susceptible to cavitation. Consequently, the miscibility of alcohol in oil increases and subsequently promotes biodiesel formation (Mahamuni & Adewuyi, 2009). In addition, the kinetic rate constant of this endothermic chemical reaction also increases since there is higher energy input for the reaction to take place (Koh & Ghazi, 2011; Mahamuni & Adewuyi, 2009). Thus, shorter reaction time can also be achieved at higher temperature. However, it is important to avoid vaporization of alcohol which will reduce the contact area with the reactant (Koh & Ghazi, 2011). In heterogeneous transesterification reaction, the effect of reaction temperature is very important as the system consists of three phases (oil-alcohol-catalyst). The reaction can be slow due to the presence of diffusion barrier among the different phases (Takase *et al.*, 2014a). The diffusion resistance between different phases will be minimized with increasing temperature as the viscosity of the reaction mixture is reduced. Therefore, solubility of alcohol in oil phase will increase and the catalyst will have a better contact with the reactants (Pukale *et al.*, 2015).

Nonetheless, beyond the optimum reaction temperature, the biodiesel yield will decrease because a higher reaction temperature will also accelerate side reactions such as saponification (Eevera *et al.*, 2009; Leung *et al.*, 2010). Another reason can be ascribed to the damping effect of the cavitation effects at higher operating temperatures (Hingu

et al., 2010; Parida *et al.*, 2016). At higher reaction temperature, the equilibrium vapour pressure will increase which leads to easier bubble formation. However, the cavitation bubbles formed contain more vapours. The release of solvent vapours interferes with the cavitation effects, causing cushioning of collapse. Therefore, bubbles implode with less intensity and reduces the mixing effect of ultrasound on the transesterification reaction, resulting in reduced mass transfer and biodiesel yield (Gude & Grant, 2013; Gupta *et al.*, 2015; Martinez-Guerra & Gude, 2015).

2.3.5 Energy consumption

In terms of energy consumption, mechanical stirring usually requires higher energy consumption than ultrasonication. It was reported that ultrasonication only required one-third to a half of the energy that was consumed by mechanical agitation (Veljković *et al.*, 2012). Yin *et al.* (2012) had recorded the energy consumption for both mechanical stirring and ultrasonic probe irradiation methods to reach biodiesel conversion of 95% from sunflower oil. It was observed that mechanical stirring required 0.31 kWh whereas ultrasonic probe irradiation only needed 0.18 kWh. Ultrasonication was also discovered to be more energy efficient than conventional stirring by other researchers such as Gupta *et al.* (2015), Yadav *et al.* (2016b) and Brasil *et al.* (2015). More energy was consumed by conventional stirring as continuous heating was required to maintain the temperature of water bath or solution (Yadav *et al.*, 2016b; Yin *et al.*, 2012). External heating source is unnecessary in biodiesel synthesis aided by ultrasonic irradiation. This is because cavitation from ultrasound will result in localized increment in temperature at the phase boundary and subsequently enhanced the reaction. Therefore, less energy is consumed in the production of biodiesel in the long run (Yin *et al.*, 2012).

Delivery of the ultrasonic power to the reaction mixture determines the degree of cavitation and thus directly affecting the biodiesel yield (Gupta *et al.*, 2015). Generally,

biodiesel conversion increases with an increment in ultrasonic power until optimum ultrasonic power is reached. When the ultrasonic power is higher, the collapse of the cavitation bubbles will be harsher due to higher jet velocity, thus enhancing micromixing between the oil and methanol phases at the phase boundary. Finer emulsion is then formed, increasing mass-transfer coefficient and biodiesel conversion. On the other hand, biodiesel conversion is reduced when further increasing the ultrasonic power beyond the optimum value. Cushioning effect at higher ultrasonic power reduces the energy transfer into the system, thus providing lower cavitation activity (Mahamuni & Adewuyi, 2009). Furthermore, huge amount of cavitation bubbles will be generated when high ultrasonic power is introduced into the reaction mixture. Merging of excessive bubbles produce bigger and more stable bubbles, acting as an obstacle to acoustic energy transfer. This phenomenon of efficiency loss in the power transfer is referred as decoupling effect (Martinez-Guerra & Gude, 2015).

2.3.6 Phase separation time

Generally, the separation of the reaction mixture containing FAME, glycerol and excess methanol requires several hours through gravity settling. The separation time depends on the amount of excess methanol used and the reaction mixture's temperature. Separation will generally occur faster in the reaction mixture containing less excess of methanol. This fact was attributed to the differences in the density of the glycerol phase due to the varying excess volume of methanol. Glycerol has much higher density (1.26 g/cm^3) than methanol (0.79 g/cm^3), and both liquids are polar compounds which will form a uniform phase at any mixing ratio. Therefore, the glycerol layer with smaller excess of methanol has a higher density, resulting in a faster phase separation between the FAME layer and the glycerol layer due to the larger difference in the density of both layers. Lower temperature of the reaction mixture will contribute to lower dissolution of glycerol

and methanol in the FAME layer, thus leading to shorter separation time (Thanh *et al.*, 2010).

As mentioned previously in Section 2.3.1 and 2.3.4, ultrasound approach requires lower alcohol to oil molar ratio and lower reaction temperature compared to conventional stirring method. Therefore, it can be assumed that lower excess of alcohol is usually present through ultrasound approach. The assumption could be further affirmed since ultrasonic transesterification requires lower reaction temperature than conventional transesterification using either mechanical or magnetic stirring. Hence, the overall temperature of the reaction mixture will be lower for ultrasonic agitation.

In the transesterification of waste vegetable oils carried out by Refaat *et al.* (2008), biodiesel yield of 96.15% was achieved under optimum conditions (methanol/oil molar ratio of 6:1, 1 wt.% KOH and 338 K) after reaction time of 1 h with the aid of mechanical stirring. These optimum conditions were then implemented again using ultrasonication (100 W, 20 kHz) in another study by Refaat and El Sheltawy (2008). It was found out that the separation time was reduced remarkably from 8 h to 25 min in addition to shorter reaction time (reduced from 1 h to 5 min) and higher yields (98–99%) were achieved. According to Kumar *et al.* (2012), ultrasonication reduced the separation time from 5 to 10 h to less than 30 min in the production of biodiesel from *Jatropha* oil at methanol: ethanol: oil molar ratio of 3:3:1 with 0.75 wt.% catalyst. The ease of separation of glycerol and catalyst was also found to be higher in the case of ultrasonication compared to mechanical stirring for the biodiesel synthesis from Nagchampa oil by Gole and Gogate (2012), which reduced the purification time and energy.

2.3.7 Ultrasonic pulse mode

Ultrasound can be applied in pulse mode or continuous mode. Examples of wave patterns for continuous and pulse sonication (5 s on/1 s off) are shown in Figure 2.3(a)

and 2.3(b), respectively. For continuous sonication (Figure 2.3(a)), ultrasound waves are delivered continuously and relaxation intervals are impossible for the liquid phase in the reaction medium, thus increasing thermal energy of the reaction medium. As a result, energy input will be partially lost as they are being transformed into vibrational or cavitation energy. Transesterification reaction may be energized by the thermal effect of the continuous sonication but prolong exposure is not recommended. This is because unfavourable emulsification of the reactants may complicate the product separation owing to over excitation of the reactants. On the contrary, relaxation intervals are possible for pulse sonication (Figure 2.3(b)), rendering excitation gap to the reaction mixture to form good emulsions without increasing thermal energy of the reaction medium significantly. Nevertheless, longer sonication time is required by pulse sonication than continuous sonication as lower excitation energy is imparted (Martinez-Guerra & Gude, 2015). Chand *et al.* (2008) had proven that pulse mode gave a greater yield of esters than continuous mode. In their study, pulse mode (5 s on/25 s off) and continuous mode (for 15 s) were compared. 96% biodiesel yield was obtained in less than 90 s in the pulse mode while 86% yield was achieved in 15 s for continuous mode. These results are in agreement with the study carried out by Martinez-Guerra and Gude (2015). In addition to lower the yield produced, application of ultrasound in continuous mode was also found to cause tip erosion and was less energy efficient than pulsed mode (Subhedar & Gogate, 2014).

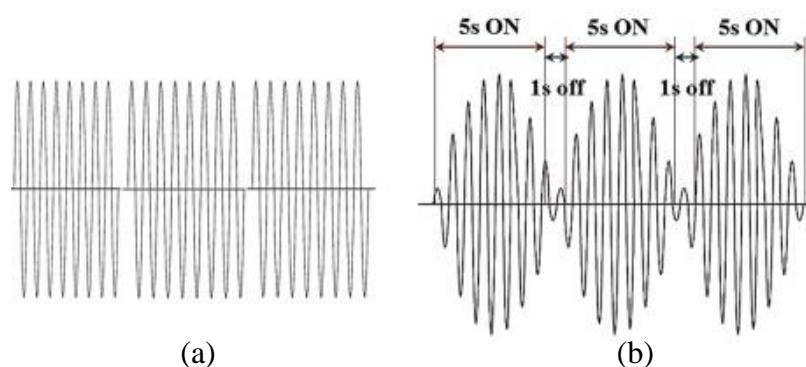


Figure 2.3: Wave profiles for (a) continuous sonication (b) pulse sonication (Martinez-Guerra & Gude, 2015).

Pulse is also known as the ratio of ultrasound working time to its idling time (Samani *et al.*, 2016). It could also be expressed in duty cycle, which is the percentage of ultrasound working time to the total ultrasound working time and idling time. At lower pulse, lower biodiesel conversion is obtained due to mild stirring effects of the ultrasound which are not strong enough to mix the immiscible reactants evenly. By increasing the pulse to a certain extent, the biodiesel conversion increases as the two immiscible layers achieve better emulsification (Hingu *et al.*, 2010). The effect of using pulsed ultrasound was investigated by Hingu *et al.* (2010) in the biodiesel synthesis from WCO for 40 min reaction time. For the pulse 2 s on/2 s off (duty cycle of 50%), the conversion was 62% and 5 s on/1 s off (duty cycle of $\approx 83\%$) increased the conversion to 65.5%. For pulse mode of 1 min on/5 s off ($\approx 92\%$), conversion of 89.5% was acquired and the yield was further increased to 94.5% after dry washing the esters. In the ultrasonic transesterification of WCO using 1 wt.% CaDG as a catalyst, methanol to oil molar ratio of 9:1 and 333 K, biodiesel yield increased when the duty cycle increased from 30% (3 s on/7s off) to 50% (7s on/3s off). However, no significant increment in the yield was detected for further enhancement in the duty cycle to 70% (7s on/3s off) (Gupta *et al.*, 2015; Hingu *et al.*, 2010). Therefore, it could be concluded that if the pulse (duty cycle) exceeded the optimum range, the biodiesel conversion or yield would increase with a lower rate. This was because in such condition, the effect of initial vibrational shock applied to the reactants by ultrasound waves would become identical with uniform waves (Samani *et al.*, 2016).

2.3.8 Biodiesel conversion and yield

In order to compare the biodiesel conversion or yield attained between conventional stirring and ultrasonication, several researchers had conducted the experiments under similar reaction conditions in which the results are tabulated in Table 2.7.

Table 2.7: Comparison of biodiesel yield or conversion of different feedstocks using ultrasound and conventional stirring approaches.

Year	Feedstock	Type of ultrasound/stirring	Ultrasonic cavitation		Conventional stirring		Increase percentage (%)	References
			Yield (%)	Conversion (%)	Yield (%)	Conversion (%)		
2010	WCO	<ul style="list-style-type: none"> • Ultrasonic horn (200 W, 20 kHz) 	–	89.5	–	57.5	32	Hingu <i>et al.</i> , 2010
2010	<i>Oreochromis niloticus</i> oil	<ul style="list-style-type: none"> • Mechanical stirring (1000 rpm) • Ultrasonic bath (60 W, 40 kHz) 	98.2	–	~85	–	14.2	Santos <i>et al.</i> , 2010
2011	Rubber seed oil	<ul style="list-style-type: none"> • Mechanical stirring • Ultrasonic bath (33±3 Hz) 	91	–	87	–	4	Ragavan & Roy, 2011
2012	<i>Jatropha</i> oil	<ul style="list-style-type: none"> • Magnetic stirring (>300 rpm) • Ultrasonic horn (400 W, 40 kHz) 	–	98	–	79	19	Worapun <i>et al.</i> , 2012
2013	WCO	<ul style="list-style-type: none"> • Mechanical stirring (600 rpm) • Stirrer (6-blade turbine, 1000 rpm) 	90	–	70	–	20	Maddikeri <i>et al.</i> , 2013
2014	WCO	<ul style="list-style-type: none"> • Ultrasonic horn (22 kHz, 375 W) 	92	–	59	–	33	Pukale <i>et al.</i> , 2015
2015	WCO	<ul style="list-style-type: none"> • Overhead stirrer (1000 rpm) • Ultrasonic horn (120 W, 22 kHz) 	93.5	–	65.6	–	27.9	Gupta <i>et al.</i> , 2015
2016	<i>Schleichera triguga</i> oil	<ul style="list-style-type: none"> • Overhead stirrer (800 rpm) • Ultrasonic probe (250 W, 20 kHz) • Conventional stirring (did not specify the condition in the paper) 	–	96.8	–	63.29	33.51	Sarve <i>et al.</i> , 2016

From Table 2.7, it can be noticed that ultrasonication can increase the biodiesel yield or conversion by 4.0% to 27.9% in comparison to conventional stirring. Since the transesterification reaction is mass controlled due to the immiscibility of methanol and oil, the micro-turbulence generated due to cavitation bubbles can result in larger interfacial area and higher temperature and pressure. For conventional stirring, agitation intensity plays an important role in the transesterification reaction. A slow mass transfer rate of the triglycerides from oil phase to methanol-oil interface will result in a slower reaction rate as this mass transfer is the rate limiting step of the transesterification process (Worapun *et al.*, 2012). In short, it can be concluded that ultrasonication can achieve higher biodiesel conversion or yield than conventional stirring under comparable reaction conditions.

2.4 Ultrasonic reactive extraction for biodiesel production

Reactive extraction is also known as in-situ transesterification in which the oil bearing materials such as oilseeds or seed cakes contacts directly with an alcohol solution at ambient temperature and pressure. Alcohol will have two roles in this process, acting as an extracting solvent and an esterification reagent, thus combining both the oil extraction and transesterification processes into one single step (Veljković *et al.*, 2012). In other words, once the oil is extracted out from seeds, it is subsequently converted to esters (Banković-Ilić *et al.*, 2012). Expensive costs employed for the oil extraction and degumming in the biodiesel production could be reduced as the isolation and possibly refining of oilseeds are not needed. In addition, the biodiesel yield could be maximized up to 98% (Baskar & Aiswarya, 2016; Veljković *et al.*, 2012). It was reported that reactive extraction can reduce biodiesel production cost by integrating multiple biodiesel processing stages which constitute over 70% of the overall cost, even when using refined oil as feedstock (Shuit *et al.*, 2010a). In order to reduce the alcohol requirement for high

efficiency of reactive extraction, the oilseeds need to be dried prior to the reaction taking place (Haas & Scott, 2007).

Integration of ultrasonication in the reactive extraction process can provide suitable pre-treatment condition to change the physical and chemical structure of the lignocellulosic seed. Ultrasound used in the process could induce physical pre-treatment through the formation of cavitation bubbles in the liquid phase that grow and violently collapse. Furthermore, addition of ultrasonication could induce mechanical treatment for disrupting biological structure and increase the surface area while enhancing the saccharification of cellulose for maximum cavitation effect at 323 K. Moreover, the thermal temperature employed in the process could deactivate the toxic phorbol ester while producing crude biodiesel, glycerol by-product and complete de-oiled seed residues (Zahari *et al.*, 2015).

However, there are only few studies conducted on ultrasound assisted RE directly from non-edible oilseeds. Chadha *et al.* (2012) achieved 94.1% of biodiesel yield with the assistance of ultrasonic probe (22 kHz; 750 W) under the optimum conditions of methanol to seed ratio (w/w) of 10:1, 2–3 mm seed size, 1 wt.% NaOH and 80 min reaction time. Zahari *et al.* (2014b) obtained 62.21% biodiesel yield with 0.15 N NaOH and <1 mm seed size. The details of methanol to seed ratio, reaction temperature and reaction time in achieving biodiesel yield of 62.21% were not mentioned in their studies. Koutsouki *et al.* (2015) synthesized biodiesel from *Cynara cardunculus* L. seeds with the assistance of ultrasonic horn (24 kHz, 400 W, 80% of ultrasonic amplitude and cycle at 0.7). Optimum biodiesel yield of 96% was achieved at methanol to oil molar ratio of 550:1, 9.5 wt.% NaOH and reaction time of 20 min. Kumar (2017) attained the maximum biodiesel conversion of 92% within 20 min by using methanol to seed ratio (w/w) of 100:1, >1–<2 mm seed size, 1.5wt.% KOH, 50% of ultrasonic amplitude and 0.3s cycle.

2.4.1 Mechanism of ultrasonic reactive extraction on oilseed for biodiesel production

The suggested ultrasonic extraction mechanism by Jadhav *et al.* (2016) is shown in Figure 2.4. In the first step of the extraction processes, the irregular dry seed particles are surrounded by a solvent layer. Uptake of the solvent by the irregular dry seed particles causes them to begin swelling, expanding and acquiring a smoother shape. A dynamic interaction is present at the surface of the seeds in the course of swelling and decreases successively upon reaching the maximum limit of swelling. Direct diffusion is then being interfered by the presence of the stagnant layer surrounding the seed particle which possibly causes the extraction process to cease. In the second step, solvated compound (seed oil) moves towards the stagnant layer and diffuses into the bulk solvent. The extraction efficiency will be hampered due to the presence of stagnant layer as a diffusion barrier. Diffusion process will become harder if the stagnant layer has high adhesiveness and the extraction yield will be lower. Moreover, blockage of crevices by the stagnant layer could hamper the diffusion of seed oil (Jadhav *et al.*, 2016).

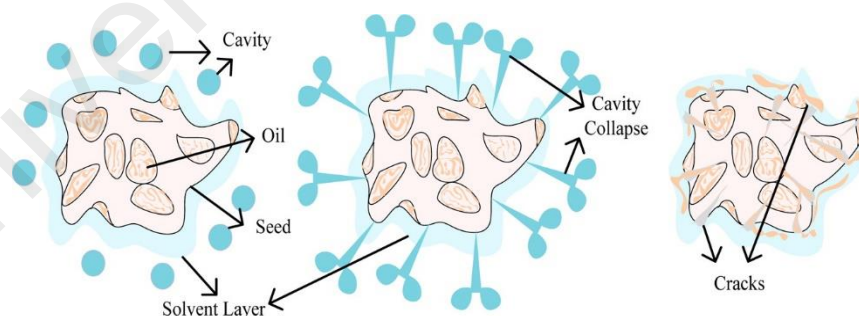


Figure 2.4: Ultrasonic extraction mechanism (Jadhav *et al.*, 2016).

By introducing ultrasonic wave with larger amplitude through the solvent medium, bubbles form and collapse in a very short time, which contain elevated pressure and temperature. Shock wave and high-speed jet are generated from the asymmetric collapse of these cavities. Striking of the shock waves on the seed surface creates microfractures,

cracks and crevices as well as breaks the stagnant layer. At the same time, impingement by high-speed jets results in surface peeling, erosion and particle breakdown. Due to these physical effects, the solvent can easily penetrate the plant's cell wall into the cell tissues, accelerate the extraction of oil bodies with solvent and permit oil bodies release into the extraction environment (solvent) (Jadhav *et al.*, 2016; Shirsath *et al.*, 2012). Once the oil bodies have been extracted, they will be converted to biodiesel simultaneously (Shuit *et al.*, 2010a).

The proposed mechanism was confirmed by Jadhav *et al.* (2016) using the field emission scanning electron microscopy (FESEM) analysis of raw and ultrasonicated date seed. Raw date seed had a smooth, intact and regular surface (as shown in Figure 2.5(a) and (c)) whereas ultrasonicated date seed had irregular shape with formation microfractures and crevices on its surface (as shown in Figure 2.5(b) and (d)). Particle size distribution of the fresh and ultrasonicated date seed powder in Figure 2.6) also affirmed the physical effect of ultrasound in seed breakdown. Ultrasonicated seed had narrower particle size distribution as compared to raw seed (in the range of 500 nm vs. 1600 nm) due to the shrinkage of seed size.

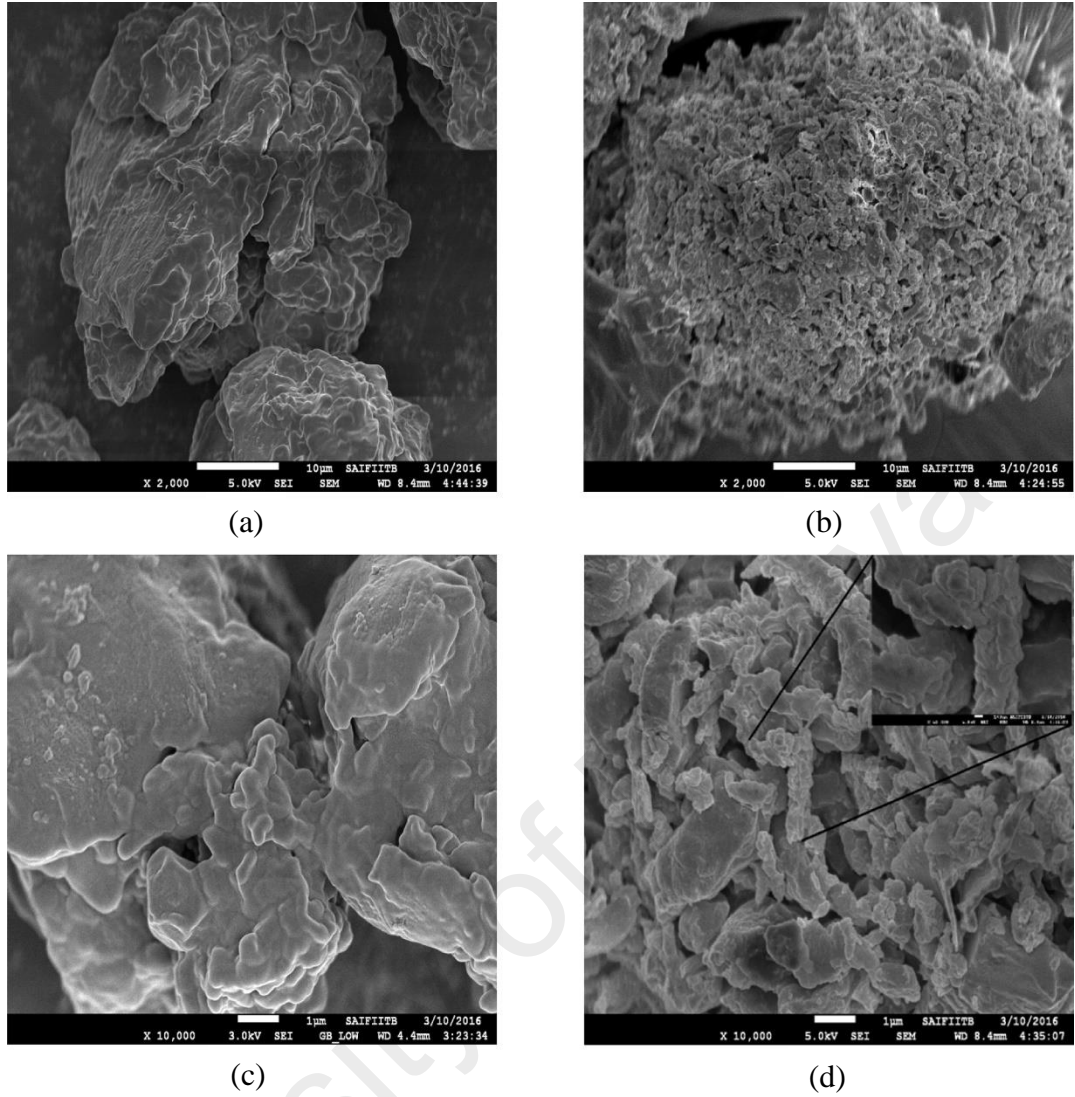


Figure 2.5: FESEM images of raw date seed at (a) 2000 \times and (c) 10000 \times and ultrasonicated date seed at (b) 2000 \times and (d) 10000 \times (Jadhav *et al.*, 2016).

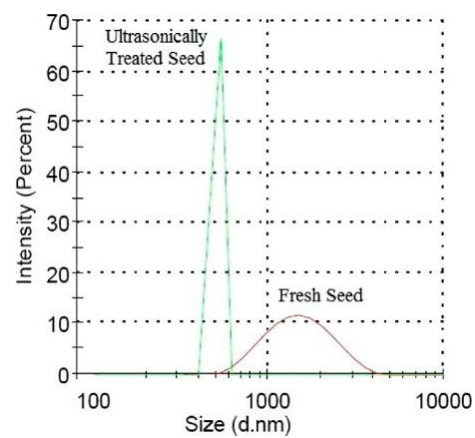


Figure 2.6: Particle size distribution of fresh date seed powder and ultrasonicated date seed powder (Jadhav *et al.*, 2016).

2.5 Research gaps

Based on the reviews discussed in this work, ultrasonic reactive extraction is a promising approach to synthesize biodiesel from oilseeds directly. However, majority of the studies had performed ultrasonic reactive extraction from liquid oil directly instead of the solid oil-bearing seeds. The optimum parameters obtained such as alcohol to oil ratio, catalyst loading, ultrasonic power and ultrasonication mode by employing ultrasonic reactive extraction from oil might not be suitable to achieve maximum biodiesel yield for ultrasonic reactive extraction from oilseeds directly. Till now, the scientific data on the ultrasonic reactive extraction from seed directly is very limited. Future research could be directed more towards the effect of parameters on biodiesel yield or conversion, especially the effect of alcohol to seed ratio instead of alcohol to oil ratio. Therefore, in the present study, *Jatropha* oilseeds were utilised as the feedstock for biodiesel synthesis with the assistance of ultrasonic reactive extraction. Few research questions to be considered are as follow:

1. Is non-edible *Jatropha* seeds capable to replace edible feedstock for biodiesel production?
2. Is ultrasonication approach able to improve mass transfer between oil and alcohol and require lower molar ratio of alcohol to oil as compared to conventional transesterification process?
3. Is the fuel properties of biodiesel produced from reactive extraction with the utilisation of oilseeds as feedstock directly able to meet the ASTM D6751 and EN14214 standards?

CHAPTER 3: MATERIALS AND METHODS

3.1 Introduction

In this research, there were three steps involved in producing *Jatropha* biodiesel. In the first step, the *Jatropha* seeds were pretreated: decortication, drying and grinding. In the second step, esterified *Jatropha* oil was synthesized by using ground *Jatropha* seeds with the assistance of ultrasound. Esterified *Jatropha* oil production was conducted based on the parameters which were ultrasonic pulse mode, particle size, n-hexane to methanol volume ratio, H_2SO_4 loading, reaction time and ultrasonic amplitude. Seed characterization tests were conducted to investigate the difference of *Jatropha* seeds before and after ultrasound assisted in-situ esterification. In the third step, *Jatropha* biodiesel production was performed and the parameters investigated were KOH loading, methanol to esterified oil molar ratio, reaction time and ultrasonic amplitude. The physicochemical properties of the biodiesel produced were determined according to ASTM and EN standards. The overview of research methodology is shown in Figure 3.1.

3.2 Materials

Jatropha seeds were procured from Indonesia. Methanol (99.8% purity), KOH (85% purity), HCl (32% purity) and nitric acid (HNO_3) (65% purity) were purchased from Merck, Germany and phenolphthalein solution (1% in ethanol) from Fluka Analytical. The remaining chemicals used in this study; toluene (99.5% purity), n-hexane (99% purity), H_2SO_4 (95-97% purity) and 2-propanol (99.7% purity) were purchased from Friendemann Schmidt. Pure methyl ester standard mixture, FAME Mix $\text{C}_8\text{--C}_{24}$ (Supelco) was used as reference and methyl nonadecanoate, C_{19} (analytical standard, 99.5%, Sigma-Aldrich) was used as internal standard (IS) in gas chromatography (GC) analysis. All the chemicals were used as received without further purification.

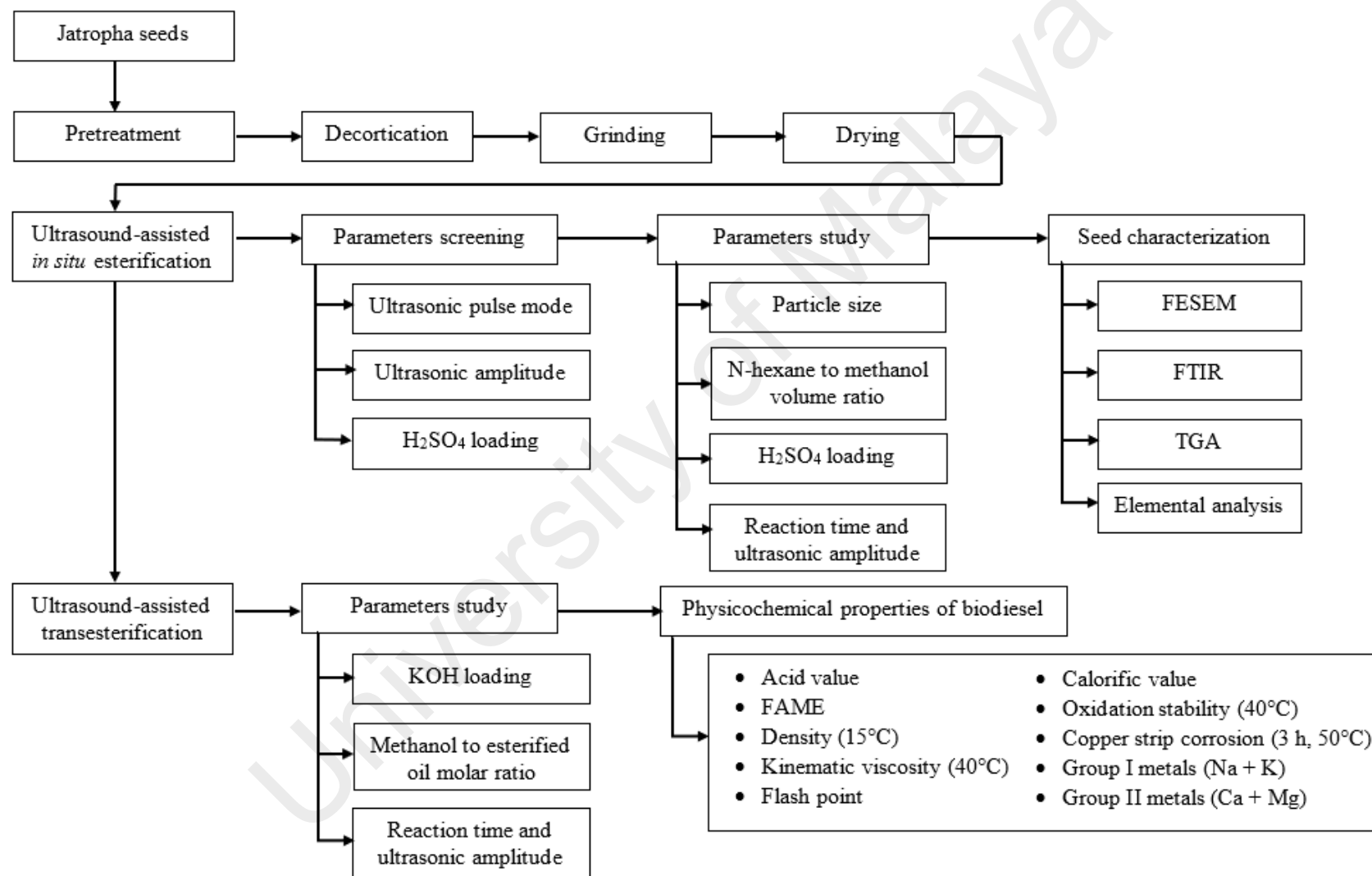


Figure 3.1: Overview of research methodology.

3.3 Equipment

Both the ultrasonic in-situ esterification and transesterification reactions were conducted in beakers made of borosilicate glass. Ultrasonic cavitation to the reaction mixture was provided by an ultrasonic probe unit of Qsonica (Q500). The ultrasonic device operated at 500 W and 20 kHz frequency. The probe amplitude and pulse were adjustable from 20% to 100% and 1 s to 1 min, respectively. Ultrasonic probe was immersed partially into the reaction mixture. No external heat source was applied apart from the ultrasonic probe itself. Ultrasonic power released by irradiation was depended on the amplitude of the ultrasonic probe (Chuah *et al.*, 2016a).

3.4 Measurement of moisture and oil content of *Jatropha* seeds

Initially, *Jatropha* seeds were weighted and dried in an oven at 60°C repeatedly until constant weight was achieved for moisture content measurement (Amalia Kartika *et al.*, 2016). Then the dried seeds were ground with a blender (Tefal La Moulinette, 1000 W). In order to determine the maximum amount of oil that could be extracted from the seeds using conventional method, Soxhlet extractor with excess n-hexane as the solvent was utilised. 25 g of ground seed was placed in the thimble of the Soxhlet extraction system with a round-bottomed flask (500 mL) and a condenser. After the extraction process, hexane was removed using rotary evaporator and the extracted oil was measured (Shuit *et al.*, 2010a). The oil extraction was performed in three replicates. The average oil yield was calculated from Equation 3.1 (Tavares *et al.*, 2017b).

$$\text{Oil yield (\%)} = \frac{\text{weight of extracted oil}}{\text{original weight of seed}} \times 100\% \quad (3.1)$$

3.5 Ultrasound assisted in-situ esterification

In each run, 20 g of crushed *Jatropha* seeds, methanol, n-hexane and H₂SO₄ were mixed in a 1 L beaker to be sonicated. Upon completion of the reaction, the mixture was

cooled to ambient temperature. Then, it was filtered to separate the filtrate and the seed cake. Excess methanol and n-hexane were removed from the filtrate by evaporation using a rotary evaporator. The filtrate was then separated into two layers by gravity. The lower layer was dark brown in colour containing glycerol. The upper layer constituted the esterified oil. The esterified oil was washed a few times with warm water (60°C) to remove all the impurities until the pH of the washing water became neutral. After that, the remaining methanol and water were evaporated using a rotary evaporator for 1 h at 70°C under vacuum. The weight of the esterified oil was measured and recorded. Extraction efficiency of oil was calculated according to Equation 3.2. AV of the esterified oil was determined by titration method and esterification efficiency was calculated according to Equation 3.3 (Trinh *et al.*, 2017). For FAME purity in the esterified oil, it was determined by GC and calculated according to Equation 3.6 in Section 3.8.2.

Extraction efficiency

$$= \frac{\text{Weight of oil extracted after ultrasonic esterification}}{\text{Weight of oil extracted after Soxhlet extraction}} \times 100\% \quad (3.2)$$

$$\text{Esterification efficiency} = \frac{\text{Initial AV} - \text{Final AV}}{\text{Initial AV}} \times 100\% \quad (3.3)$$

Where

Initial AV=Initial acid value (mg KOH/g)

Final AV=Final acid value (mg KOH/g)

The optimum reaction parameters of ultrasonic pulse mode, particle size, n-hexane to methanol volume ratio, H₂SO₄ loading (Appendix A), reaction time and ultrasonic amplitude which influence the esterification and extraction efficiencies and FAME purity were identified using one factor at a time method. Each experiment was conducted in duplicate to ensure data reproducibility. The reported values were the average of the individual runs. The overall flowchart of esterification process is depicted in Figure 3.2.

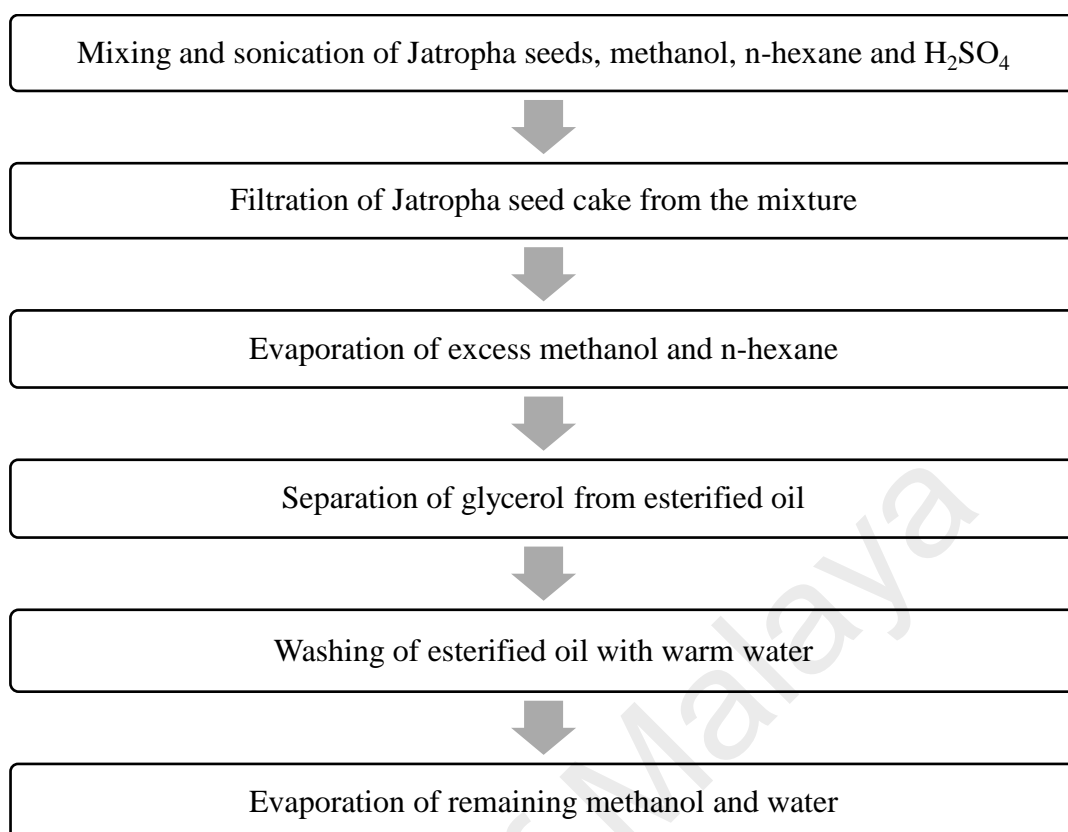


Figure 3.2: Overall flowchart of ultrasound assisted in-situ esterification process.

3.6 Ultrasound assisted transesterification

Firstly, 10 g of esterified oil from ultrasound assisted in-situ esterification reaction was poured into a 50 mL beaker. KOH pellets were dissolved in methanol before being added into the beaker containing esterified oil. The mixture was being sonicated for transesterification process. After completion of the reaction, the mixture was cooled to ambient temperature. Then, it was allowed to settle in a separating funnel. Glycerol settled at the bottom was subsequently removed. The top layer which consisted of biodiesel was washed a few times with warm water (60°C) to remove impurities until the pH of the washing water became neutral. Finally, the water and residual methanol in the biodiesel phase was evaporated by using rotary evaporator for 1 h at 70°C under vacuum. The biodiesel weight was measured and recorded. The FAME purity of biodiesel produced was determined by GC and calculated according to Equation 3.6. Biodiesel yield was then

calculated according to Equation 3.4. The difference between FAME yield and biodiesel yield is FAME purity represents how pure is the biodiesel obtained whereas biodiesel yield represents how much biodiesel is obtained.

$$\text{Biodiesel yield (\%)} = \frac{\text{FAME purity} \times W_{BD}}{W_{EO}} \quad (3.4)$$

Where

W_{BD} = Weight of biodiesel (g)

W_{EO} = Weight of esterified oil (g)

Fuel characteristics of the biodiesel produced were identified using the methods discussed in Section 3.8. The optimum reaction parameters of KOH loading (Appendix B), methanol to esterified oil molar ratio (Appendix C), reaction time and ultrasonic amplitude which influence the FAME purity and biodiesel yield were identified using one factor at a time method. Similar to ultrasonic esterification, each experiment was conducted in duplicate to ensure data reproducibility. The reported values were the average of the individual runs. The overall flowchart of ultrasound assisted transesterification process is depicted in Figure 3.3.

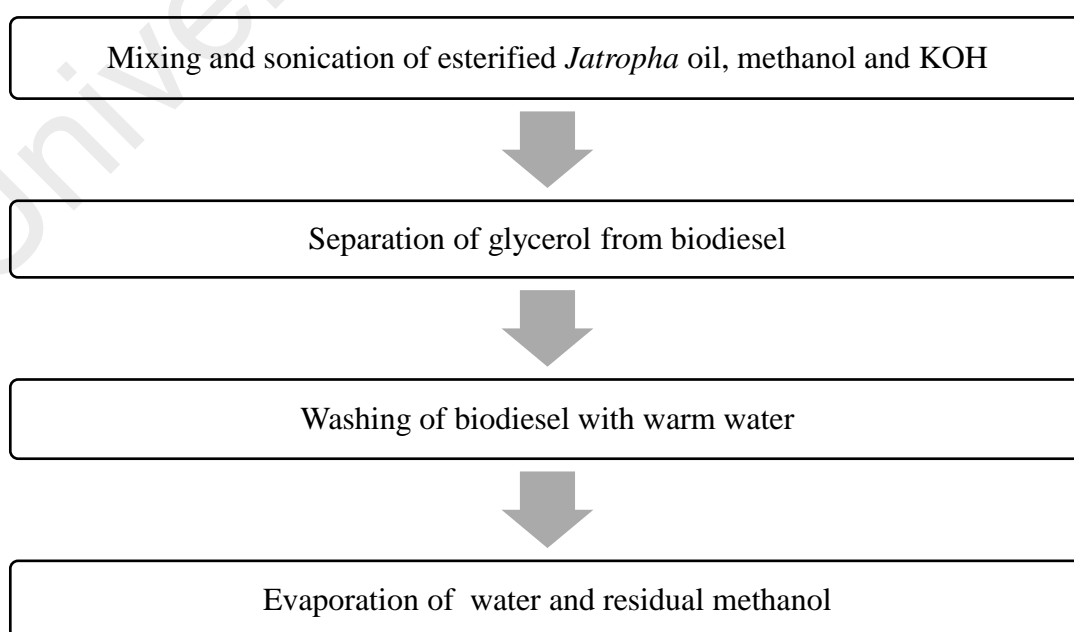


Figure 3.3: Overall flowchart of ultrasound assisted transesterification process.

3.7 Seed characterization

The solid seeds before and after ultrasonic esterification were characterized using FESEM, thermal gravimetric analysis (TGA), fourier-transform infrared spectroscopy (FTIR) and elemental analyses to ascertain its changes in physical morphology and chemical characteristics.

3.7.1 FESEM

FESEM analysis was performed using a field emission scanning electron microscope (Zeiss, model Auriga) at accelerating voltage of 1 to 1.1 kV to analyze the surface morphology and physical structure of the seeds before and after ultrasound assisted *in-situ* esterification at room temperature. Single layer of samples was put carefully on the clean disk attached with double sided tapes for the FESEM imaging.

3.7.2 TGA

Thermal behaviour of seeds before and after ultrasound assisted in-situ esterification was characterized by TGA. This thermal decomposition analysis was performed by using a thermogravimetric analyzer (Perkin Elmer, model TGA 4000). Nitrogen was used as the carrier gas with a flow rate of 100 mL/min. The sample (around 5 mg) was heated from ambient temperature to a final temperature of 900°C at a rate of 10°C/min.

3.7.3 FTIR

FTIR was performed to identify the dominant chemical bonds and functional groups such as oxygen containing groups, carbonyl, hydroxyl and carboxylic groups. FTIR was conducted using FTIR spectrometer (Perkin Elmer, model Spectrum 400). About 2–3 mg of sample was mixed with 100 mg of potassium bromide (KBr) and ground to uniform particle size before pressed as KBr pellet using hydraulic press. The spectra were obtained

in the vibrational absorption range 4000–450 cm^{-1} , at a resolution of 4 cm^{-1} and four cumulative scans.

3.7.4 Elemental analysis

Elemental compositions (carbon (C), hydrogen (H), nitrogen (N) and oxygen (O)) were analyzed using an elemental analyser (Perkin Elmer, model 2400 Series II). Sample of 0.5 g was weighed accurately and heated to 1150°C and the corresponding elements were determined through the weight percentage composition.

3.8 Fuel properties

The physicochemical properties and qualities of biodiesel must meet the international specification standards such as ASTM D6751 and EN14214 before being utilised as fuel in engines. Therefore, physicochemical properties of *Jatropha* biodiesel such as AV, FAME, density, kinematic viscosity, flash point, calorific value, oxidation stability, copper strip corrosion, group I metals (Na + K) and group II metals (Ca + Mg) were determined and then compared with ASTM D6751 and EN14214 standards. All the relevant equipment and test methods are listed in Table 3.1.

Table 3.1: List of equipment for fuel properties tests.

Properties	Equipment	Test Method
AV	– (Manual titration)	D664
FAME purity	Agilent GC-7890A	EN14103
Density (15°C)	Density meter DM 40 (Mettler Toledo)	D127
Kinematic viscosity (40°C)	Stabinger viscometer SVM 3000 (Anton Paar)	D445
Flash point	Flash point tester NPM 440 (Normalab)	D93
Calorific value	6100 oxygen bomb calorimeter (Parr)	D240
Oxidation stability (110°C)	873 biodiesel rancimat (Metrohm)	EN14112

Table 3.1, continued

Properties	Equipment	Test Method
Copper strip corrosion (3 h, 50°C)	Copper corrosion bath (Stanhope Seta)	EN ISO 2160
Group I metals (Na + K)	Inductively coupled plasma mass spectrometry (ICP-MS) 7500 series (Agilent Technologies)	EN14538
Group II metals (Ca + Mg)	ICP-MS 7500 series (Agilent Technologies)	EN 14538

3.8.1 Acid value (AV)

AV measures the amount of carboxylic acid groups in a chemical compound, such as fatty acid. It is measured in terms of the mass (mg) of KOH required to neutralize the FFAs present in 1 g of sample. The AV of the sample was determined using acid-base titration technique. A standard solution of 0.1 N KOH was prepared as titrant. 5 g of sample was weighed and poured into a conical flask. 25 mL of 2-propanol was measured and poured into the conical flask containing the sample. The mixture was stirred and heated for 5 min. Ten drops of phenolphthalein were added to the mixture as indicator. The sample was then titrated against KOH until the colour of the mixture changed to pink and lasted for 30 s. The AV was calculated using Equation 3.5 (Trinh *et al.*, 2017).

$$AV = \frac{(A-B) \times M \times \text{Molecular weight of KOH}}{m} \quad (3.5)$$

Where

A = Volume of KOH solution used in the titration of the sample (mL)

B = Volume of KOH solution used in the titration of the blank (mL)

M = Molarity of KOH solution (mol/L)

m = Mass of sample (g)

3.8.2 FAME purity

The FAME purity of esterified oil and prepared biodiesel was determined by GC (Agilent GC-7890A). The system was equipped with a HP-INNOWAX capillary column (0.32 mm internal diameter \times 30 m length \times 0.25 μ m film thickness) and a flame ionization detector (FID). The injector and detector were maintained at 250°C. Helium was used as the carrier gas with a constant flow rate of 1.5 mL/min. The oven temperature was programmed according to EN14103:2011 standard as follows: 60°C held for 2 min, then raised to 200°C at a rate of 10°C/min and further increased to 240°C at 5°C/min and held for 7 min. Analysis of each sample was done by dissolving 20 mg of esterified oil or biodiesel with 2 mL of toluene (solvent) in the presence of methyl nonadecanoate as IS. A sample of volume 1 μ L was injected into GC using split mode with a split ratio of 100:1.5. The resulted chromatogram was compared with chromatogram obtained from C8–C24 FAME mix to determine the methyl ester peaks. FAME purity was obtained by comparing the area of methyl ester peaks with IS peak using the Equation 3.6:

$$FAME\ purity = \frac{(\sum A) - A_{EI}}{A_{EI}} \times \frac{w_{EI}}{m} \times 100\% \quad (3.6)$$

In this equation, $\sum A$ is the sum of the peak areas of the FAME content from C8:0 to C24:0, A_{EI} is the peak area of the IS (methyl nonadecanoate), w_{EI} is the weight (mg) of IS and m is the weight (mg) of the sample.

3.8.3 Density at 15°C

Density is the relationship between the mass and volume of a liquid or a solid and can be expressed in grams per liter (g/L). Density of biodiesel was measured by using a density meter. The compartment cell of the density meter was cleaned and dried. The sampling was made and once the oscillation frequency became stable, the density value would be shown (Kamel *et al.*, 2016).

3.8.4 Calorific value

Calorific value shows the energy content in a substance, by measuring the amount of heat produced in a complete combustion. The unit used is usually joules per kilogram, or in this study, megajoules per kilogram (MJ/kg). A bomb calorimeter was used to measure the calorific value of biodiesel. Firstly, a known amount of biodiesel was weighted and put in a crucible. A cotton thread was attached to the fuse wire and positioned just above the surface of biodiesel. After the sample and the cotton thread were placed properly in the bomb, it was charged with oxygen gas from a cylinder. The assembled bomb was then placed in a bucket containing 2 L of distilled water. The biodiesel was burnt in a sealed chamber and the energy released to heat the water could be determined based on the temperature difference.

3.8.5 Flash point

Flash point is the temperature at which the fuel will ignite when exposed to a flame or a spark. It is the lowest temperature at which the fuel will emit enough vapours to ignite and it varies inversely with the volatility of the fuel (Atabani *et al.*, 2013). The flash point of biodiesel was determined by a flash point tester. 75 mL of biodiesel was measured and poured into a brass cup with covered lid. Biodiesel was heated and stirred at specific rate. An ignition source was directed into the brass cup at regular intervals with simultaneous interruption of the stirring until a flash was detected.

3.8.6 Kinematic viscosity at 40°C

Viscosity is defined as the resistance of liquid to flow. It refers to the thickness of the oil, and is determined by measuring the amount of time taken for the oil to pass through an orifice of a specified size (Atabani *et al.*, 2013). Kinematic viscosity is the ratio of the dynamic viscosity to the density of the liquid. Kinematic viscosity of biodiesel was

measured by a viscometer. It uses a rotational coaxial cylinder measuring system which has an integrated density measuring cell. The schematic diagram of measuring cell is shown in Figure 3.4. An outer cylindrical tube is driven by a motor at a constant speed and is filled with the biodiesel sample. A low-density inner cylinder (rotor) is held in the centre of the higher-density sample by buoyancy forces. Consequently, a measuring gap is formed between the tube and the rotor. The rotor is forced to rotate by shear stress in the liquid and is guided axially by a magnet and a soft iron ring. A permanent magnet in the inner cylinder induces eddy currents in the surrounding copper casing. The sample's shear forces drive the rotor while magnetic effects retard its rotation. Shortly after the start of the measurement, the rotor reaches a stable speed. This is determined by the equilibrium between the effect of the eddy current brake and the shear forces at work in the sample. The dynamic viscosity [mPa·s] is calculated from the rotor speed. The integrated density [g/cm³] measurement is carried out by the oscillating U-tube principle. This allows the calculations of the corresponding kinematic viscosity [mm²/s]. To start the kinematic viscosity test, a minimum of 3 mL of biodiesel was loaded to a 5 mL syringe. At least 2 mL of the biodiesel was drawn into the measuring cell and the measurement was started. The value of kinematic viscosity was then recorded.

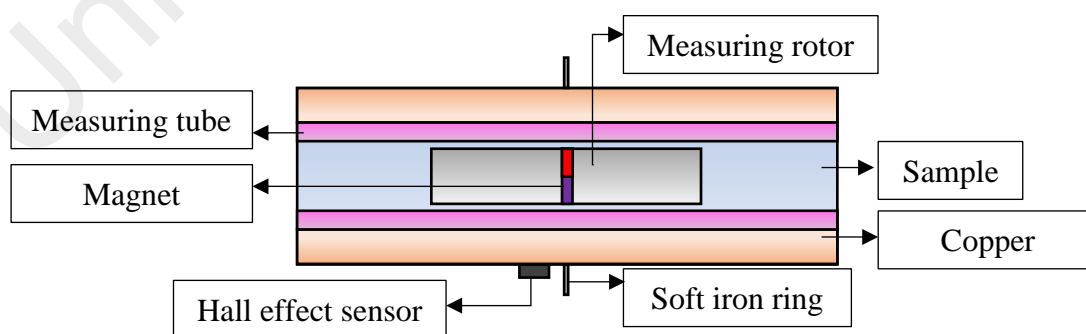


Figure 3.4: Measuring cell of viscometer.

3.8.7 Oxidation stability

Oxidation stability is the tendency of the fuel to react with oxygen at ambient temperature, and it reflects the relative vulnerability of the fuel to be degraded by oxidation (Dharma *et al.*, 2016b). It is one of the critical properties affecting the usage of biodiesel because the presence of unsaturated fatty acid in biodiesel can render it susceptible to oxidation, thus inducing ester polymerisation and formation of insoluble gums that are capable of clogging fuel filters, fouling injectors and interfering with engine performance (Chuah *et al.*, 2016c; Durrett *et al.*, 2008). The oxidative stability test measures the rate at which biodiesel fuel decomposes when subjected to elevated temperatures and vigorous aeration. These conditions accelerate the aging of biodiesel and allow for a rapid measure of fuel stability that has been shown to correlate to the slower oxidative process that occurs under normal storage conditions. During oxidation stability test, 7.5 g of biodiesel was heated to 110°C by a heating block with an air flow of 10 L/h passing through the biodiesel. When biodiesel was exposed to air, acids began to form, which were transferred to a measuring vessel containing 60 mL of distilled water and fitted with an electrode for measuring the conductivity. In the measuring vessel, the change in the conductivity of distilled water caused by the formation of volatile short-chain carboxylic acids (mainly formic and acetic) in the biodiesel was recorded by a computer continuously. Once the acid concentration in the water was high enough, the conductivity underwent a rapid increase that was called an induction period. In other words, induction period is expressed as the time that passes between the moment when the measurement is started and the moment when the formation of oxidation products at 110°C begins to increase rapidly.

3.8.8 Copper strip corrosion

Copper strip corrosion test is used to indicate the presence of components that may be corrosive to copper that come into contact with the biodiesel. It is a qualitative method that is used to determine the level of corrosion of biodiesel product (Hafez *et al.*, 2017). Polished copper strip was put into a tube and biodiesel sample was poured inside the tube until the strip was fully immersed. The tube was then put in the water bath for 3 h at 50°C. The colour and tarnish level of the copper strip after 3 h were then assessed using the corrosion standards following ASTM D130 as shown in Figure 3.5. A visual guide with four categories (1–4) was used to classify the degree of corrosion, with category 1 corresponding to the lowest degree of corrosion (“slight tarnish”) and category 4 corresponding to the highest degree (“corrosion”). A classification number was given after comparing to the ASTM strips.

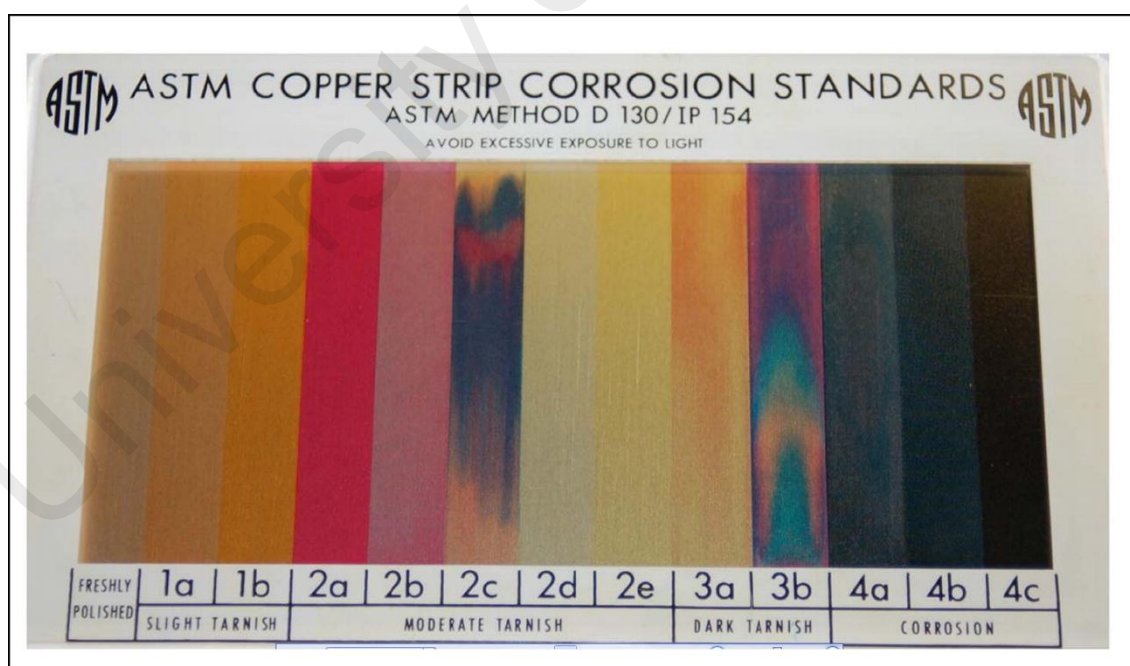


Figure 3.5: Corrosion standards according to ASTM D130 (Hafez *et al.*, 2017).

3.8.9 Group I and II metals

Elements such as Na, K, Ca and Mg are quantified in accordance to biodiesel quality standards. Na and K originate from the biodiesel processing that uses alkaline hydroxides (NaOH or KOH) as catalysts while Ca and Mg are introduced into biodiesel during the purification process as anhydrous MgSO_4 and CaO are used as drying agents. These chemical species may also be inherently present in the raw materials and remain in the final product. The presence of such alkaline and alkaline earth ions may produce residual deposits that clogs the fuel injection system (Almeida *et al.*, 2014). The concentrations of Na, K, Ca and Mg elements in biodiesel were determined through ICP-MS. The biodiesel sample must be subjected to microwave digestion for total decomposition prior to ICP-MS test. Initially, 0.5 g of biodiesel was weighed and poured into an acid-rinsed fluorocarbon digestion vessel. Then 9 mL of HNO_3 and 1 mL of HCl were added to the vessel. The mixture was subjected to a digestion program: ramped to 150°C in 12 min and held for 2 min; then further ramped to 180°C in 5 min and held for 10 min. After digestion and subsequent cooling, 1 mL of the mixture was diluted with distilled water at dilution factor of 100:1 (v/v) for the analysis by ICP-MS.

CHAPTER 4: RESULTS AND DISCUSSION

This chapter includes the results obtained from the research works as well as critical analysis, discussion and comparison with the results from previous studies. There were three sections in this chapter. The first section discusses the impacts of moisture and oil contents in *Jatropha* seeds on the reaction. The second section presents the optimum reaction conditions in producing esterified oil from raw *Jatropha* oilseeds through ultrasound assisted *in-situ* esterification. The parameters such as ultrasonic pulse mode, particle size, n-hexane to methanol volume ratio, H₂SO₄ loading, reaction time and ultrasonic amplitude were evaluated in term of extraction efficiency, esterification efficiency and FAME purity. The seeds before and after ultrasound assisted *in-situ* esterification were then compared through FESEM, TGA, FTIR and elemental analysis. In the third section, biodiesel was synthesized from esterified *Jatropha* oil through ultrasound assisted transesterification. The reaction parameters (KOH loading, methanol to esterified oil molar ratio, reaction time and ultrasonic amplitude) were studied in relation to FAME purity and biodiesel yield. Lastly, the physicochemical properties of *Jatropha* biodiesel produced were characterized and compared with ASTM and EN international standards.

4.1 Moisture and oil contents of *Jatropha* seeds

The presence of water content in seeds > 6.7 wt.% could induce saponification of FFAs, triglycerides and esters which would then reduce the ester yield. For extraction process, water might further reduce the solubility of triglycerides in methanol due to its polarity (Zakaria & Harvey, 2012). The water molecules inside the solid seeds might also hinder the diffusion process and obstruct the extraction efficiency. Since the water content in *Jatropha* seeds was determined to be 1.89 wt.%, there would be minimal detrimental effect on this process. The total oil yield of *Jatropha* seeds was found to be 53.96% by

using Soxhlet extraction after three replicates. The extracted oil content was in line with the reported values from the literature which ranged from 40% to 60% (Kumar & Sharma, 2008).

4.2 Parameters screening for ultrasound assisted in-situ esterification

4.2.1 Effect of ultrasonic pulse mode

The effects of ultrasonic pulse mode (3 s on/2 s off, 5 s on/2 s off, 7 s on/2 s off) on oil extraction efficiency, esterification efficiency and FAME purity are plotted in Figure 4.1. The extraction efficiency did not show appreciable difference at different ultrasonic pulse modes, ranging from 84.58% to 86.36%. It was noticed that ultrasonic pulse mode of 5 s on/2 s off achieved the highest esterification efficiency of 54.85% and FAME purity of 26.64%. Lower esterification efficiency and FAME purity with pulse on time of 3 s were attributed to the mild stirring effects of the ultrasound which are not strong enough to mix the immiscible reactants evenly. By increasing the pulse on time to 5 s, the esterification efficiency and FAME purity increased as better emulsification of the two immiscible layers was achieved (Hingu *et al.*, 2010). However, further increment of the pulse on time to 7 s resulted in decrements of the esterification efficiency and FAME purity. This might be due to the initial vibrational shock experienced by the reactants becoming symmetrical with uniform waves (Samani *et al.*, 2016). Optimum pulse mode of 5 s on/2 s off was then used to optimize the next parameter.

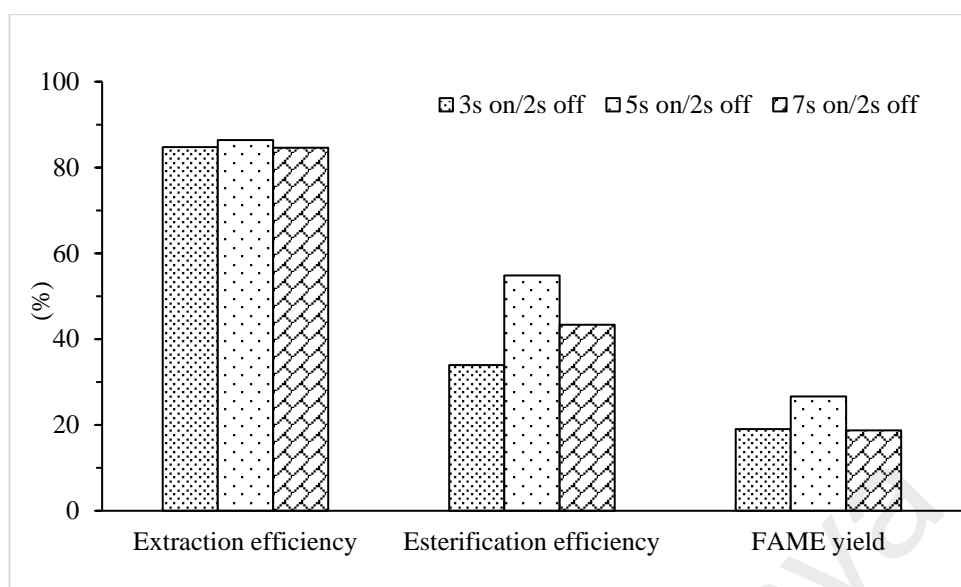


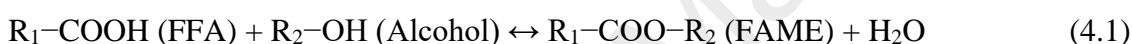
Figure 4.1: Effects of ultrasonic pulse mode on extraction efficiency, esterification efficiency and FAME purity at n-hexane to methanol volume ratio of 3:1, 5 vol.% H₂SO₄, 50% ultrasonic amplitude and 150 min reaction time.

4.2.2 Effect of ultrasonic amplitude

As shown in Figure 4.2, the extraction efficiency increased from 80.62% to 86.36% when ultrasonic amplitude increased from 40% to 50%. It was then declined gradually from 86.36% to 74.69% when amplitude increased from 50% to 70%. At higher ultrasonic amplitude, the cavitation bubble collapses would be harsher, the microjet velocity targeted on the *Jatropha* seed particles would be higher, facilitating the disruption of the plant tissue and increasing the contact area of the seeds to the solvents. Therefore, diffusion of oil into solvents was easier and the extraction efficiency was higher. However, cavitation intensity decreased beyond the optimum ultrasonic amplitude, causing reduction in extraction efficiency. This was because higher ultrasonic amplitude led to higher temperature and vapour pressure which then led to an increment in bubble formation. However, the cavitation bubbles formed contained more vapours. The release of solvent vapours interfered with the cavitational effects, causing cushioning of collapse and less cavitation intensity (Hu *et al.*, 2012; Koutsouki *et al.*, 2016; Tavares *et al.*, 2017b). Similar scenario was observed by Jadhav *et al.* (2016) in the oil extraction from

waste date seeds assisted by ultrasound. In their study, the extraction yield increased from 5.0 to 6.4 g oil per 100 g of seed when the ultrasonic amplitude increased from 22% to 30%. There was no increment detected in the oil extraction yield beyond 30%.

FAME purities of 21.94%, 26.64%, 38.58% and 39.10% were achieved in the ascending order of ultrasonic amplitudes (40, 50, 60 and 70%). When the ultrasonic amplitude was higher, more oil would leach out from the seeds (owing to the phenomenon as described above) and react with the reactants in the presence of H_2SO_4 . Higher temperature attained at higher amplitude further promoted the forward esterification of reversible reaction, as shown in Equation 4.1 by evaporation of H_2O (Andrade-Tacca *et al.*, 2014).



Hence, FAME purity increased. Although the maximum FAME purity was achieved at 70% amplitude, ultrasonic probe suffered from overheating frequently. Since there was only little difference (0.52%) in the FAME purities between 60% and 70% amplitudes, amplitude of 60% was chosen as the optimum value by considering its high esterification efficiency of 71.10%.

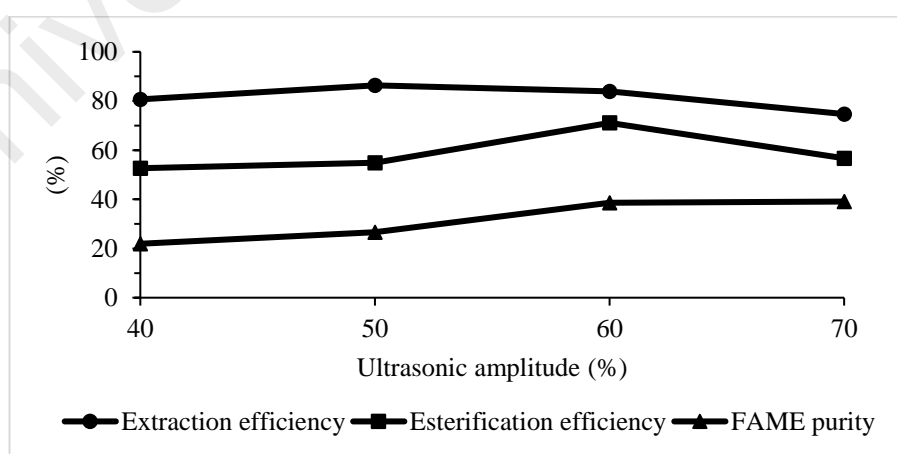


Figure 4.2: Effects of ultrasonic amplitude on extraction efficiency, esterification efficiency and FAME purity at n-hexane to methanol volume ratio of 3:1, 5 vol.% H_2SO_4 , pulse mode of 5 s on/2 s off and 150 min reaction time.

4.2.3 Effect of H₂SO₄ loading

The effects of H₂SO₄ loading (5 to 30 vol.% with a step of 5 vol.%) on oil extraction efficiency, esterification efficiency and FAME purity are depicted in Figure 4.3. Extraction efficiency increased from 83.96% to 89.58% when H₂SO₄ loading increased from 5 to 15 vol.%. It was then dropped to 83.33% with addition of 30 vol.% H₂SO₄. A sudden drop in extraction efficiency at 20 vol.% H₂SO₄ was probably due to more oil lost during washing or oil transferring step. Although increasing trend was observed with addition of H₂SO₄ loading from 5 to 15 vol.% and decreasing trend with 20 vol.% H₂SO₄ loading onwards, H₂SO₄ loading only showed minimum effect in extraction efficiency by observing insignificant difference (0.63%) in the extraction efficiencies between 5 vol.% (83.96%) and 30 vol.% H₂SO₄ (83.33%). On the other hand, larger difference (11.67%) in the extraction efficiency was observed for ultrasonic amplitudes of 40% and 70% (86.36% versus 74.69%). Therefore, it could be deduced that extraction efficiency was more depended on ultrasonic amplitude as compared to H₂SO₄ loading. This might be due to the extraction of triglycerides from the oil solid seeds which depended mainly on the solvation power of the solvents (n-hexane and methanol) (Amalia Kartika *et al.*, 2016).

In term of esterification efficiency, 71.10% was obtained with 5 vol.% H₂SO₄. Increasing trend was noted in general except a significant drop by increasing H₂SO₄ loading from 20 vol.% onwards. There were two possible reasons for this observation. Firstly, there was an increment in the water content in the reaction mixture at high H₂SO₄ loading, reducing the catalytic activity of H₂SO₄ (Santos *et al.*, 2010). Secondly, triglyceride was hydrolysed to form FFAs and low-molecular weight alcohols at high H₂SO₄ loading according to Equation 4.2 (Deng *et al.*, 2010). This claim was supported by Saha and Goud (2014) in the esterification of karanja oil. They observed that the AV of karanja oil decreased from 33 to 4.8 mg KOH/g when H₂SO₄ concentration increased from 0.25 to 0.5 wt.%. However, AV of karanja oil increased slightly when H₂SO₄

concentration was further increased to 1.0 wt.%. In addition, the colour of esterified oil was significantly darkened with the addition of 10 vol.% H₂SO₄ onwards. It was possibly due to the oxidation or cracking of carbon chains (Liu *et al.*, 2012). Choudhury *et al.* (2013) also discovered the darkening of *Jatropha* oil with the addition of H₂SO₄ concentration above 5 wt.% due to the formation of sulfones.



The highest FAME purity of 38.58% was obtained with 5 vol.% H₂SO₄. By increasing H₂SO₄ loading from 10 to 25 vol.%, FAME purity showed an increment from 29.26% to 36.30% and showed a slight decrement to 31.15% when further increasing the H₂SO₄ loading to 30 vol.%. Based on the FAME purity results, one interesting scenario was noticed: 5 and 25 vol.% H₂SO₄ had only a slight difference in FAME purity (38.58% versus 36.30%). Considering the appreciable reduction in esterification efficiency with the addition of 25 vol.% H₂SO₄, it was essential to investigate the effect of esterification efficiency on FAME purity during subsequent transesterification. The esterified oils produced from 5 and 25 vol.% H₂SO₄ were subjected to ultrasound assisted transesterification at methanol to esterified oil molar ratio of 12:1, KOH loading of 1.0 wt.%, 60% ultrasonic amplitude and pulse mode of 5s on/2s off. After 15 min of transesterification, the latter offered higher FAME purity of 99.43% than the former (92.29% FAME purity). In view of economic perspective, higher amount of catalyst will not be profitable due to the cost of the catalysts itself and also subsequent purification process post-reaction (Nigade *et al.*, 2015). Therefore, 5 vol.% H₂SO₄ loading was chosen as the optimum value.

In a similar study, Shuit *et al.* (2010a) had conducted in-situ esterification of *Jatropha* seeds with the assistance of magnetic stirring and heating. Extraction efficiency of 91.20% and FAME purity of 99.80% were achieved in reaction time of 24 h. Although FAME purity obtained in this study was about 2.59-fold lower than their reported FAME

purity (38.58% versus 99.80%), the reaction time was much shorter which was 9.6-fold shorter (2.5 h versus 24 h) and the extraction efficiency only showed a slight difference of 7.24% (83.96% versus 91.20%). It was evident from this comparison that ultrasound can serve as an effective approach as it does not require external agitation or stirring. In addition, it could achieve comparable extraction efficiency and FAME purity in short reaction time as compared to the method of magnetic stirring with external heating.

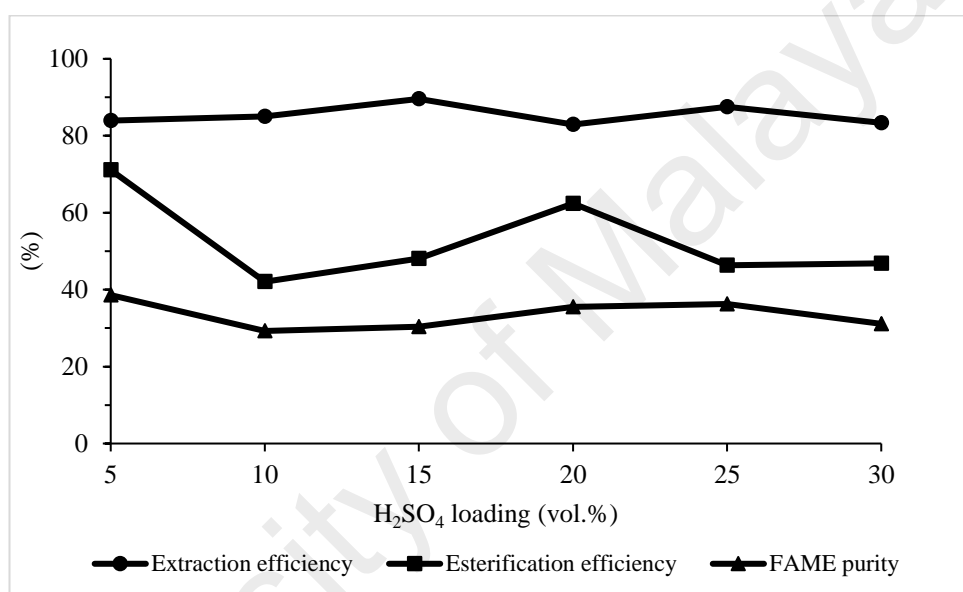


Figure 4.3: Effects of H₂SO₄ loading on extraction efficiency, esterification efficiency and FAME purity at n-hexane to methanol volume ratio of 3:1, 60% ultrasonic amplitude, pulse mode of 5 s on/2 s off and 150 min reaction time.

4.3 Parameters study of ultrasound assisted in-situ esterification

From the results of parameters screening in Section 4.2, it was found out that the optimum H₂SO₄ loading and ultrasonic amplitude were 5 vol.% and 60%, respectively. In order to ensure these two parameters obtained were optimum, further parameter study was conducted to verify the results. For H₂SO₄ loading, values of 3, 4 and 6 vol.% were tested. For ultrasonic amplitude, combination of various reaction times (30 to 150 min) and ultrasonic amplitudes (40%–80%) were examined. In addition, parameters such as particle size and n-hexane to methanol volume ratio were assayed. Considering high n-

hexane to methanol volume ratio and long reaction time in the previous parameters screening, n-hexane to methanol volume ratio was reduced from 3:1 to 1.5:1 and reaction time was reduced from 150 to 60 min for further investigation.

4.3.1 Effect of particle size

In the ultrasound assisted in-situ esterification, particle size plays an important role in extracting oil from *Jatropha* seeds. Effect of particle size (<1, 1–2 and >2 mm) on the oil extraction efficiency, esterification efficiency and FAME purity were investigated at a fixed condition (n-hexane to methanol volume ratio of 1.5:1, 5 vol.% H₂SO₄, 60% amplitude and reaction time of 60 min). From Figure 4.4, it was observed that particle size of 1–2 mm showed the highest oil extraction efficiency, followed by particle sizes of <1 and >2 mm. Smaller particle size has larger interfacial area that facilitates the oil extraction of oil from the seeds, leading to higher oil extraction efficiency (Banković-Ilić *et al.*, 2012). However, particle size of <1 mm had slightly lower oil extraction efficiency than particle size of 1–2 mm as there was positive agglomeration of fine particles due to the sticky oil particles which resulted in reduction of surface area (Mathiarasi & Partha, 2016). For larger particle size, mass transfer limitation existed where oil particles were being trapped deep in the core of the seeds and thus solvent penetration was more difficult for oil leaching (Banković-Ilić *et al.*, 2012; Mathiarasi & Partha, 2016; Shuit *et al.*, 2010a). Therefore, particle size of >2 mm had the lowest oil extraction efficiency. It was also noticed from Figure 4.4 that both the esterification efficiency and FAME purity exhibited similar trend as the oil extraction efficiency for all the three different particle sizes. Nonetheless, particle size had more significant effect in extraction efficiency than esterification efficiency and FAME purity. Higher extraction efficiency would lead to more oil content being extracted out from the seed and thus helped to increase the esterification efficiency and FAME purity.. Particle size of <1 mm had slightly lower

esterification efficiency and FAME purity than particle size of 1–2 mm. This was because smaller particle size than a critical range would be affected more by moisture content produced during esterification which reduced the catalytic activity of H_2SO_4 (Kumar, 2017; Santos *et al.*, 2010). Similar results were observed in the ultrasonic transesterification of *Jatropha* oilseeds conducted by Kumar (2017). Biodiesel conversion of 92.63% was achieved with particle size of 1–2 mm in reaction time of 20 min at 1:100 seed/methanol (w/w) ratio, 1.5 wt.% KOH, 50% ultrasonic amplitude and 0.3 s cycle.

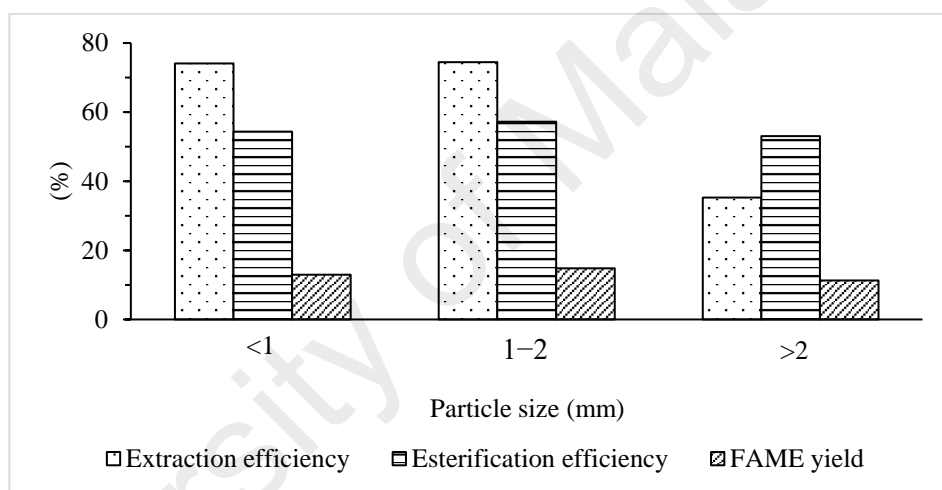


Figure 4.4: Effect of particle size on extraction efficiency, esterification efficiency and FAME purity at n-hexane to methanol volume ratio of 1.5:1, 5 vol.% H_2SO_4 , 60% ultrasonic amplitude and reaction time of 60 min.

4.3.2 Effect of n-hexane to methanol volume ratio

In the ultrasound assisted in-situ esterification of *Jatropha* oilseeds, it is important to ensure that majority of the oil content has been extracted from the seeds. Since the miscibility of methanol and oil is very low, methanol is usually not an effective solvent in oil extraction. Triglycerides are commonly non-polar hydrocarbon molecules, thus n-hexane can be utilised as non-polar co-solvent so as to promote the triglycerides extraction from seeds and enhance the mass transfer of oil into methanol (Amalia Kartika

et al., 2016; Shuit *et al.*, 2010a). In order to investigate the influence of n-hexane on the reactive extraction of *Jatropha* seeds, five different volume ratios of n-hexane to methanol (1:1, 1.5:1, 2:1, 3:1 and 4:1, which corresponds to molar ratio of 0.31:1, 0.46:1, 0.62:1, 0.93:1 and 1.24:1, respectively) were investigated. Other reaction parameters were remained constant (5 vol.% H₂SO₄, 60% amplitude and reaction time of 60 min). From Figure 4.5, it was noticed that n-hexane to methanol volume ratio of 3:1 exhibited the highest extraction efficiency (81.87%) whereas volume ratio of 1:1 showed the lowest extraction efficiency (37.25%). This observation could be explained by the concentration gradient of oil between the inner cell walls of the seed and the bulk solvent (methanol and n-hexane). The volume of total solvent for n-hexane to methanol volume ratio of 1:1 was less than that in the case of n-hexane to methanol volume ratio of 3:1. When the solvent amount was reduced, the concentration gradient decreased and thus extraction efficiency showed a decrement (Amalia Kartika *et al.*, 2016). It was observed from Figure 4.5 that volume ratio of n-hexane to methanol did not show significant effect in esterification efficiency and FAME purity. This observation was similar with the in-situ transesterification of castor seeds conducted by Hincapié *et al.* (2011). However, Dasari *et al.* (2016) reported that n-hexane had an insignificant effect on castor oil biodiesel conversion as well as extraction. From the results obtained in this study, it was revealed that n-hexane participated only in the extraction but not in the reaction. Further increment of the n-hexane to methanol ratio beyond 3:1 did not show positive impact on the extraction efficiency. Therefore, volume ratio of 3:1 was chosen as the optimum volume ratio for further studies.

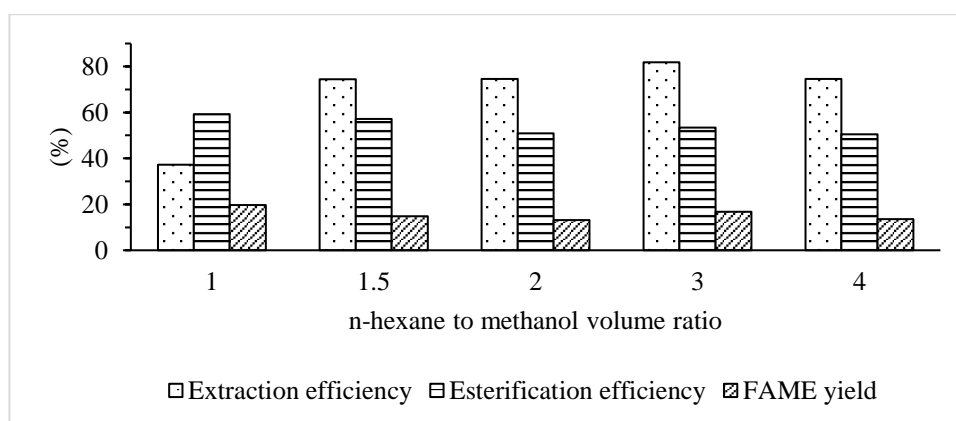


Figure 4.5: Effect of n-hexane to methanol volume ratio on extraction efficiency, esterification efficiency and FAME purity at particle size of 1–2 mm, 5 vol.% H₂SO₄, 60% ultrasonic amplitude and reaction time of 60 min.

4.3.3 Effect of H₂SO₄ loading

To study the effect of H₂SO₄ loading on the oil extraction efficiency, esterification efficiency and FAME purity, ultrasound assisted in-situ esterification reaction was conducted at four different H₂SO₄ loadings (3, 4, 5 and 6 vol.%). As observed from Figure 9, the extraction efficiency increased with the H₂SO₄ amount until 5 vol%. The role of H₂SO₄ in reactive extraction was not only as catalyst but it also helped in accelerating the oil extraction from *Jatropha* seeds as oil dissolved better in acidic solvent (Hensarling & Jacks, 1983; Shuit *et al.*, 2010b). Therefore, increment in the H₂SO₄ loading in the reaction mixture would allow more oil molecules to be diffused faster and easier before subsequently be transesterified to FAME. However, extraction efficiency was discovered to decrease with the addition of 6 vol% H₂SO₄. The esterification efficiency and FAME yield also increased with the H₂SO₄ amount until 5 vol%. This was because by increasing the amount of acid catalyst, there will be more interaction between the proton generated by the acid catalyst and the triglyceride increased, thus pushing the equilibrium of the reaction towards FAME formation (Parkar *et al.*, 2012). In other words, FFA was reduced which corresponded to higher esterification efficiency. However, esterification efficiency decreased slightly with addition of 6 vol.% H₂SO₄ which was possibly due to over-

saturation of catalyst and dilution of reactants from larger amount of water molecules produced from the esterification reaction (Pan *et al.*, 2016). FAME purity also showed a decrement from 16.73% to 15.52% with the addition of 6 vol.% H_2SO_4 . There are two possible reasons for the decrement of FAME purity with the addition of H_2SO_4 loading from 5 to 6 vol.%. Firstly, there was an increment in the water content in the reaction mixture at high H_2SO_4 loading. Secondly, triglyceride molecules were hydrolysed to form FFAs and low-molecular weight alcohols at high H_2SO_4 loading according to Equation 4.2 (Deng *et al.*, 2010). Deng *et al.* (2010) encountered similar scenario in the ultrasound assisted acid esterification of *Jatropha* oil at methanol to *Jatropha* oil ratio of 40 vol.%, 60°C in 1 h reaction time. The AV of *Jatropha* oil decreased from 10.45 to 1.21 mg KOH/g when H_2SO_4 concentration increased from 1 to 4 vol.%. However, the AV rose again from 1.21 to approximately 6 mg KOH/g when further increased H_2SO_4 concentration from 4 to 6 vol.%. Saha and Goud (2014) also asserted the similar view about the increase in AV with an increment in the H_2SO_4 loading.

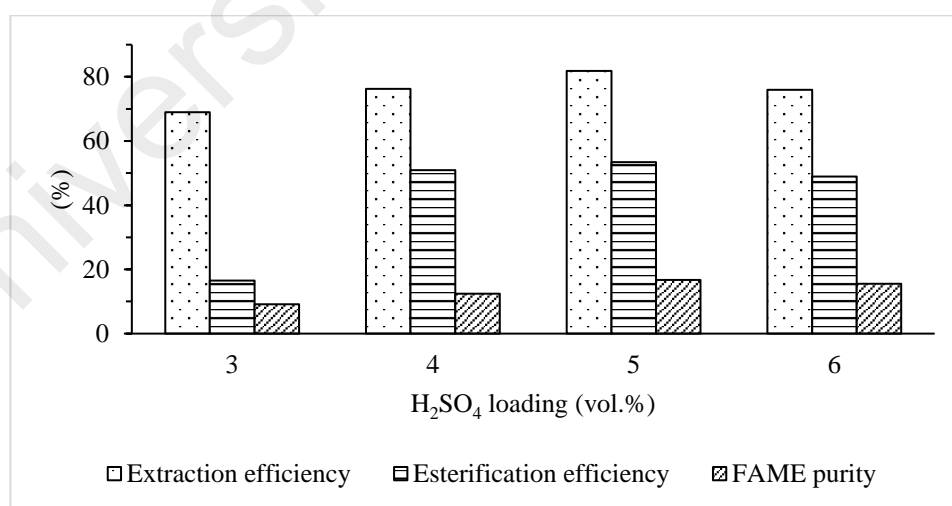


Figure 4.6: Effect of H_2SO_4 loading on extraction efficiency, esterification efficiency and FAME purity at particle size of 1–2 mm, n-hexane to methanol volume ratio of 3:1, 60% ultrasonic amplitude and reaction time of 60 min.

4.3.4 Reaction time and ultrasonic amplitude

Sufficient contact time is important to ensure completion of the esterification reaction (Hayyan *et al.*, 2011). In addition, ultrasonic amplitude is also taken into account in esterification reaction. Reaction time and ultrasonic amplitude are inter-related to each other (Somnuk *et al.*, 2013). FFA reduction cannot be attained within a short reaction time when low amplitude is introduced thus esterification efficiency and FAME purity will be lower (Somnuk *et al.*, 2013). The effect of various reaction times (30 to 150 min) and ultrasonic amplitudes (40 to 80%) on the extraction efficiency is presented in Figure 4.7. Generally, extraction efficiency increased with reaction time at any amplitude. This was because the impact of ultrasound on ultrasound would be greater when reaction time was prolonged. More cracks and microfractures would be created on the seed surface. At the same time, impingement by high-speed jets results in surface peeling, erosion and particle breakdown. Due to these, the solvent (methanol and hexane) can easily penetrate the plant's cell wall into the cell tissues, accelerate the oil bodies with solvent and permit oil bodies release into the solvent (Jadhav *et al.*, 2016; Shirsath *et al.*, 2012). Towards the end of the reaction, extraction efficiencies of 86.36% and 83.96% were found to be the highest and second highest extraction efficiencies at 50% and 60% amplitudes, respectively.

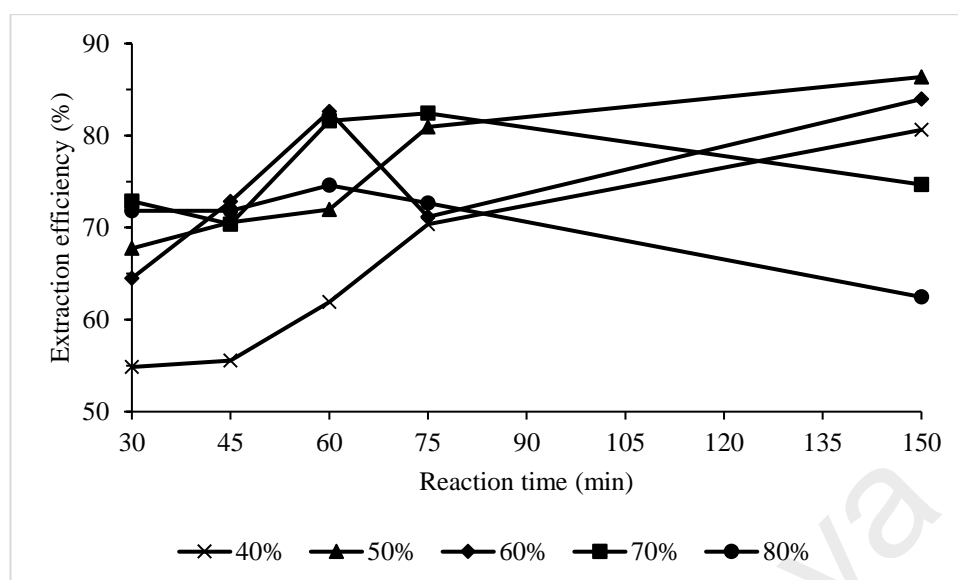


Figure 4.7: Effect of various reaction times and ultrasonic amplitudes on extraction efficiency at particle size of 1–2 mm, n-hexane to methanol volume ratio of 3:1, 5 vol.% H₂SO₄.

The effect of various reaction times and ultrasonic amplitudes on the esterification efficiency is shown in Figure 4.8. As it can be observed, the esterification efficiency increased with reaction time until 60 min and decreased with further increased in reaction time for amplitudes 40%, 70% and 80%. For amplitude 50%, esterification efficiency showed a decrement after 75 min. Increment in reaction time beyond optimum causes the esterification reaction to proceed in backward direction since it is reversible process and hence reduction in the esterification efficiency was observed. For amplitude 60%, esterification efficiency exhibited increasing trend in general. The highest esterification efficiency of 71.10% was found at 60% amplitude with reaction time of 150 min.

The effect of various reaction times and ultrasonic amplitudes on the FAME purity is illustrated in Figure 4.9. It was noticed from Figure 4.9 that FAME purity increased with an increment in reaction time at any amplitude. For amplitudes 40% and 50%, the FAME purity increased in a slower rate with an increment in reaction time. For amplitudes 60% onwards, the FAME purity increased in a faster rate especially from 75 min to 150 min. The highest FAME purity of 40.03% was achieved at 80%, followed by FAME purity of

39.10% at 70% and FAME purity of 38.58% at 60% with reaction time of 150 min. Higher FAME purities acquired at 70% and 80% amplitudes were attributed to higher temperature attained when higher amplitude was introduced, which further promoted the forward esterification of reversible reaction as shown in Equation 4.1 by H₂O evaporating (Andrade-Tacca *et al.*, 2014).

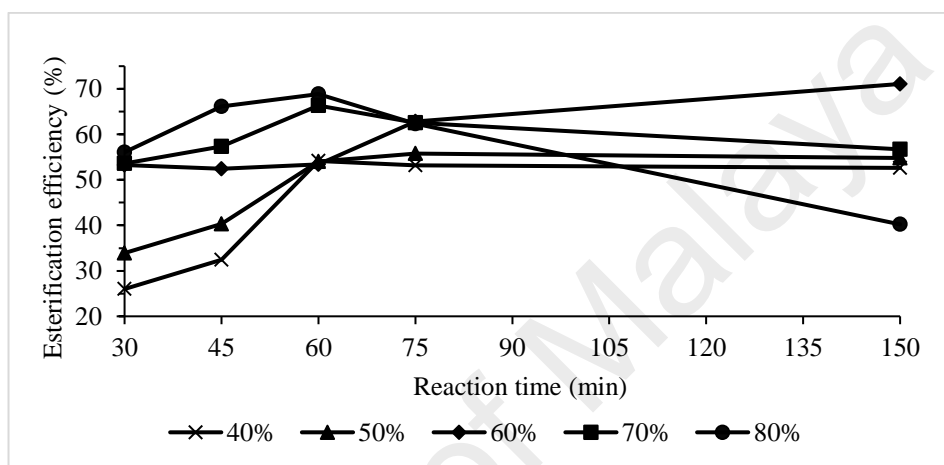


Figure 4.8: Effect of various reaction times and ultrasonic amplitudes on esterification efficiency at particle size of 1–2 mm, n-hexane to methanol volume ratio of 3:1, 5 vol.% H₂SO₄.

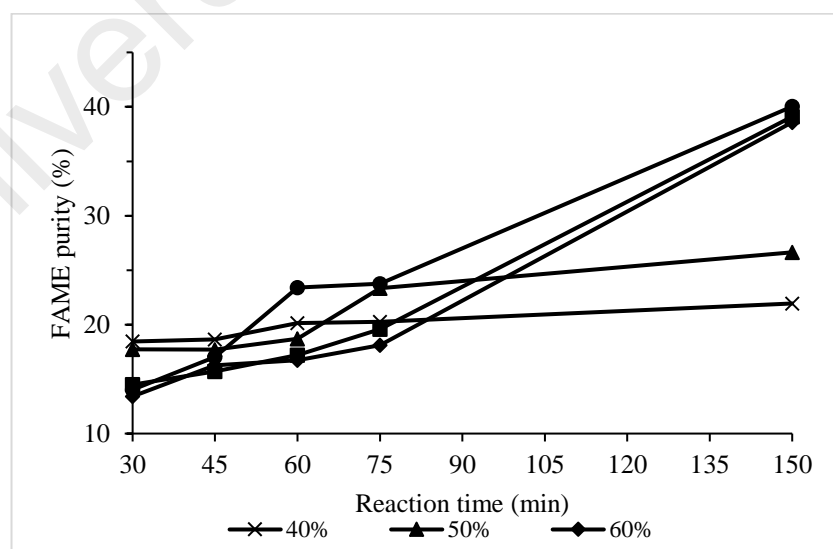


Figure 4.9: Effect of various reaction times and ultrasonic amplitudes on FAME purity at particle size of 1–2 mm, n-hexane to methanol volume ratio of 3:1, 5 vol.% H₂SO₄.

However, overheating of the ultrasonic probe was being encountered at 70% and 80% amplitudes which affected the consistency of the experimental results. Therefore, it was suggested that 150 min reaction time and 60% amplitude were chosen as the optimum parameters as they were sufficient for the completion of the esterification reaction as well as having high extraction efficiency of 83.96%. Somehow, it was found that AV of esterified *Jatropha* oil was reduced from 18.18 to 5.26 mg KOH/g at 60% amplitude with reaction time of 150 min. Apparently, the final AV was higher than the acceptable limit (4 mg KOH/g) for further transesterification. However, Canakci and Van Gerpen (2001) had reported that transesterification would not occur if FFAs content in the oil was about 3 wt.%. Preliminary transesterification was conducted to determine the viability of esterified oil containing AV of 5.26 mg KOH/g to undergo transesterification. Biodiesel yield of 92.29% was obtained at methanol to esterified oil molar ratio of 12:1, 1 wt.% KOH and 60% ultrasonic amplitude in reaction time of 15 min. AV was reduced from 5.26 to 1.64 mg KOH/g, corresponding to esterification efficiency of 68.82%. Therefore, it was proven that this novel method could allow oil containing high FFA content more than 3 wt.% to undergo transesterification process. Consequently, limitation of FFA content can be reduced considerably.

4.4 Seed characterization

4.4.1 FESEM

After ultrasound assisted in-situ esterification, the *Jatropha* seeds showed notable differences in surface morphology compared to the raw de-oiled *Jatropha* seeds as revealed through the micrographs shown in Figure 4.10. It was observed from Figure 4.10(a) and (b) that raw de-oiled *Jatropha* seed particles were isolated from each other and the *Jatropha* seed particles after ultrasound assisted in-situ esterification agglomerated with each other as depicted in Figure 4.10(c) and (d). Agglomeration of the

ultrasonic esterified *Jatropha* seed particles could be attributed to the presence of stronger functional groups bonding between them. More intense peaks were found in the *Jatropha* seeds after ultrasound assisted in-situ esterification as revealed through FTIR analyses in Section 4.4.2. In addition, it was noticeable from Figure 4.10(b) that the raw de-oiled seed particles had relatively smooth and intact surface. On the other hand, the ultrasonic esterified seed particles possessed uneven, disrupted and irregular surface which as observed from Figure 4.10(d). It could be deduced that when ultrasonic waves passed through the reaction mixture, the cavities (bubbles) were generated and collapsed. The asymmetric collapse of these cavities resulted in the generation of a violent shock wave and high-speed jet. These shock waves then struck the seed surface, which broke the stagnant layer as well as created cracks, crevices, and microfractures. At the same time, impingement by high-speed jets results in surface peeling, erosion and particle breakdown (Jadhav *et al.*, 2016; Shirsath *et al.*, 2012).

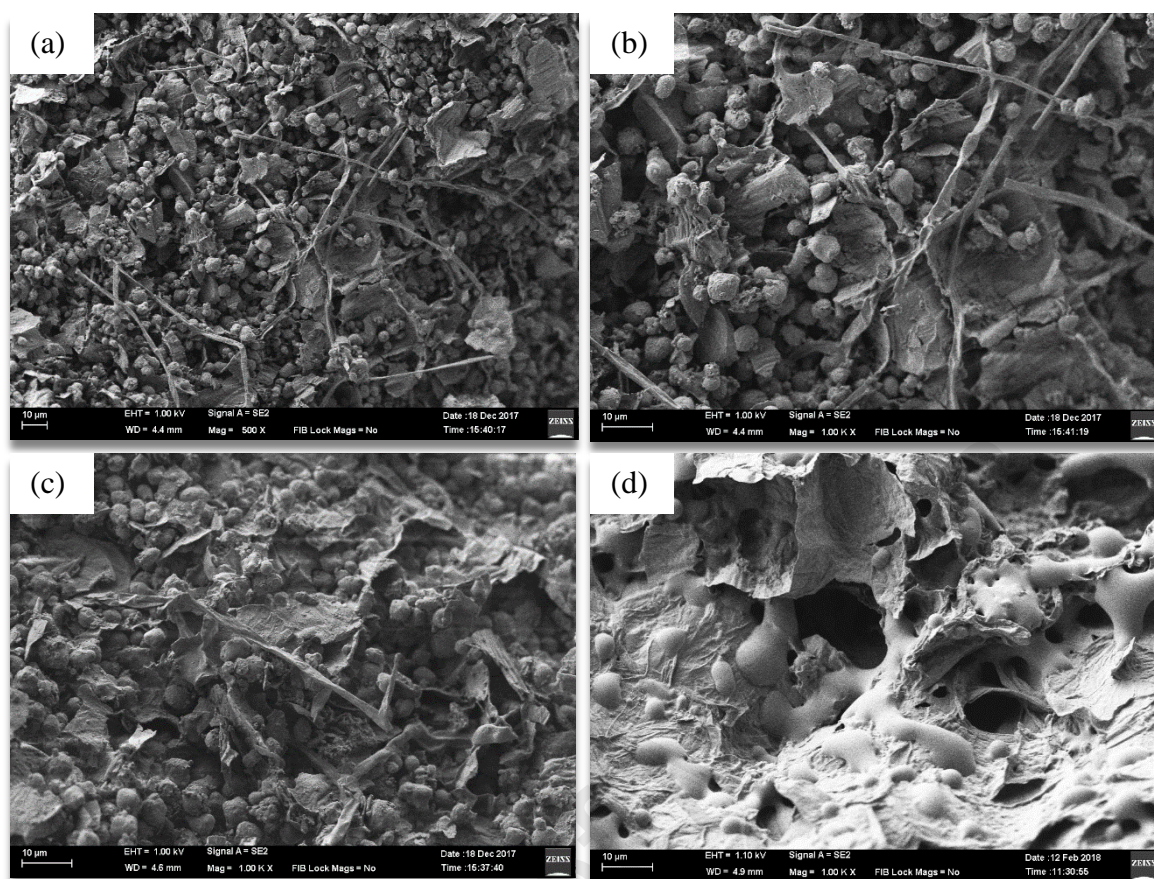


Figure 4.10: FESEM images of raw de-oiled *Jatropha* seeds at magnification of (a) 500× (b) 1000× and ultrasonic esterified *Jatropha* seeds at magnification of (c) 500× (d) 1000×.

4.4.2 FTIR

Figure 4.11 presents the FTIR spectra of the *Jatropha* seeds before and after ultrasound assisted in-situ esterification. Peaks observed at 3007 and 3274 cm^{-1} in respective Figure 4.11(a) and (b) were associated to O–H stretching vibration, denoting the presence of alcohols, phenolic groups of cellulose and lignin, carboxylic acids or water (Abdullah *et al.*, 2017; Sait *et al.*, 2012). Sharp peaks at 2851–2918 and 2854–2924 cm^{-1} in respective to Figure 4.11(a) and (b) were attributed to the symmetrical and asymmetrical C–H stretching vibrations (CH_2 group), owing to the presence of fatty acids in the *Jatropha* seeds (Shak & Wu, 2014). The raw *Jatropha* seeds showed band at 1653–1741 cm^{-1} was attributed to the stretching vibration of C=O in hemicelluloses (Briones *et al.*, 2011; Sait *et al.*, 2012). On the other hand, ultrasonic esterified seeds showed bands with higher

peak intensity at 1625–1741 cm^{-1} which was assigned to C=O stretching of esters (Briones *et al.*, 2011). The presence of ester was resulted from the esterification reaction between FFA and methanol with the aid of H_2SO_4 . The bands that appeared at 1541 and 1526 cm^{-1} in respective Figure 4.11(a) and (b) were likely due to aromatic ring in phenolic compounds in seeds (Balasundram *et al.*, 2006; Sait *et al.*, 2012). The peaks found at 1463 and 1449 cm^{-1} in respective raw and ultrasonic esterified seeds could possibly indicate the presence of alkanes (C–H bending) (Sait *et al.*, 2012). C–O stretching vibrations were observed within the range of 1039–1237 cm^{-1} in both raw and ultrasonic esterified *Jatropha* seeds which were due to existence of carboxylic acids, esters and alcohols (Sait *et al.*, 2012). However, ultrasonic esterified seeds had two peaks with high intensity as compared to five peaks with low intensity. The possible reason could be due to the FFA in the *Jatropha* seed was converted to biodiesel towards the end of the esterification reaction. Lastly, band at 456–863 cm^{-1} related to the long chain band was discovered with more intense in ultrasonic esterified seeds than raw seeds (Abdullah *et al.*, 2017).

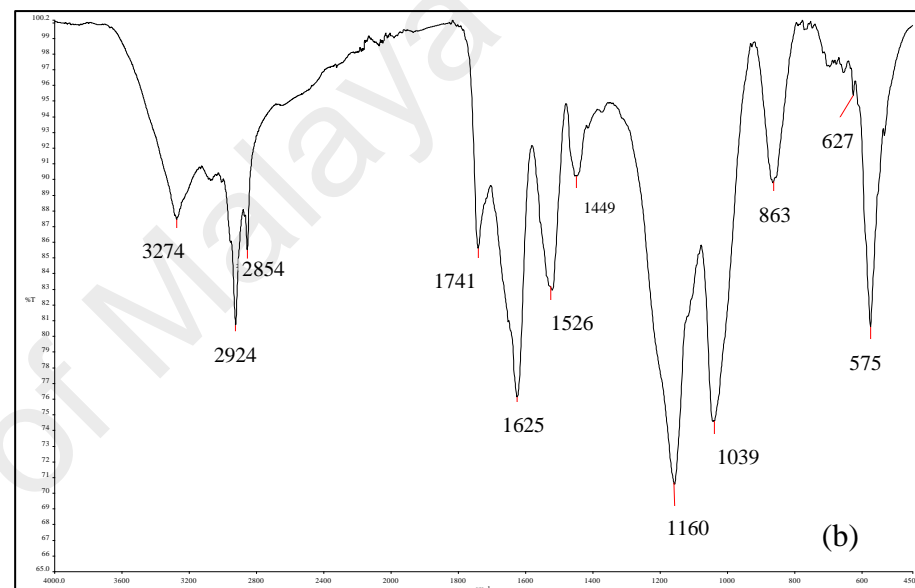
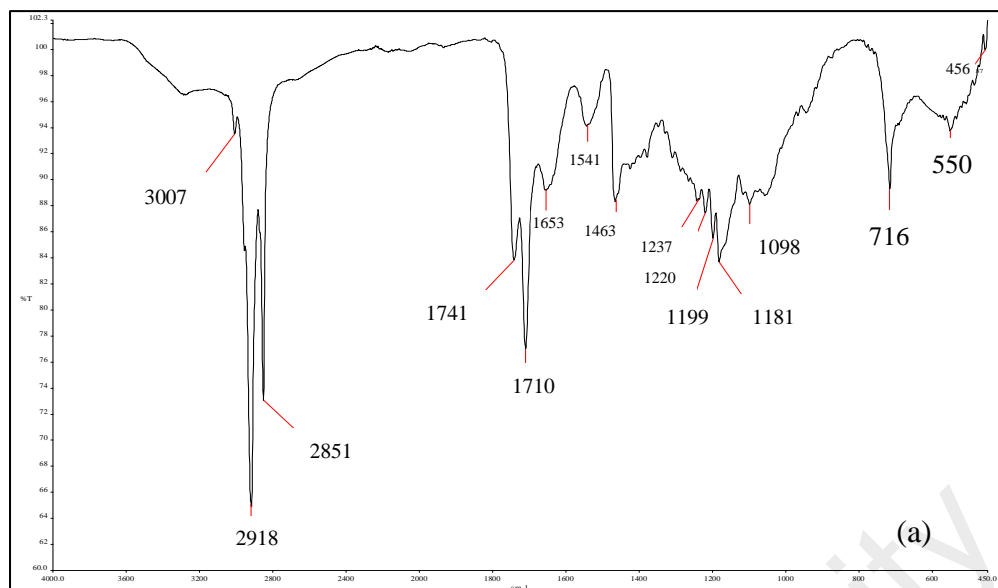


Figure 4.11: FTIR spectra of *Jatropha* seeds (a) before and (b) after ultrasound assisted in-situ esterification.

4.4.3 TGA

The TGA profiles of the *Jatropha* seeds before and after ultrasound assisted in-situ esterification are shown in Figure 4.12. The TGA curves measure the seed weight loss against temperature. There were two significant weight losses which could be observed for raw and ultrasonic esterified *Jatropha* seeds. The first weight loss occurred between temperature range of 200°C to 300°C which was attributed to the thermal decomposition of hemicellulose. The second weight loss took place between 300°C and 450°C which was attributed to the thermal decomposition of cellulose. Hemicellulose is amorphous which is thermally unstable due to the presence of acetyl groups. On the other hand, cellulose is highly crystalline and thus it is thermally stable (Ke *et al.*, 2012). A similar trend was exhibited by both types of *Jatropha* seeds but ultrasonic esterified *Jatropha* seeds had better decomposition at lower temperature. It was proposed from the results that ultrasound could break down the seed matrix, rendering the biomass compounds to be more susceptible to thermal degradation (Zahari *et al.*, 2015). It was also noted that there was no significant weight loss after 700°C while ultrasonic esterified seed still suffered from weight loss until 900°C. This phenomenon might be due to the reduction of lignin content in the ultrasonic esterified seed after breakage by the ultrasonic energy waves (Thiagarajan *et al.*, 2016).

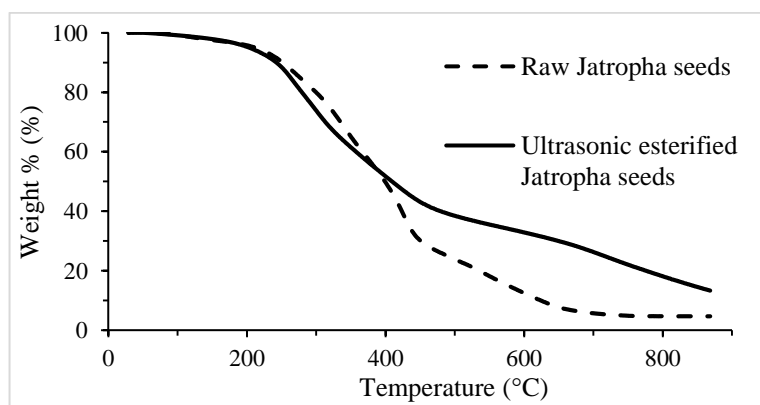


Figure 4.12: TGA curves of raw *Jatropha* seeds and ultrasonic esterified *Jatropha* seeds.

4.4.4 Elemental analysis

As inferred from Figure 4.13, the major components found in both of the raw *Jatropha* seeds and ultrasonic esterified *Jatropha* seeds were carbon and oxygen. Decrement in the carbon content after ultrasound assisted in-situ esterification was attributed to the extraction of oil (Zahari *et al.*, 2015). The presence of nitrogen would indicate the existence of protein in the seeds (Singh & Bothara, 2014). The crude protein content could be estimated from the nitrogen composition ($N \times 6.25$) (Schroeder *et al.*, 2017). From the calculation, ultrasonic esterified *Jatropha* seeds was found to have higher crude protein content than raw *Jatropha* seeds, which were 48.18% and 26.75%, respectively. This difference could indicate that ultrasonic esterification did not significantly remove those nutrients that could serve as valuable source of nitrogen during the bioethanol fermentation process (Zahari *et al.*, 2015). Similar trends in all the elemental compositions were also observed in the ultrasound assisted reactive extraction of *Jatropha* seeds undertaken by Zahari *et al.* (2014a) in the presence of H_2SO_4 as catalyst.

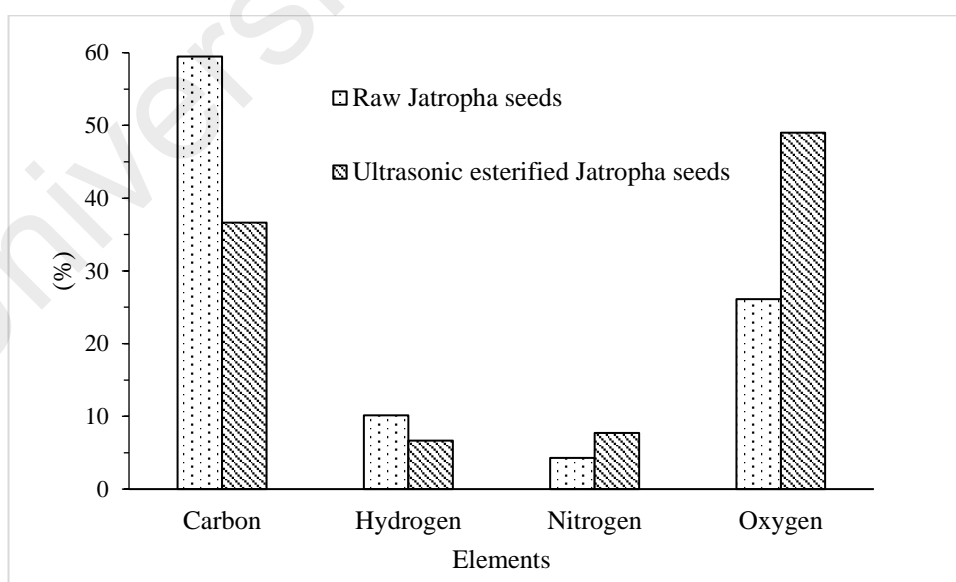


Figure 4.13: Elemental analyses of raw *Jatropha* seeds and ultrasonic esterified *Jatropha* seeds.

4.5 Parameter study of ultrasound assisted transesterification

4.5.1 Effect of KOH loading

The effect of KOH loading (0.5 to 2.0 wt.% with increment of 0.5 wt.%) on FAME purity and biodiesel yield was evaluated at methanol to esterified oil molar ratio of 12:1, amplitude of 60% in reaction time of 15 min. It was noticed from Figure 4.14 that FAME purity increased from 18.28% to 99.03% and biodiesel yield increased from 15.11% to 83.09% as the KOH loading increased from 0.5 to 1.5 wt.%. Thereafter, when KOH loading further increased from 1.5 to 2.0 wt.%, FAME purity decreased from 99.03% to 98.77% and biodiesel yield decreased from 83.09% to 81.86%. Further increment in the catalyst loading caused a decrement in the yield obtained as the addition of excessive alkaline catalyst could cause more triglycerides to react with the catalyst through saponification (Encinar *et al.*, 2012b). Emulsions were observed in the washing step and thus hindered the purification of ester from soap. In addition, large amount of catalyst increases the solubility of FAME in the glycerol, resulting in a noticeable amount of FAME remaining in the glycerol phase after phase separation (Noureddini *et al.*, 1998).

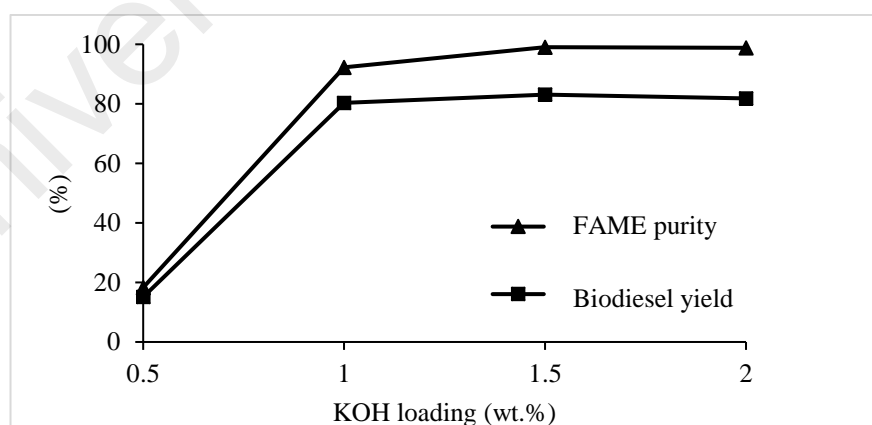


Figure 4.14: Effect on KOH loading on FAME purity and biodiesel yield at methanol to esterified oil molar ratio of 12:1, amplitude of 60% and reaction time of 15 min.

4.5.2 Effect of methanol to esterified oil molar ratio

The effect of methanol to esterified oil molar ratio (9:1, 12:1, 15:1 and 18:1) on the FAME purity and biodiesel yield was investigated at KOH loading of 1.5 wt.% and 60% amplitude with reaction time of 15 min. By observing Figure 4.15, when methanol to esterified oil molar ratio increased from 9:1 to 12:1, FAME purity increased from 93.31% to 99.03% and biodiesel yield increased from 76.68% to 85.20%. Further increasing molar ratio from 12:1 to 18:1, FAME purity decreased from 99.03 to 92.82% and biodiesel yield decreased from 85.20 to 72.42%. It could be noticed that biodiesel and FAME purities showed decreasing trends when further increasing the molar ratio from 12:1 onwards. This was because there might be less effect of methanol to oil molar ratio on the biodiesel yield beyond the optimum molar ratio (12:1) under ultrasonication process. The decrease in the biodiesel yield with an increase of molar ratio from 12:1 onwards might be attributed to the over dilution of biodiesel and glycerol and might also be due to the shifting of the equilibrium reaction towards the reactant side, which reduced the effective yield (Pukale *et al.*, 2015). It was noticed also that the FAME purity decreased beyond the optimum molar ratio (12:1). This was due to higher dissolution of glycerol and alcohol in biodiesel which affected the purity of biodiesel when the amount of methanol increased in the mixture (Samani *et al.*, 2016).

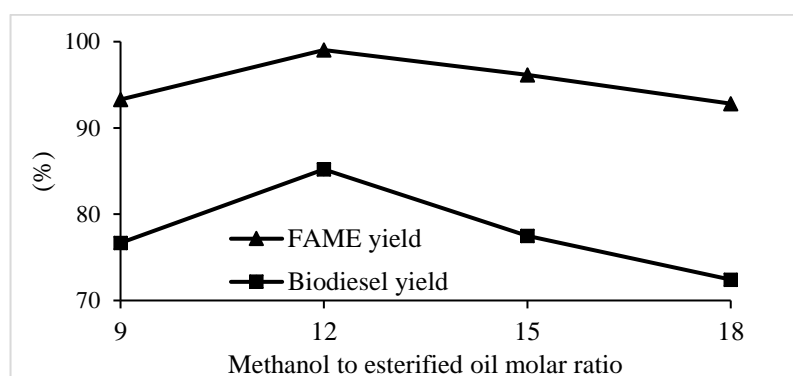


Figure 4.15: Effect of methanol to esterified oil molar ratio on FAME purity and biodiesel yield at KOH loading of 1.5 wt.%, ultrasonic amplitude of 60% and reaction time of 15 min.

4.5.3 Effect of reaction time and ultrasonic amplitude

In the absence of external heat supply to the reaction, reaction time and ultrasonic amplitude play important roles in driving the reaction to completion. Reaction time and ultrasonic amplitude should be sufficient to rise the reaction temperature significantly and provide efficient mixing to overcome heterogeneity in the reaction mixture (Gude & Grant, 2013). From Figure 4.16, it could be noticed that FAME purity increased slightly with reaction time without a drop for ultrasonic amplitude of 50% which indicated that the reaction was not complete. FAME purity at 20 min was 94.66% which had not fulfilled the FAME purity requirement of 96.5% as per EN14214. This observation could be explained through lower reaction temperature at 50% amplitude, the viscosity of oil was higher which then impeded the bubble formation, resulting in poor mixing between the oil and alcohol-catalyst phases (Gude & Grant, 2013; Takase *et al.*, 2014b). From Figure 4.17, it could be observed that biodiesel yield at 50% ultrasonic amplitude had the same trend as FAME purity.

For ultrasonic amplitude of 60%, FAME purity increased from 98.67% to 99.03% and biodiesel yield increased from 79.32% to 85.20% by increasing the reaction time from 10 to 15 min. This was because reaction temperature would increase as higher ultrasonic amplitude was introduced. The viscosity of oil would also decrease and it could become susceptible to cavitation. Consequently, the miscibility of alcohol in oil increased and subsequently promoted biodiesel formation (Mahamuni & Adewuyi, 2009). However, prolonged reaction time to 20 min had resulted in a decrement in FAME purity and biodiesel yield to 96.01% and 80.94%, respectively. This scenario might be due to vaporization of alcohol which reduced the contact area with the reactant (Koh & Ghazi, 2011).

For ultrasonic amplitude of 70%, FAME purity and biodiesel yield showed decreasing trend generally. FAME purity of 97.13% was achieved at reaction time of 10 min but it

decreased to 96.42% and 95.77% at reaction time of 15 min and 20 min, respectively. Similarly, biodiesel yield of 73.23% was achieved at reaction time of 10 min but it decreased to 70.53% and 70.28% at reaction time of 15 min and 20 min, respectively. Beyond the optimum reaction time and ultrasonic amplitude, higher reaction temperature accelerated side reactions such as saponification (Eevera *et al.*, 2009; Leung *et al.*, 2010). Another reason could be ascribed to the damping effect of the cavitation effects at higher operating temperatures (Hingu *et al.*, 2010; Parida *et al.*, 2016). At higher reaction temperature, the equilibrium vapour pressure increased which led to easier bubble formation. However, the cavitation bubbles formed would contain more vapours. The release of solvent vapours interfered with the cavitation effects, causing cushioning of collapse. Therefore, bubbles imploded with less intensity and reduced the mixing effect of ultrasound on the transesterification reaction, resulting in reduced mass transfer and biodiesel yield (Gude & Grant, 2013; Gupta *et al.*, 2015; Martinez-Guerra & Gude, 2015).

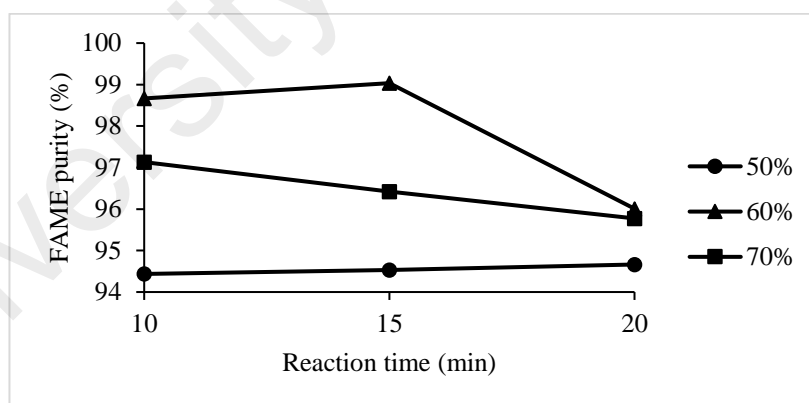


Figure 4.16: Effect of various reaction times and ultrasonic amplitudes on FAME purity at methanol to esterified oil molar ratio of 12:1 and KOH loading of 1.5 wt.%.

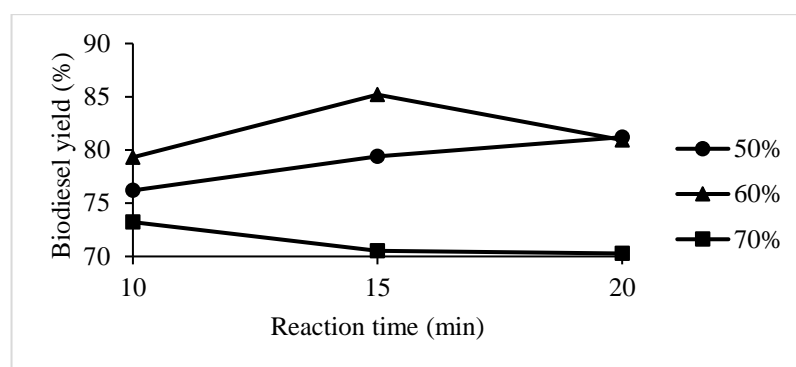


Figure 4.17: Effect of various reaction times and ultrasonic amplitudes on biodiesel yield at methanol to esterified oil molar ratio of 12:1 and KOH loading of 1.5 wt.%.

4.5.4 Physicochemical properties of biodiesel

The properties of biodiesel were tabulated in Table 4.1 together with limits of international standards of biodiesel: ASTM D6751 and EN14214. It could be noticed that all the *Jatropha* biodiesel properties met the standards as per ASTM D6751 and EN14214 except AV. Generally, biodiesel with high AV is undesirable as it can cause severe corrosion of the fuel supply system and internal combustion engine, resulting from degradation of the fuel in service (Dharma *et al.*, 2016a). In this study, the AV of *Jatropha* biodiesel was determined as 0.605 mg KOH/g which was beyond the minimum acceptable limits specified in ASTM D7651 and EN14214 (0.5 mg KOH/g). Nonetheless, high FAME purity of 99.03% was achieved which was above the minimum required limit (96.5%) given in EN14214.

Table 4.1: Properties of *Jatropha* biodiesel in comparison to standards.

Properties	Unit	ASTM D6751	EN14214	This study
AV	mg KOH/g	Max. 0.5	Max. 0.5	0.605
FAME purity	wt. %	–	Min. 96.5	99.03
Density (15°C)	kg/m ³	Max. 880	860–900	881.2
Kinematic viscosity (40°C)	mm ² /s	1.9–6.0	3.5–5.0	4.44
Flash point	°C	Min. 130	Min. 101	220.5
Calorific value	MJ/kg	–	–	39.90
Oxidation stability (110°C)	h	Min. 3	Min. 6	11.96

Table 4.1, continued

Properties	Unit	ASTM D6751	EN14214	This study
Copper strip corrosion (3 h, 50°C)	–	Max. No. 3	Max. No. 1	No. 1b
Group I metals (Na + K)	mg/kg	Max. 5	Max. 5	1.86
Group II metals (Ca + Mg)	mg/kg	Max. 5	Max. 5	3.90

Density is a very important property to gauge diesel engine performance as it affects the fuel injection process as well as pump and pipeline design. All diesel injection systems measure the fuel on a volume basis, so fuel density affects the total mass of fuel injected. Delivery of the exact fuel amount by injection system would ensure proper combustion (Atabani *et al.*, 2013; Dharma *et al.*, 2016b; Encinar *et al.*, 2012a). In this study, the density of biodiesel was 881.2 kg/m³ which was between the range of 860–900 kg/m³ according to EN14214. However, the density value of *Jatropha* biodiesel was slightly higher as compared to ASTM D6751 (maximum 880 kg/m³).

Viscosity plays a major role in fuel injection and combustion process. Higher viscosity affects the fuel fluidity and leads to a higher drag in the injection pump, causing higher pressures and injection volumes, especially at low engine operating temperatures. As a result, a delay in the mixing of air with fuel occurs in the combustion chamber due to a reduction in intake stroke. The timing for fuel injection and ignition tends to be slightly advanced for biodiesel, which may, in turn, lead to higher NO_x emissions due to higher maximum combustion temperatures (Dharma *et al.*, 2016b; Encinar *et al.*, 2012a). The formation of NO_x is very sensitive to temperature and it increases with increasing combustion temperature of biodiesel (>1800 K) (Altun *et al.*, 2008). Plus, fuel with high viscosity tends to form larger droplets on injection which can cause poor combustion, increasing exhaust smoke and emissions (Mohod *et al.*, 2014). Carbon deposition on the injectors also occurs due to insufficient atomization (Atabani *et al.*, 2013; Encinar *et al.*,

2012b). On the other hand, the lower the viscosity of fuel, the easier it is to pump and atomize and achieve finer droplets for combustion. However, fuel with low viscosity may not be able to supply sufficient fuel to fill the pumping chamber, and again this effect will be a loss in engine power (Mohod *et al.*, 2014). Therefore, it is essential that the kinematic viscosity of biodiesel must follow the standard requirements according to ASTM D 6751 (1.9–6.0 mm²/s) and EN 14214 (3.5–5.0 mm²/s) (Atabani *et al.*, 2013). In this study, the kinematic viscosity of *Jatropha* biodiesel was 4.44 mm²/s which indicated that the biodiesel is easier to pump and atomize and achieve finer droplets for combustion.

The flash point of biodiesel (usually more than 150 °C) is higher than the conventional diesel fuel (55–66 °C) which makes it safer as high flash point value will decrease the risk of fire. Low flash point will also indicate the presence of alcohol or other low boiling-point solvents and therefore it is a very important parameter to be determined considering handling, storage and safety of the fuel (Atabani *et al.*, 2013; Dharma *et al.*, 2016b; Dias *et al.*, 2008). It is essential that the biodiesel component must meet flash point criteria, prior to blending, for the purpose of assuring that the biodiesel component does not contain alcohol (Hingu *et al.*, 2010). In this study, the flash point of *Jatropha* biodiesel was 220.5°C which was higher than the minimum limits prescribed in ASTM D6751 (130°C) and EN14214 (101°C). This high flash point value would account for safe storage and transportation due to the reduced risk of fire (Mathiarasi & Partha, 2016).

In general, a high calorific value is desirable since it is indicative of the energy content of the fuel. The *Jatropha* biodiesel produced in this study had a high calorific value of 39.90 MJ/kg. For oxidation stability, the influence of molecular structure on the rate of oxidation of biodiesel is greater than the influence of environmental conditions such as air, light, heat and the presence of metal, traces and peroxides (Chuah *et al.*, 2016c; Durrett *et al.*, 2008). The fatty acid composition with a high percentage of unsaturated fatty acids could lead to poor oxidation stability, unless antioxidants are added to the

biodiesel (Chuah *et al.*, 2016c). Poor oxidation stability would increase viscosity of fuel and cause formation of contaminants such as sediment and gums, thus leading to poor engine performance (Hoekman *et al.*, 2012). In this study, the oxidation stability was 11.96 h which was much better than the minimum duration specified in the ASTM D7651 and EN14214 standards.

Copper strip corrosion test is an indication of the presence of components that may be corrosive to copper that come into contact with the fuel. The test is generally assumed to be due to the presence of sulphur compounds in the fuel (Hafez *et al.*, 2017). In this study, the result of the copper strip corrosion test was 1b which indicated the absence of corrosive compounds or acids that potentially affects the copper (Torrentes-Espinoza *et al.*, 2017). As mentioned in Section 3.8.9, the presence of such alkaline and alkaline earth ions (Na, K, Ca and Mg) may produce residual deposits that clogs the fuel injection system (Almeida *et al.*, 2014). In this study, both of the combined Na + K and Ca + Mg amounts found in the *Jatropha* biodiesel fulfilled the specifications as given in ASTM D6751 and EN14214. The amount of combined Na + K in *Jatropha* biodiesel was found to be 1.86 mg/kg which indicated that wash out of the trace catalyst of KOH from the biodiesel was sufficient. On the other hand, the amount of combined Ca + Mg in *Jatropha* biodiesel was found to be and 3.90 mg/kg. Higher amount of combined Ca + Mg than Na + K might be due to the inherently presence of Ca and Mg in the raw materials and remain in the final product (Almeida *et al.*, 2014).

The comparison between the *Jatropha* biodiesel properties obtained in this study and existing literatures using the same ultrasonication technique have been tabulated in Table 4.2. It could be observed from Table 4.2 that the *Jatropha* biodiesel properties in the study conducted by Kumar *et al.* (2012) fulfilled the standards except density and oxidation stability did not fulfil ASTM D6751 and EN14214 standards, respectively. For the study conducted by Chadha *et al.* (2012), only oxidation stability of *Jatropha* biodiesel did not

fulfil the EN14214 requirement. The *Jatropha* biodiesel synthesized in the study has better oxidation stability and higher calorific value, FAME purity and flash point than their studies. These properties would indicate that the energy content of *Jatropha* biodiesel in the present study was higher, the risk of fire hazard was lower, the biodiesel produced was also purer and less susceptible to be degraded by oxidation. However, the AV of *Jatropha* biodiesel in the present study was higher than that of their studies.

Table 4.2: Comparison of *Jatropha* biodiesel properties with existing literatures using ultrasonication technique.

Properties	Unit	This study	Kumar <i>et al.</i> (2012)	Chadha <i>et al.</i> (2012)
AV	mg KOH/g	0.605	0.18	0.421
FAME purity	wt. %	99.03	>96	94.1
Density (15°C)	kg/m ³	881.2	888.7	852
Kinematic viscosity (40°C)	mm ² /s	4.44	4.70	4.394
Flash point	°C	220.5	135	163
Calorific value	MJ/kg	39.90	—	39.23
Oxidation stability (110°C)	h	11.96	5	3.23
Copper strip corrosion (3 h, 50°C)	—	No. 1b	<No. 1	No. 1

4.6 Comparison of ultrasound technique with conventional stirring approach

In order to clearly confirm the merit of ultrasound technique over conventional stirring approach, the comparison of the FAME purity, biodiesel yield and AV reduction efficiency between them under the same optimized conditions was presented in Table 4.3. It could be noticed that ultrasound technique could obtain higher FAME purity (99.03% vs 91.79%), biodiesel yield (85.20% vs 75.62%) and AV reduction efficiency (88.50% vs 88.20%) compared to magnetic stirring approach. This was because the generation of micro-turbulence in the reactants from the rapid formation of cavitation bubbles could induce larger effective contact area with higher localized temperature and pressure. Therefore, reaction rate increased and shifted the equilibrium towards the product side, rendering higher FAME purity and biodiesel yield. Comparing to conventional stirring,

mixing intensity also played a major role during the reaction between the triglycerides and alcohol molecules. The diffusion of triglyceride molecules from triglyceride-rich phase towards the methanol interface could be the rate limiting step. Therefore, ineffective mass transfer at their phase boundary would result in low reaction rate (Tan *et al.*, 2019; Worapun *et al.*, 2012). Similar findings were also discovered by Sarve *et al.* (2016). Under the same optimized parameters (methanol to *Schleichera triguga* oil of 9:1, Ba(OH)₂ of 3 wt.% and reaction temperature of 50°C), FAME purity of 96.8% was achieved by ultrasonication whereas conventional stirring only achieved 63.29% FAME purity after similar reaction time of 100 min. Worapun *et al.* (2012) had also compared the performance of ultrasound and conventional mechanical stirring under the similar optimized reaction conditions (methanol to oil ratio of 15% w/w, KOH loading of 1 wt.%, reaction temperature of 30°C and reaction time of 25 min). Biodiesel conversion of 98% was achieved by ultrasound technique but 79% of biodiesel conversion was achieved by mechanical stirring method.

Table 4.3: Comparison between ultrasound technique and conventional magnetic stirring approach.

Techniques	FAME purity (%)	Biodiesel yield (%)	AV reduction efficiency (%)
Ultrasound	99.05	85.20	88.50
Magnetic stirring	91.79	75.62	88.20

4.7 Brief summary

Water content in *Jatropha* oilseeds was determined to be 1.89 wt.% which was less than 6.7 wt.%, indicating that there would be minimal detrimental effect on oil extraction process. *Jatropha* seeds were also found to have high oil content (53.96 wt.%), making it suitable to be utilised as feedstock for biodiesel synthesis.

In the parameter screening for ultrasound assisted in-situ esterification, H₂SO₄ loadings of 5 and 25 vol.% had only a slight difference in FAME purity (38.58% versus

36.30%). In the subsequent ultrasound assisted transesterification, the latter offered higher FAME purity of 99.43% than the former (92.29%). In view from the economic perspective, higher amount of catalyst would not be profitable due to the cost of the catalysts itself and also subsequent purification process post-reaction. Therefore, 5 vol.% H_2SO_4 was chosen as the optimum value.

In the parameter study of ultrasound assisted in-situ esterification, extraction efficiency of 83.96%, esterification efficiency of 71.10% and FAME purity of 38.58% were attained at optimum reaction parameters of ultrasonic pulse mode of 5 s on/2 s off, *Jatropha* oilseed particle size of 1–2 mm, n-hexane to methanol volume ratio of 3:1, H_2SO_4 loading of 5 vol.%, reaction time of 150 min and amplitude of 60%. Although the final AV of esterified oil was 5.26 mg KOH/g, transesterification still could be performed with satisfactory FAME purity of 92.29% at methanol to esterified oil molar ratio of 12:1, 1 wt.% KOH and 60% ultrasonic amplitude in reaction time of 15 min. AV was reduced from 5.26 to 1.64 mg KOH/g, corresponding to esterification efficiency of 68.82%. This proved that this novel method could allow oil containing more than 3 wt.% FFA to undergo transesterification process.

Violent shock waves and high-speed jets generated from the asymmetric collapse of cavities struck the seed surface and created cracks and microfractures. On the other hand, *Jatropha* seeds had smooth and intake surface before ultrasonication. It was observed from FTIR spectra that ultrasonic esterified seeds had two peaks with high intensity as compared to five peaks with low intensity. The possible reason could be due to the FFA content in the *Jatropha* seed was converted to biodiesel towards the end of the esterification reaction. From the TGA curves, it was noted that there was no significant weight loss after 700°C for raw *Jatropha* seeds while ultrasonic esterified seed still suffered from weight loss till 900°C. This phenomenon might be due to the reduction of lignin content in the ultrasonic esterified seed after breakage by the ultrasonic energy

waves. From the elemental analysis, carbon content of *Jatropha* seeds was found to reduce greatly after ultrasound assisted in-situ esterification which was attributed to the extraction of fat and lipid (long chain carbon molecules).

For ultrasonic transesterification, FAME purity of 99.03% and biodiesel yield of 85.20% were achieved at KOH loading of 1.5 wt.% and methanol to esterified oil molar ratio of 12:1 at ultrasonic amplitude of 60% in reaction time of 15 min. AV was reduced from 5.26 to 0.605 mg KOH/g which corresponded to AV reduction efficiency of 88.50%. All the biodiesel properties fulfilled the ASTM and EN standards except AV (0.605 wt.%) which exceeded slightly the acceptable limit (0.5 wt.%) in both standards and density (881.2 kg/m^3) beyond the acceptable limit in ASTM standard (880 kg/m^3).

The comparison with conventional magnetic stirring had demonstrated the efficiency of ultrasound to induce effective emulsion and mass transfer. With the application of ultrasound in transesterification, fine emulsion was formed which maximize the interfacial area for the reaction between two immiscible phases (oil and methanol). The cavitation also led to a localized increment of temperature at the phase boundary. As a consequence, both mass transfer and overall reaction rates were expected to increase which helped to attain higher FAME purity (99.03% vs 91.79%) and biodiesel yield (85.20% vs 88.20%) compared to magnetic stirring approach.

CHAPTER 5: CONCLUSIONS AND RECOMMENDATIONS

The present study clearly demonstrated that two-step ultrasound assisted in-situ esterification and transesterification ultrasound is an efficient and time-saving approach to produce biodiesel with satisfactory FAME purity of 99.03% from raw *Jatropha* seeds directly without separate pre-extraction stage.

Results from the ultrasound assisted in-situ esterification had revealed that it was a feasible approach to extract oil from *Jatropha* oilseeds and reduce AV of extracted *Jatropha* oil simultaneously. High AV of the extracted *Jatropha* oil could be reduced to less than 3 wt.% FFA. Ultrasonic pulse mode was found to have a nominal effect on extraction efficiency but had obvious effects on esterification efficiency and FAME purity. On the other hand, particle size and n-hexane to methanol volume ratio significantly affected extraction efficiency but had only a nominal effect on esterification efficiency and FAME purity. Other reaction variables (H_2SO_4 loading, reaction time and ultrasonic amplitude) were found to have considerable effects on extraction, esterification efficiencies and FAME purity.

After transesterification process, high FAME purity of 99.03% and biodiesel yield of 85.20% were achieved within a short reaction time of 15 min at KOH loading of 1.5 wt.%, methanol to esterified oil molar ratio of 12:1 and ultrasonic amplitude of 60%. AV was reduced from 5.26 to 0.605 mg KOH/g which corresponded to AV reduction efficiency of 88.50%.

Jatropha seed particles were found to exhibit smooth and intact surface before ultrasonication. After ultrasonication, the seed particles possessed uneven, disrupted and irregular surface due to the striking of ultrasonic shock waves on the seed's surface as well as created cracks, crevices and microfractures. Ultrasound could also break down the seed matrix, rendering the biomass compounds easier to be thermally degraded. In addition, ultrasound assisted in-situ esterification did not significantly remove the protein

content in the seeds which indicated that ultrasonic esterified *Jatropha* seeds could probably serve as valuable nitrogen source during the bioethanol fermentation process. All the *Jatropha* biodiesel properties fulfilled the ASTM and EN standards except AV and density.

This research work was the first attempt of ultrasound assisted in-situ esterification of *Jatropha* oilseeds with acid catalyst. Therefore, detailed and in-depth information of the influence of each reaction parameters on extraction efficiency, esterification efficiency and FAME purity was contributed to current literatures, specific to *Jatropha* oilseeds. These results warrant more in-depth optimization and fundamental studies such as kinetics and mechanism to be carried out in future.

5.1 Recommendations for future work

It would be feasible to apply ultrasonic reactive extraction to produce biodiesel after the *Jatropha* biodiesel produced has been blended with diesel to achieve AV of lower than 0.5 mg KOH/g and density of less than 880 kg/m³. It had been proven from the study conducted by Ong *et al.* (2014) that AV and density could be reduced with an increment of the biodiesel percentage in the biodiesel-diesel blend. Future work could be done to verify the aforementioned recommendation by varying the biodiesel percentage in diesel. It is also essential to conduct engine performance (engine torque, brake power, brake specific fuel consumption and brake thermal efficiency) and emissions (oxides of nitrogen, HC, CO₂ and CO) testing by using *Jatropha* biodiesel-diesel blend in diesel engine. The findings obtained could be compared with the case of utilising palm oil biodiesel-diesel blend in order to ensure *Jatropha* biodiesel-diesel blend is suitable to replace palm oil biodiesel-diesel blend as transportation fuel. Therefore, the fuel versus food crisis arising from utilisation of palm oil for blending with diesel could be alleviated. In addition, it is important to conduct kinetic modelling of ultrasound assisted in-situ

esterification by using oil-bearing seeds as feedstock. This information will help researchers to ascertain the optimum reaction pathway and determine the rate limiting step. Reactor volume, reactor design and flow rate on the micro bubble's behavior in ultrasound assisted in-situ esterification and transesterification also require further investigation. These findings would be beneficial for the pilot-scale set up and commercialisation in the future.

University of Malaya

REFERENCES

- Abbasi, S., & Diwekar, U. M. (2014). Characterization and stochastic modeling of uncertainties in the biodiesel production. *Clean Technologies and Environmental Policy*, 16(1), 79-94
- Abdullah, N. S., Hussin, M. H., Sharifuddin, S. S., & Yusoff, M. A. M. (2017). Preparation and characterization of activated carbon from *Moringa Oleifera* seed pod. *Science International*, 29(1), 7-11
- Ali, S. D., Javed, I. N., Rana, U. A., Nazar, M. F., Ahmed, W., Junaid, A., . . . Nazir, R. (2017). Novel SrO-CaO mixed metal oxides catalyst for ultrasonic-assisted transesterification of jatropha oil into biodiesel. *Australian Journal of Chemistry*, 70(3), 258
- Almeida, J. M., Dornellas, R. M., Yotsumoto-Neto, S., Ghisi, M., Furtado, J. G., Marques, E. P., . . . Marques, A. L. (2014). A simple electroanalytical procedure for the determination of calcium in biodiesel. *Fuel*, 115, 658-665
- Altun, Ş., Bulut, H., & Öner, C. (2008). The comparison of engine performance and exhaust emission characteristics of sesame oil–diesel fuel mixture with diesel fuel in a direct injection diesel engine. *Renewable Energy*, 33(8), 1791-1795
- Amalia Kartika, I., Evon, P., Cerny, M., Suparno, O., Hermawan, D., Ariono, D., & Rigal, L. (2016). Simultaneous solvent extraction and transesterification of jatropha oil for biodiesel production, and potential application of the obtained cakes for binderless particleboard. *Fuel*, 181, 870-877
- Andrade-Tacca, C. A., Chang, C. C., Chen, Y. H., Ji, D. R., Wang, Y. Y., Yen, Y. Q., & Chang, C. Y. (2014). Reduction of FFA in jatropha curcas oil via sequential direct-ultrasonic irradiation and dosage of methanol/sulfuric acid catalyst mixture on esterification process. *Energy Conversion and Management*, 88, 1078-1085
- Aransiola, E., Ojumu, T., Oyekola, O., Madzimbamuto, T., & Ikhu-Omoregbe, D. (2014). A review of current technology for biodiesel production: state of the art. *Biomass and Bioenergy*, 61, 276-297
- Asif, S., Ahmad, M., Bokhari, A., Chuah, L. F., Klemeš, J. J., Akbar, M. M., . . . Yusup, S. (2017a). Methyl ester synthesis of *Pistacia khinjuk* seed oil by ultrasonic-assisted cavitation system. *Industrial Crops and Products*, 108, 336-347

- Asif, S., Chuah, L. F., Klemeš, J. J., Ahmad, M., Akbar, M. M., Lee, K. T., & Fatima, A. (2017b). Cleaner production of methyl ester from non-edible feedstock by ultrasonic-assisted cavitation system. *Journal of Cleaner Production*, 161, 1360-1373
- Atabani, A. E., Silitonga, A. S., Ong, H. C., Mahlia, T. M. I., Masjuki, H. H., Badruddin, I. A., & Fayaz, H. (2013). Non-edible vegetable oils: a critical evaluation of oil extraction, fatty acid compositions, biodiesel production, characteristics, engine performance and emissions production. *Renewable and Sustainable Energy Reviews*, 18, 211-245
- Badday, A. S., Abdullah, A. Z., Lee, K. T., & Khayoon, M. S. (2012). Intensification of biodiesel production via ultrasonic-assisted process: a critical review on fundamentals and recent development. *Renewable and Sustainable Energy Reviews*, 16(7), 4574-4587
- Bahadur, S., Goyal, P., & Sudhakar, K. (2015). Ultrasonic assisted transesterification of neem oil for biodiesel production. *Energy Sources, Part A: Recovery, Utilization, and Environmental Effects*, 37(17), 1921-1927
- Bahadur, S., Goyal, P., Sudhakar, K., & Prakash Bijarniya, J. (2015). A comparative study of ultrasonic and conventional methods of biodiesel production from mahua oil. *Biofuels*, 6(1), 107-113
- Balasundram, N., Sundram, K., & Samman, S. (2006). Phenolic compounds in plants and agri-industrial by-products: antioxidant activity, occurrence, and potential uses. *Food Chemistry*, 99, 191-203
- Banković-Ilić, I. B., Stamenković, O. S., & Veljković, V. B. (2012). Biodiesel production from non-edible plant oils. *Renewable and Sustainable Energy Reviews*, 16(6), 3621-3647
- Baskar, G., & Aiswarya, R. (2016). Trends in catalytic production of biodiesel from various feedstocks. *Renewable and Sustainable Energy Reviews*, 57, 496-504
- Boffito, D. C., Galli, F., Pirola, C., Bianchi, C. L., & Patience, G. S. (2014). Ultrasonic free fatty acids esterification in tobacco and canola oil. *Ultrasonics Sonochemistry*, 21(6), 1969-1975
- Brasil, A. N., Oliveira, L. S., & Franca, A. S. (2015). Circulation flow reactor with ultrasound irradiation for the transesterification of vegetable oils. *Renewable Energy*, 83, 1059-1065

- Briones, R., Serrano, L., Younes, R. B., Mondragon, I., & Labidi, J. (2011). Polyol production by chemical modification of date seeds. *Industrial Crops and Products*, 34(1), 1035-1040
- Canakci, M., & Van Gerpen, J. (2001). Biodiesel production from oils and fats with high free fatty acids. *Transactions of the American Society of Agricultural Engineers*, 44(6), 1429-1436
- Chadha, P., Arora, A. K., Prakash, S., Jha, M. K., Puri, S. K., Tuli, D. K., & Malhotra, R. K. (2012). Ultrasonic assisted in situ transesterification of jatropha seed to biodiesel. *Journal of Scientific and Industrial Research*, 71(4), 290-294
- Chand, P., Reddy, C. V., Verkade, J. G., & Grewell, D. (2008). Enhancing biodiesel production from soybean oil using ultrasonics. *Energy & Fuels*, 24(3), 2010-2015
- Chen, G., Shan, R., Shi, J., & Yan, B. (2014). Ultrasonic-assisted production of biodiesel from transesterification of palm oil over ostrich eggshell-derived CaO catalysts. *Bioresource Technology*, 171, 428-432
- Choudhury, H. A., Malani, R. S., & Moholkar, V. S. (2013). Acid catalyzed biodiesel synthesis from jatropha oil: mechanistic aspects of ultrasonic intensification. *Chemical Engineering Journal*, 231, 262-272
- Choudhury, H. A., Srivastava, P., & Moholkar, V. S. (2014). Single-step ultrasonic synthesis of biodiesel from crude jatropha curcas oil. *American Institute of Chemical Engineers Journal*, 60(5), 1572-1581
- Chuah, L. F., Amin, M. M., Yusup, S., Bokhari, A., Klemeš, J. J., & Alnarabiji, M. S. (2016a). Influence of green catalyst on transesterification process using ultrasonic-assisted. *Journal of Cleaner Production*, 136, 14-22
- Chuah, L. F., Bokhari, A., Yusup, S., Klemeš, J. J., Akbar, M. M., & Saminathan, S. (2016b). Optimisation on pretreatment of kapok seed (*Ceiba pentandra*) oil via esterification reaction in an ultrasonic cavitation reactor. *Biomass Conversion and Biorefinery*, 7(1), 91-99
- Chuah, L. F., Yusup, S., Aziz, A. R. A., Klemeš, J. J., Bokhari, A., & Abdullah, M. Z. (2016c). Influence of fatty acids content in non-edible oil for biodiesel properties. *Clean Technologies and Environmental Policy*, 18(2), 473-482

- Dasari, S. R., Borugadda, V. B., & Goud, V. V. (2016). Reactive extraction of castor seeds and storage stability characteristics of produced biodiesel. *Process Safety and Environmental Protection*, 100, 252-263
- Deng, X., Fang, Z., & Liu, Y. H. (2010). Ultrasonic transesterification of *Jatropha curcas* L. oil to biodiesel by a two-step process. *Energy Conversion and Management*, 51(12), 2802-2807
- Deng, X., Fang, Z., Liu, Y.-h., & Yu, C.-L. (2011). Production of biodiesel from jatropha oil catalyzed by nanosized solid basic catalyst. *Energy*, 36(2), 777-784
- Dharma, S., Masjuki, H. H., Ong, H. C., Sebayang, A. H., Silitonga, A. S., Kusumo, F., & Mahlia, T. M. I. (2016a). Optimization of biodiesel production process for mixed *Jatropha curcas*–*Ceiba pentandra* biodiesel using response surface methodology. *Energy Conversion and Management*, 115, 178-190
- Dharma, S., Ong, H. C., Masjuki, H., Sebayang, A., & Silitonga, A. (2016b). An overview of engine durability and compatibility using biodiesel–bioethanol–diesel blends in compression-ignition engines. *Energy Conversion and Management*, 128, 66-81
- Dias, J. M., Alvim-Ferraz, M. C., & Almeida, M. F. (2008). Comparison of the performance of different homogeneous alkali catalysts during transesterification of waste and virgin oils and evaluation of biodiesel quality. *Fuel*, 87(17), 3572-3578
- dos Santos Ribeiro, J., Celante, D., Simões, S. S., Bassaco, M. M., da Silva, C., & de Castilhos, F. (2017). Efficiency of heterogeneous catalysts in interesterification reaction from macaw oil (*Acrocomia aculeata*) and methyl acetate. *Fuel*, 200, 499-505
- Durrett, T. P., Benning, C., & Ohlrogge, J. (2008). Plant triacylglycerols as feedstocks for the production of biofuels. *The Plant Journal*, 54(4), 593-607
- Eevera, T., Rajendran, K., & Saradha, S. (2009). Biodiesel production process optimization and characterization to assess the suitability of the product for varied environmental conditions. *Renewable Energy*, 34(3), 762-765
- Ejikeme, P., Anyaogu, I., Ejikeme, C., Nwafor, N., Egbuonu, C., Ukogu, K., & Ibemesi, J. (2010). Catalysis in biodiesel production by transesterification processes-an insight. *Journal of Chemistry*, 7(4), 1120-1132

- El-Ibiari, N., El-Enin, S. A., Gadalla, A., El-Ardi, O., & El-Diwani, G. (2014). Biodiesel production from castor seeds by reactive extraction conventionally and via ultrasound using response surface methodology. *International Journal of Innovative Science, Engineering & Technology*, 1(6), 300-311
- Encinar, J., González, J., & Pardal, A. (2012a). Transesterification of castor oil under ultrasonic irradiation conditions. Preliminary results. *Fuel processing technology*, 103, 9-15
- Encinar, J., Gonzalez, J., Rodriguez, J., & Tejedor, A. (2002). Biodiesel fuels from vegetable oils: transesterification of *Cynara cardunculus* L. oils with ethanol. *Energy & Fuels*, 16(2), 443-450
- Encinar, J., Pardal, A., & Martínez, G. (2012b). Transesterification of rapeseed oil in subcritical methanol conditions. *Fuel processing technology*, 94(1), 40-46
- Fayyazi, E., Ghobadian, B., Najafi, G., & Hosseinzadeh, B. (2014). Genetic algorithm approach to optimize biodiesel production by ultrasonic system. *Chemical Product and Process Modeling*, 9(1), 59-70
- Freedman, B., Pryde, E., & Mounts, T. (1984). Variables affecting the yields of fatty esters from transesterified vegetable oils. *Journal of the American Oil Chemists Society*, 61(10), 1638-1643
- Gaikwad, N. D., & Gogate, P. R. (2015). Synthesis and application of carbon based heterogeneous catalysts for ultrasound assisted biodiesel production. *Green Processing and Synthesis*, 4(1), 17-30
- Gogate, P. R., Tayal, R. K., & Pandit, A. B. (2006). Cavitation: a technology on the horizon. *Current Science*, 91(1), 35-46
- Gole, V. L., & Gogate, P. R. (2012). Intensification of synthesis of biodiesel from nonedible oils using sonochemical reactors. *Industrial & Engineering Chemistry Research*, 51(37), 11866-11874
- Gude, V. G., & Grant, G. E. (2013). Biodiesel from waste cooking oils via direct sonication. *Applied Energy*, 109, 135-144
- Guldhe, A., Singh, B., Rawat, I., & Bux, F. (2014). Synthesis of biodiesel from *Scenedesmus* sp. by microwave and ultrasound assisted in situ transesterification using tungstated zirconia as a solid acid catalyst. *Chemical Engineering Research and Design*, 92(8), 1503-1511

- Gupta, A. R., Yadav, S. V., & Rathod, V. K. (2015). Enhancement in biodiesel production using waste cooking oil and calcium diglyceroxide as a heterogeneous catalyst in presence of ultrasound. *Fuel*, 158, 800-806
- Haas, M. J., McAloon, A. J., Yee, W. C., & Foglia, T. A. (2006). A process model to estimate biodiesel production costs. *Bioresource Technology*, 97(4), 671-678
- Haas, M. J., & Scott, K. M. (2007). Moisture removal substantially improves the efficiency of in situ biodiesel production from soybeans. *Journal of the American Oil Chemists' Society*, 84(2), 197-204
- Hafez, A. I., Gerges, N. S., Ibrahim, H. N., Abou El-magd, W. S. I., & Hashem, A. I. (2017). Evaluation of kaolin clay as natural material for transformer oil treatment to reduce the impact of ageing on copper strip. *Egyptian Journal of Petroleum*, 26(2), 533-539
- Hajinezhad, A., Abedi, S., Ghobadian, B., & Noorollahi, Y. (2015). Biodiesel production from norouzak (*Salvia lerifolia*) seeds as an indigenous source of bio fuel in Iran using ultrasound. *Energy Conversion and Management*, 99, 132-140
- Hajjari, M., Tabatabaei, M., Aghbashlo, M., & Ghanavati, H. (2017). A review on the prospects of sustainable biodiesel production: a global scenario with an emphasis on waste-oil biodiesel utilization. *Renewable and Sustainable Energy Reviews*, 72, 445-464
- Hara, M. (2009). Environmentally benign production of biodiesel using heterogeneous catalysts. *ChemSusChem*, 2(2), 129-135
- Hayyan, A., Alam, M. Z., Mirghani, M. E. S., Kabbashi, N. A., Hakimi, N. I. N. M., Siran, Y. M., & Tahiruddin, S. (2011). Reduction of high content of free fatty acid in sludge palm oil via acid catalyst for biodiesel production. *Fuel Processing Technology*, 92(5), 920-924
- He, B., & Van Gerpen, J. H. (2012). Application of ultrasonication in transesterification processes for biodiesel production. *Biofuels*, 3(4), 479-488
- Helwani, Z., Othman, M., Aziz, N., Fernando, W., & Kim, J. (2009). Technologies for production of biodiesel focusing on green catalytic techniques: a review. *Fuel Processing Technology*, 90(12), 1502-1514
- Hensarling, T. N., & Jacks, T. (1983). Solvent extraction of lipids from soybeans with acidic hexane. *Journal of the American Oil Chemists' Society*, 60(4), 783-784

- Hincapié, G., Mondragón, F., & López, D. (2011). Conventional and in situ transesterification of castor seed oil for biodiesel production. *Fuel*, 90(4), 1618-1623
- Hingu, S. M., Gogate, P. R., & Rathod, V. K. (2010). Synthesis of biodiesel from waste cooking oil using sonochemical reactors. *Ultrasonics Sonochemistry*, 17(5), 827-832
- Ho, W. W. S., Ng, H. K., & Gan, S. (2016). Advances in ultrasound-assisted transesterification for biodiesel production. *Applied Thermal Engineering*, 100, 553-563
- Hoekman, S. K., Broch, A., Robbins, C., Cenicerros, E., & Natarajan, M. (2012). Review of biodiesel composition, properties, and specifications. *Renewable and Sustainable Energy Reviews*, 16(1), 143-169
- Hong, I. K., Jeon, H., & Lee, S. B. (2014). Effect of mixed alcohol reactants on ultrasonic alcoholysis of canola oil. *Journal of Industrial and Engineering Chemistry*, 20(3), 911-915
- Hu, A. J., Feng, Q. Q., Zheng, J. I. E., Hu, X. H., Wu, C., & Liu, C. Y. (2012). Kinetic model and technology of ultrasound extraction of safflower seed oil. *Journal of Food Process Engineering*, 35(2), 278-294
- Islam, A., Taufiq-Yap, Y. H., Chan, E. S., Moniruzzaman, M., Islam, S., & Nabi, M. N. (2014). Advances in solid-catalytic and non-catalytic technologies for biodiesel production. *Energy Conversion and Management*, 88, 1200-1218
- Jadhav, A. J., Holkar, C. R., Goswami, A. D., Pandit, A. B., & Pinjari, D. V. (2016). Acoustic cavitation as a novel approach for extraction of oil from waste date seeds. *ACS Sustainable Chemistry & Engineering*, 4(8), 4256-4263
- Ji, J., Wang, J., Li, Y., Yu, Y., & Xu, Z. (2006). Preparation of biodiesel with the help of ultrasonic and hydrodynamic cavitation. *Ultrasonics*, 44, e411-e414
- Jogi, R., Murthy, Y. S., Satyanarayana, M., Rao, T. N., & Javed, S. (2016). Biodiesel production from degummed *Jatropha curcas* oil using constant-temperature ultrasonic water bath. *Energy Sources, Part A: Recovery, Utilization, and Environmental Effects*, 38(17), 2610-2616

- Kamel, D. A., Farag, H. A., Amin, N. K., & Fouad, Y. O. (2016). Biodiesel synthesis from non-edible oils by transesterification using the activated carbon as heterogeneous catalyst. *International Journal of Environmental Science and Technology*, 14(4), 785-794
- Ke, J., Laskar, D. D., Ellison, M. T., Zemetra, R. S., & Chen, S. (2012). Modulation of lignin deposition/composition via phytic acid reduction in seed improves the quality of barley straw for sugar release and ethanol production. *Biomass and Bioenergy*, 46, 584-592
- Kesgin, C., Yücel, S., Özçimen, D., Terzioğlu, P., & Attar, A. (2014). Transesterification of hazelnut oil by ultrasonic irradiation. *International Journal of Green Energy*, 13(3), 328-333
- Khosravi, E., Shariati, A., & Nikou, M. R. K. (2016). Instant biodiesel production from waste cooking oil under industrial ultrasonic irradiation. *International Journal of Oil, Gas and Coal Technology*, 11(3), 308-317
- Kiss, A. A. (2009). Novel process for biodiesel by reactive absorption. *Separation and Purification Technology*, 69(3), 280-287
- Kiss, A. A., & Bildea, C. S. (2012). A review of biodiesel production by integrated reactive separation technologies. *Journal of Chemical Technology and Biotechnology*, 87(7), 861-879
- Koh, M. Y., & Ghazi, T. I. M. (2011). A review of biodiesel production from *Jatropha curcas* L. oil. *Renewable and Sustainable Energy Reviews*, 15(5), 2240-2251
- Koutsouki, A., Tegou, E., Kontakos, S., Kontominas, M., Pomonis, P., & Manos, G. (2015). In situ transesterification of *Cynara cardunculus* L. seed oil via direct ultrasonication for the production of biodiesel. *Fuel Processing Technology*, 134, 122-129
- Koutsouki, A. A., Tegou, E., Badeka, A., Kontakos, S., Pomonis, P. J., & Kontominas, M. G. (2016). In situ and conventional transesterification of rapeseeds for biodiesel production: the effect of direct sonication. *Industrial Crops and Products*, 84, 399-407
- Krishnaiah, G., Pasnoori, S., Santhoshi, P., Rajanna, K., Rao, Y. R., & Patnaik, K. R. (2016). Ultrasonic and microwave effects on crystalline Mn(II) carbonate catalyzed biodiesel production using watermelon (*Citrullus vulgaris*) seed oil and alcohol (fibrous flesh) as exclusive green feedstock. *Biofuels*, 1-7

- Kumar, A., & Sharma, S. (2008). An evaluation of multipurpose oil seed crop for industrial uses (*Jatropha curcas* L.): a review. *Industrial Crops and Products*, 28(1), 1-10
- Kumar, D., & Ali, A. (2013). Transesterification of low-quality triglycerides over a Zn/CaO heterogeneous catalyst: kinetics and reusability studies. *Energy & Fuels*, 27(7), 3758-3768
- Kumar, D., Kumar, G., Johari, R., & Kumar, P. (2012). Fast, easy ethanomethanolysis of *Jatropha curcas* oil for biodiesel production due to the better solubility of oil with ethanol in reaction mixture assisted by ultrasonication. *Ultrasonics Sonochemistry*, 19(4), 816-822
- Kumar, D., Kumar, G., & Singh, C. (2010a). Fast, easy ethanolysis of coconut oil for biodiesel production assisted by ultrasonication. *Ultrasonics Sonochemistry*, 17(3), 555-559
- Kumar, D., Kumar, G., & Singh, C. (2010b). Ultrasonic-assisted transesterification of *Jatropha curcas* oil using solid catalyst, Na/SiO₂. *Ultrasonics Sonochemistry*, 17(5), 839-844
- Kumar, G. (2017). Ultrasonic-assisted reactive-extraction is a fast and easy method for biodiesel production from *Jatropha curcas* oilseeds. *Ultrasonics Sonochemistry*, 37, 634-639
- Lam, M. K., Lee, K. T., & Mohamed, A. R. (2010). Homogeneous, heterogeneous and enzymatic catalysis for transesterification of high free fatty acid oil (waste cooking oil) to biodiesel: a review. *Biotechnology Advances*, 28(4), 500-518
- Lee, K. T., Lim, S., Pang, Y. L., Ong, H. C., & Chong, W. T. (2014). Integration of reactive extraction with supercritical fluids for process intensification of biodiesel production: prospects and recent advances. *Progress in Energy and Combustion Science*, 45, 54-78
- Leung, D. Y., Wu, X., & Leung, M. (2010). A review on biodiesel production using catalyzed transesterification. *Applied Energy*, 87(4), 1083-1095
- Liu, Y., Lu, H., Jiang, W., Li, D., Liu, S., & Liang, B. (2012). Biodiesel production from crude *Jatropha curcas* L. oil with trace acid catalyst. *Chinese Journal of Chemical Engineering*, 20(4), 740-746

- Maddikeri, G. L., Pandit, A. B., & Gogate, P. R. (2012). Intensification approaches for biodiesel synthesis from waste cooking oil: a review. *Industrial & Engineering Chemistry Research*, 51(45), 14610-14628
- Maddikeri, G. L., Pandit, A. B., & Gogate, P. R. (2013). Ultrasound assisted interesterification of waste cooking oil and methyl acetate for biodiesel and triacetin production. *Fuel Processing Technology*, 116, 241-249
- Maghami, M., Sadrameli, S., & Ghobadian, B. (2015). Production of biodiesel from fishmeal plant waste oil using ultrasonic and conventional methods. *Applied Thermal Engineering*, 75, 575-579
- Mahamuni, N. N., & Adewuyi, Y. G. (2009). Optimization of the synthesis of biodiesel via ultrasound-enhanced base-catalyzed transesterification of soybean oil using a multifrequency ultrasonic reactor. *Energy & Fuels*, 23(5), 2757-2766
- Manickam, S., Arigela, V. N. D., & Gogate, P. R. (2014). Intensification of synthesis of biodiesel from palm oil using multiple frequency ultrasonic flow cell. *Fuel Processing Technology*, 128, 388-393
- Martinez-Guerra, E., & Gude, V. G. (2015). Continuous and pulse sonication effects on transesterification of used vegetable oil. *Energy Conversion and Management*, 96, 268-276
- Mathiarasi, R., & Partha, N. (2016). Optimization, kinetics and thermodynamic studies on oil extraction from *Daturametel Linn* oil seed for biodiesel production. *Renewable Energy*, 96, 583-590
- Meira, M., Quintella, C. M., Ribeiro, E. M. O., Silva, H. R. G., & Guimarães, A. K. (2014). Overview of the challenges in the production of biodiesel. *Biomass Conversion and Biorefinery*, 5(3), 321-329
- Mohan, S., Pal, A., & Singh, R. (2017). The production of semal oil methyl esters through a combined process reactor. *Energy Sources, Part A: Recovery, Utilization, and Environmental Effects*, 39(10), 955-962
- Mohapatra, S., Das, P., Swain, D., Satapathy, S., & Sahu, S. R. (2016). A review on rejuvenated techniques in biodiesel production from vegetable oils. *International Journal of Current Engineering and Technology*, 6, 100-111

- Mohod, A. V., Subudhi, A. S., & Gogate, P. R. (2017). Intensification of esterification of non edible oil as sustainable feedstock using cavitational reactors. *Ultrasonics Sonochemistry*, 36, 309-318
- Mohod, T. R., Bhansali, S., Moghe, S., & Kathoke, T. (2014). Preheating of biodiesel for the improvement of the performance characteristics of di engine: a review. *International Journal of Engineering Research and General Science*, 2(4), 747-753
- Monisha, J., Harish, A., Sushma, R., Krishna Murthy, T., Blessy, B. M., & Ananda, S. (2013). Biodiesel: a review. *International Journal of Engineering Research and Applications*, 3(6), 902-912
- Mootabadi, H., Salamatinia, B., Bhatia, S., & Abdullah, A. Z. (2010). Ultrasonic-assisted biodiesel production process from palm oil using alkaline earth metal oxides as the heterogeneous catalysts. *Fuel*, 89(8), 1818-1825
- Nigade, S. S., Jadhav, S. D., & Chandgude, A. K. (2015). Development of transesterification system with acid and base homogeneous catalysts for Mangifera Indica seed oil to Mangifera Indica Methyl Ester (MOME biodiesel). *International Journal of Energy and Power Engineering*, 4(5-1), 48-53
- Noureddini, H., Harkey, D., & Medikonduru, V. (1998). A continuous process for the conversion of vegetable oils into methyl esters of fatty acids. *Journal of the American Oil Chemists' Society*, 75(12), 1775-1783
- Oh, P. P., Lau, H. L. N., Chen, J., Chong, M. F., & Choo, Y. M. (2012). A review on conventional technologies and emerging process intensification (PI) methods for biodiesel production. *Renewable and Sustainable Energy Reviews*, 16(7), 5131-5145
- Ong, H. C., Masjuki, H. H., Mahlia, T. M. I., Silitonga, A. S., Chong, W. T., & Yusaf, T. (2014). Engine performance and emissions using *Jatropha curcas*, *Ceiba pentandra* and *Calophyllum inophyllum* biodiesel in a CI diesel engine. *Energy*, 69, 427-445
- Pan, Y., Alam, M. A., Wang, Z., Wu, J., Zhang, Y., & Yuan, Z. (2016). Enhanced esterification of oleic acid and methanol by deep eutectic solvent assisted amberlyst heterogeneous catalyst. *Bioresource Technology*, 220, 543-548
- Parida, S., Sahu, D. K., & Misra, P. K. (2016). A rapid ultrasound-assisted production of biodiesel from a mixture of Karanj and soybean oil. *Energy Sources, Part A: Recovery, Utilization, and Environmental Effects*, 38(8), 1110-1116

- Parkar, P. A., Choudhary, H. A., & Moholkar, V. S. (2012). Mechanistic and kinetic investigations in ultrasound assisted acid catalyzed biodiesel synthesis. *Chemical Engineering Journal*, 187, 248-260
- Prakash Maran, J., & Priya, B. (2015). Modeling of ultrasound assisted intensification of biodiesel production from neem (*Azadirachta indica*) oil using response surface methodology and artificial neural network. *Fuel*, 143, 262-267
- Pukale, D. D., Maddikeri, G. L., Gogate, P. R., Pandit, A. B., & Pratap, A. P. (2015). Ultrasound assisted transesterification of waste cooking oil using heterogeneous solid catalyst. *Ultrasonics Sonochemistry*, 22, 278-286
- Ragavan, S. N., & Roy, D. V. (2011). Transesterification of rubber seed oil by sonication technique for the production of methyl esters. *Biomass Conversion and Biorefinery*, 1(2), 105-110
- Ramachandran, K., Al-Zuhair, S., Fong, C., & Gak, C. (2006). Kinetic study on hydrolysis of oils by lipase with ultrasonic emulsification. *Biochemical Engineering Journal*, 32(1), 19-24
- Ramadhass, A. S., Jayaraj, S., & Muraleedharan, C. (2005). Biodiesel production from high FFA rubber seed oil. *Fuel*, 84(4), 335-340
- Refaat, A., Attia, N., Sibak, H. A., El Sheltawy, S., & ElDiwani, G. (2008). Production optimization and quality assessment of biodiesel from waste vegetable oil. *International Journal of Environmental Science & Technology*, 5(1), 75-82
- Refaat, A., & El Sheltawy, S. (2008). Comparing three options for biodiesel production from waste vegetable oil. *Waste Management and the Environment IV*, 109, 133-140
- Saha, R., & Goud, V. V. (2014). Ultrasound assisted transesterification of high free fatty acids karanja oil using heterogeneous base catalysts. *Biomass Conversion and Biorefinery*, 5(2), 195-207
- Sait, H. H., Hussain, A., Salema, A. A., & Ani, F. N. (2012). Pyrolysis and combustion kinetics of date palm biomass using thermogravimetric analysis. *Bioresource Technology*, 118, 382-389

- Salamatinia, B., Mootabadi, H., Hashemizadeh, I., & Abdullah, A. Z. (2013). Intensification of biodiesel production from vegetable oils using ultrasonic-assisted process: optimization and kinetic. *Chemical Engineering and Processing: Process Intensification*, 73, 135-143
- Saleh, J., Tremblay, A. Y., & Dubé, M. A. (2010). Glycerol removal from biodiesel using membrane separation technology. *Fuel*, 89(9), 2260-2266
- Samani, B. H., Zareiforoush, H., Lorigooini, Z., Ghobadian, B., Rostami, S., & Fayyazi, E. (2016). Ultrasonic-assisted production of biodiesel from *Pistacia atlantica* Desf. oil. *Fuel*, 168, 22-26
- Santos, F. F., Malveira, J. Q., Cruz, M. G., & Fernandes, F. A. (2010). Production of biodiesel by ultrasound assisted esterification of *Oreochromis niloticus* oil. *Fuel*, 89(2), 275-279
- Sarve, A. N., Varma, M. N., & Sonawane, S. S. (2016). Ultrasound assisted two-stage biodiesel synthesis from non-edible *Schleichera triguga* oil using heterogeneous catalyst: kinetics and thermodynamic analysis. *Ultrasonics Sonochemistry*, 29, 288-298
- Schroeder, P., Nascimento, B. P. d., Romeiro, G. A., Figueiredo, M. K. K., & Veloso, M. C. D. C. (2017). Chemical and physical analysis of the liquid fractions from soursop seed cake obtained using slow pyrolysis conditions. *Journal of Analytical and Applied Pyrolysis*, 124, 161-174
- Sebayang, D., Agustian, E., & Praptijanto, A. (2010, Dec). *Transesterification of biodiesel from waste cooking oil using ultrasonic technique*. Paper presented at the International Conference on Environment 2010, Penang, Malaysia.
- Shak, K. P. Y., & Wu, T. Y. (2014). Coagulation–flocculation treatment of high-strength agro-industrial wastewater using natural *Cassia obtusifolia* seed gum: treatment efficiencies and flocs characterization. *Chemical Engineering Journal*, 256, 293-305
- Shirsath, S., Sonawane, S., & Gogate, P. (2012). Intensification of extraction of natural products using ultrasonic irradiations—a review of current status. *Chemical Engineering and Processing: Process Intensification*, 53, 10-23
- Shuit, S. H., Lee, K. T., Kamaruddin, A. H., & Yusup, S. (2010a). Reactive extraction and in situ esterification of *Jatropha curcas* L. seeds for the production of biodiesel. *Fuel*, 89(2), 527-530

- Shuit, S. H., Lee, K. T., Kamaruddin, A. H., & Yusup, S. (2010b). Reactive extraction of *Jatropha curcas* L. seed for production of biodiesel: process optimization study. *Environmental Science & Technology*, 44(11), 4361-4367
- Singh, B. (2014). Production of biodiesel from plant oils-an overview. *Journal of Biotechnology, Bioinformatics and Bioengineering*, 1(2), 33-42
- Singh, B., Bux, F., & Sharma, Y. (2011). Comparison of homogeneous and heterogeneous catalysis for synthesis of biodiesel from *Madhuca indica* oil. *Chemical Industry and Chemical Engineering Quarterly*, 17(2), 117-124
- Singh, S., & Bothara, S. B. (2014). Physico-chemical and structural characterization of mucilage isolated from seeds of *Diospyros melonoxylon* Roxb. *Brazilian Journal of Pharmaceutical Sciences*, 50(4), 713-725
- Somnuk, K., Smithmaitrie, P., & Prateepchaikul, G. (2013). Optimization of continuous acid-catalyzed esterification for free fatty acids reduction in mixed crude palm oil using static mixer coupled with high-intensity ultrasonic irradiation. *Energy Conversion and Management*, 68, 193-199
- Su, C. H. (2013). Recoverable and reusable hydrochloric acid used as a homogeneous catalyst for biodiesel production. *Applied Energy*, 104, 503-509
- Subhedar, P. B., & Gogate, P. R. (2014). Alkaline and ultrasound assisted alkaline pretreatment for intensification of delignification process from sustainable raw-material. *Ultrasonics Sonochemistry*, 21(1), 216-225
- Subhedar, P. B., & Gogate, P. R. (2016). Ultrasound assisted intensification of biodiesel production using enzymatic interesterification. *Ultrasonics Sonochemistry*, 29, 67-75
- Takase, M., Chen, Y., Liu, H., Zhao, T., Yang, L., & Wu, X. (2014a). Biodiesel production from non-edible *Silybum marianum* oil using heterogeneous solid base catalyst under ultrasonication. *Ultrasonics sonochemistry*, 21(5), 1752-1762
- Takase, M., Feng, W., Wang, W., Gu, X., Zhu, Y., Li, T., . . . Wu, X. (2014b). *Silybum marianum* oil as a new potential non-edible feedstock for biodiesel: a comparison of its production using conventional and ultrasonic assisted method. *Fuel Processing Technology*, 123, 19-26

- Talebian-Kiakalaieh, A., Amin, N. A. S., & Mazaheri, H. (2013). A review on novel processes of biodiesel production from waste cooking oil. *Applied Energy*, 104, 683-710
- Tan, S. X., Lim, S., Ong, H. C., & Pang, Y. L. (2019). State of the art review on development of ultrasound-assisted catalytic transesterification process for biodiesel production. *Fuel*, 235, 886-907
- Tavares, G. R., Gonçalves, J. E., dos Santos, W. D., & da Silva, C. (2017a). Enzymatic interesterification of crambe oil assisted by ultrasound. *Industrial Crops and Products*, 97, 218-223
- Tavares, G. R., Massa, T. B., Gonçalves, J. E., da Silva, C., & dos Santos, W. D. (2017b). Assessment of ultrasound-assisted extraction of crambe seed oil for biodiesel synthesis by in situ interesterification. *Renewable Energy*, 111, 659-665
- Thanh, L. T., Okitsu, K., Sadanaga, Y., Takenaka, N., Maeda, Y., & Bandow, H. (2010). Ultrasound-assisted production of biodiesel fuel from vegetable oils in a small scale circulation process. *Bioresource Technology*, 101(2), 639-645
- Thiagarajan, J., Srividya, P., & Balasubramanian, P. (2016). Thermogravimetric and decomposition analysis of jatropha, castor and pongamia deoiled seed cakes. *International Journal of Innovations in Engineering and Technology*, 7 (2), 417-425
- Tian, Y., Xiang, J., Verni, C. C., & Soh, L. (2018). Fatty acid methyl ester production via ferric sulfate catalyzed interesterification. *Biomass and Bioenergy*, 115, 82-87
- Torrentes-Espinoza, G., Miranda, B. C., Vega-Baudrit, J., & Mata-Segreda, J. F. (2017). Castor oil (*Ricinus communis*) supercritical methanolysis. *Energy*, 140, 426-435
- Trinh, H., Yusup, S., & Uemura, Y. (2017). Optimization and kinetic study of ultrasonic assisted esterification process from rubber seed oil. *Bioresource Technology*, 247, 51-57
- Veljković, V. B., Avramović, J. M., & Stamenković, O. S. (2012). Biodiesel production by ultrasound-assisted transesterification: state of the art and the perspectives. *Renewable and Sustainable Energy Reviews*, 16(2), 1193-1209
- Vyas, A. P., Verma, J. L., & Subrahmanyam, N. (2010). A review on FAME production processes. *Fuel*, 89(1), 1-9

- Wang, Y. Y., D  ng, T. N. H. P., Chen, B. H., & Lee, D. J. (2012). Transesterification of triolein to biodiesel using sodium-loaded catalysts prepared from zeolites. *Industrial & Engineering Chemistry Research*, 51(30), 9959-9965
- Worapun, I., Pianthong, K., & Thaiyasuit, P. (2012a). Two-step biodiesel production from crude *Jatropha curcas* L. oil using ultrasonic irradiation assisted. *Journal of oleo science*, 61(4), 165-172
- Yadav, A. K., Khan, M. E., Pal, A., & Dubey, A. M. (2016a). Biodiesel production from Nerium oleander (Thevetia peruviana) oil through conventional and ultrasonic irradiation methods. *Energy Sources, Part A: Recovery, Utilization, and Environmental Effects*, 38(23), 3447-3452
- Yadav, A. K., Khan, M. E., Pal, A., & Singh, B. (2016b). Ultrasonic-assisted optimization of biodiesel production from karabi oil using heterogeneous catalyst. *Biofuels*, 9(1), 101-112
- Yang, N., Su, Y., Wang, H., Wu, Z., & Huang, X. (2011). Experimental study on preparation of biodiesel through transesterification with ultrasonic assistant. *Materials for Renewable Energy & Environment*, 1, 284-287
- Yin, X., Ma, H., You, Q., Wang, Z., & Chang, J. (2012). Comparison of four different enhancing methods for preparing biodiesel through transesterification of sunflower oil. *Applied Energy*, 91(1), 320-325
- Zahari, M. S. M., Ibrahim, M. Z., Lam, S. S., & Mat, R. (2014a). Prospect of parallel biodiesel and bioethanol production from *Jatropha curcas* seed. *Applied Mechanics and Materials*. 663, 44-48.
- Zahari, M. S. M., Ismail, S., Ibrahim, M. Z., Lam, S. S., & Mat, R. (2014b). Study of enhanced reactive extraction process using ultrasonication for jatropha curcas seed. *Applied Mechanics & Materials*, 699, 522-527
- Zahari, M. S. M., Ismail, S., Ibrahim, M. Z., Lam, S. S., & Mat, R. (2015). Ultrasonicated *Jatropha curcas* seed residual as potential biofuel feedstock. *Jurnal Teknologi*, 77(1), 133-138
- Zakaria, R., & Harvey, A. P. (2012). Direct production of biodiesel from rapeseed by reactive extraction/in situ transesterification. *Fuel Processing Technology*, 102, 53-60

Zhang, F., Fang, Z., & Wang, Y. T. (2015). Biodiesel production directly from oils with high acid value by magnetic $\text{Na}_2\text{SiO}_3/\text{Fe}_3\text{O}_4/\text{C}$ catalyst and ultrasound. *Fuel*, 150, 370-377

Zou, H., & Lei, M. (2012). Optimum process and kinetic study of *Jatropha curcas* oil pre-esterification in ultrasonical field. *Journal of The Taiwan Institute of Chemical Engineers*, 43(5), 730-735

University of Malaya

LIST OF PUBLICATIONS AND PAPERS PRESENTED

- Tan, S. X., Ong, H. C., Lim, S., & Pang, Y. L. (2018). In-situ reactive extraction of *Jatropha curcas* L. seeds assisted by ultrasound: preliminary studies. *Energy Sources, Part A: Recovery, Utilization, and Environmental Effects*, 40(14), 1772-1779.
- Tan, S. X., Lim, S., Ong, H. C., & Pang, Y. L. (2019). State of the art review on development of ultrasound assisted catalytic transesterification process for biodiesel production. *Fuel*, 235, 886-907.

University of Malaya